Development of Proliposomal and Liposomal Formulations with Poorly Water-soluble Drugs

Der Naturwissenschaftlichen Fakultät

der Friedrich-Alexander-Universität Erlangen-Nürnberg

zur Erlangung des Doktorgrades Dr. rer. nat.

vorgelegt von

Christina Rödel

aus Bayreuth

Als Dissertation von der Naturwissenschaftlichen Fakultät der Friedrich-Alexander-Universität Erlangen-Nürnberg genehmigt.

Tag der mündlichen Prüfung:	31.10.2019
Vorsitzender des Promotionsorgans:	Prof. Dr. Georg Kreimer
Gutachter:	Prof. Dr. Geoffrey Lee
	PD Dr. Henning Gieseler

Für meine Familie

“If we knew what it was we were doing,
it would not be called research, would it?”

Albert Einstein (1879 - 1955)

Parts of this thesis have already been presented:

C. Rödel, S. Seyferth and G. Lee (2016):
The influence of pH-value on liposomal size, PDI and zeta potential.
10th World Meeting on Pharmaceutics, Biopharmaceutics and Pharmaceutical Technology (PBP 2016)
Glasgow (United Kingdom), April 4 - 7, 2016. Poster presentation.

C. Rödel, S. Seyferth and G. Lee (2017):
Proliposomes: development of a coating method on spherical carriers for the manufacturing of small unilamellar vesicles.
6th FIP Pharmaceutical Sciences World Congress (FIP PSWC 2017)
Stockholm (Sweden), May 21 - 24, 2017. Poster presentation.

C. Rödel, S. Seyferth and G. Lee (2018):
Development of a formulation and tableting process of proliposomes.
11th World Meeting on Pharmaceutics, Biopharmaceutics and Pharmaceutical Technology (PBP 2018)
Granada (Spain), March 19 - 22, 2018. Poster presentation.

List of abbreviations

Expressions

API	Active pharmaceutical ingredient
BCS	Biopharmaceutics Classification System
CMC	Critical micelle concentration
COX	Cyclooxygenase
DLS	Dynamic light scattering
DNA	Deoxyribonucleic acid
DoE	Design of experiments
DPI	Dry powder inhaler
DSC	Differential scanning calorimetry
EE	Encapsulation efficiency
EMA	European Medicines Agency
ESEM	Environmental scanning electron microscopy
ESR	Erythrocyte sedimentation rate
FFF	Field-flow fractionation
FRVs	Freeze-dried rehydration vesicles
GC	Gas chromatography
GHP	Globuli Homeopathic Pharmacopeia
HCl	Hydrochloric acid
HDL	High-density lipoprotein
HPLC	High-performance liquid chromatography
HPTLC	High-performance thin-layer chromatography
i.m.	Intramuscular
i.v.	Intravenous
LD	Laser diffraction
LDL	Low-density lipoprotein
LNP	Lipid nanoparticle
LOD	Limit of detection
LOQ	Limit of quantification
LUVs	Large unilamellar vesicles
MCC	Microcrystalline cellulose

MLVs	Multilamellar vesicles
MPS	Mononuclear phagocyte system
NaOH	Sodium hydroxide
NMR	Nuclear magnetic resonance spectroscopy
NSAID	Non-steroidal anti-inflammatory drug
PCS	Photon correlation spectroscopy
PDI	Polydispersity index
PEG	Poly(ethylene glycol)
Ph.Eur.	European Pharmacopoeia
PLs	Proliposomes
plv.	Pulverized
$PPAR_\alpha$	Peroxisome proliferator receptor alpha
RC	Regenerated cellulose
RES	Reticuloendothelial system
REV	Reverse-phase evaporation
RI	Refractive index
SAS	Supercritical anti-solvent
SC-CO_2	Supercritical carbon dioxide
SEC	Size-exclusion chromatography
SEM	Scanning electron microscopy
SFD	Spray freeze drying
siRNA	Small interfering ribonucleic acid
SNALP	Stable nucleic acid lipid particle
SUVs	Small unilamellar vesicles
TBA	Thiobarbituric acid
TEM	Transmission electron microscopy
TLC	Thin-layer chromatography
ULV	Unilamellar vesicle
WAXD	Wide-Angle-X-Ray diffraction
Z-ave	Z-average
ZP	Zeta potential

Lipids

CL	Cardiolipin
DEPC	1,2-dierucoylphosphatidylcholine
DMPC	1,2-dimyristoyl-*sn*-glycero-3-phosphocholine
DMPG	1,2-ditetradecanoyl-*sn*-glycero-3-phospho-(1'-*rac*-glycerol) (14:0)
DOPC	1,2-di-(9Z-octadecenoyl)-*sn*-glycero-3-phosphocholine (18:1)
DOPE	1,2-dioleoyl-*sn*-glycero-3-phosphoethanolamine (18:0)
DOPS	1,2-di-(9Z-octadecenoyl)-*sn*-glycero-3-phospho-L-serine (18:1)
DOTAP	1,2-dioleoyl-3-trimethylammonium-propane (18:1)
DPPC	1,2-dipalmitoyl-*sn*-glycero-3-phosphocholine
DPPG	1,2-dihexadecanoyl-*sn*-glycero-3-phospho-(1'-*rac*-glycerol) (16:0)
DSPC	1,2-dioctadecanoyl-*sn*-glycero-3-phosphocholine (18:0)
DSPE	1,2-distearoyl-*sn*-glycero-3-phosphoethanolamine (18:0)
DSPE-PEG-2000	1,2-distearoyl-*sn*-glycero-3-phosphoethanolamine-N-[amino(polyethylene glycol)-(MW 2000)] (18:0)
DSPG	1,2-distearoyl-*sn*-glycero-3-phospho-(1'-*rac*-glycerol) (18:0)
Egg-PC	L-α-phosphatidylcholine (egg, soybean)
HSPC	L-α-phosphatidylcholine, hydrogenated (soybean)
MPEG-2000-DSPE	Methoxy polyethylene glycolf-(MW 2000)-1,2-distearoyl-*sn*-glycero-3-phosphoethanolamine (18:0)
PA	Phosphatidic acid
PC	Phosphatidylcholine
PE	Phosphatidylethanolamine
PG	Phosphatidylglycerol
PI	Phosphatidylinositol
POPC	1-hexadecanoyl-2-(9Z-octadecenoyl)-*sn*-glycero-3-phosphocholine (16:0/18:1)
PS	Phosphatidylserine
SM	Sphingomyelin

Capital letters

D	Diffusion coefficient
MW	Molecular weight
T_{inlet}	Air inlet temperature
T_m	Phase transition temperature
T_{outlet}	Air outlet temperature

Small letters

c	Concentration
d(H)	Hydrodynamic diameter
d_{50}	Median value of a volume based size distribution
k	Boltzmann constant
m	Mass
pK_a	Acid dissociation constant
t	Time

Greek letters

η	Dynamic viscosity
λ	Wavelength
ψ	Membrane potential

Table of contents

1 INTRODUCTION 1

2 THEORETICAL BACKGROUND 5

2.1 Classification of liposomes 5
2.2 Classical preparation techniques of liposomes 9
2.3 Techniques to control liposomal size and size distribution 13
2.4 Drug loading of liposomes 16
2.5 Liposome components 19
  2.5.1 Phospholipids 19
  2.5.2 Role of cholesterol 22
2.6 Characterization of liposomes 23
  2.6.1 Chemical analysis of liposomal components 25
  2.6.2 Physical characterization of liposomes 26
2.7 State of the art of liposomal formulations 29
  2.7.1 Approved liposomal formulations 29
  2.7.2 Liposomal formulations in clinical use 32
2.8 Preparation techniques of proliposomes 36
  2.8.1 Lipid film deposition method 36
  2.8.2 Fluidized bed method 36
  2.8.3 Spray drying method 37
  2.8.4 Lipid drug matrix method 40
  2.8.5 Supercritical anti-solvent method 40
  2.8.6 Lyophilization method 42
2.9 Potential routes of application of proliposomes 43

3 MATERIALS AND METHODS 47

3.1 Materials 47
  3.1.1 Active pharmaceutical ingredients 47
  3.1.2 Lipids 49
  3.1.3 Excipients and reagents 50
  3.1.4 Further materials 55
3.2 Methods 56

3.2.1 Preparation of liposomes 56
3.2.2 Preparation of proliposomes 57
3.2.3 Characterization of liposomes...60
3.2.4 Encapsulation efficiency..63
3.2.5 Release studies..64
3.2.6 HPLC analysis..64
3.2.7 Optical analysis 65
3.2.8 Characterization of dried powder samples using X-Ray diffraction 67
3.2.9 Tableting 67
3.2.10 Stability 68
3.2.11 Design of experiments approach..68
3.2.12 Scale-up production of proliposomes 68

4 RESULTS AND DISCUSSION 71

4.1 Investigation of various techniques for homogenization of liposomes manufactured with the round bottom flask method 71
4.1.1 Variation in sample treatment by filtration, ultrasonic sound and vortexing 71
4.1.2 Improvement of liposomal stability *via* pH variation.......................77
4.2 Production of proliposomes using coating methods...................................82
4.2.1 Characterization of carrier materials 82
4.2.2 Microscopic studies using polarized light microscopy and (cryo-) TEM as tool for proof of liposomes...88
4.2.3 Characterization of liposomes before and after extrusion in comparison with conventional round bottom flask method.........................92
4.2.4 Stability study of liposomal formulations 96
4.2.5 Influence of carrier material, shape and carrier-to-lipid ratio 99
4.2.6 Effect of lipid species on size and number of liposomes 101
4.2.7 Comparison of liposomal size with modified round bottom flask method 105
4.2.8 Tableting of proliposomal granules 106
4.2.9 Release studies of proliposomal formulations 113
4.2.10 Design of experiments approach..116
4.2.11 Scale-up of proliposomal preparation..123

4.3 Production of proliposomes *via* spray drying ... 127
    4.3.1 Production of microparticulated mannitol as carrier for proliposomal formulations ... 127
    4.3.2 Characterization of proliposomes and liposomes ... 132
4.4 Summary of the spray drying experiment and coating method applied 137

5 CONCLUSION / ZUSAMMENFASSUNG ... 143

6 APPENDIX ... 155

7 REFERENCES ... 159

8 CURRICULUM VITAE ... 173

9 ACKNOWLEDGEMENTS / DANKSAGUNG ... 175

1 INTRODUCTION

In 1964, the British haematologists Alec D. Bangham and R.W. Horne were the first who described the discovery of liposomal structures and published electron microscope images of multilamellar phospholipid vesicles [1]. Bangham was famous for doing research on “multilamellar smectic mesophases”. According to his surname, these vesicles were called colloquially “banghasome”. One of the first visitors in Bangham’s laboratory, Gerald Weissmann, established the term “liposomes” about 50 years ago for this kind of particles (Greek; *lipos* “fat” and *soma* “body”), defined as microscopic vesicles with one or more lipid layers [2]. Liposomes have become more and more important as drug carriers in recent years. Bulbake *et al.* list 28 liposomal formulations (status: 2017) which have reached approval phases of clinical I to III trials, others are well established products, which were approved many years ago [3, 4]. Amphotericin B (Abelcet®, Ambisome®, Amphotec®) is an example for an encapsulated active substance with reduced toxicity in liposomal dosage forms [5]. Another advantage of liposomes is the purposeful and selective accumulation or release of active ingredients *via* drug targeting. This mechanism has great importance in cancer therapy [3]. Other fields of liposomal application are diagnostics, gene transfection or cosmetics [6-8]. Liposomes are colloidal, spherical, self-closed lipid vesicles with a diameter range from 20 nm to several microns [9]. The classification is based on composition or size [10]. The basic structure is a lipid bilayer which encloses an aqueous core. The formation of the bilayer is similar to those of cell membranes, in which surfactant alike molecules mark the smallest unit with a hydrophilic head and a hydrophobic tale. Due to the structurally related amphiphilic properties, it is possible to encapsulate both, hydrophilic (in the core) and lipophilic active ingredients (in the bilayer) [11]. One drawback in the handling of liposomes is their low stability. Their tendency to hydrolysis of the phospholipids, aggregation or drug leakage often limits the shelf life of liposomal preparations [12]. One approach to avoid these shortcomings is the formation of proliposomes (PLs). Payne *et al.* were the first who reported in 1986 on PLs as dry, free-flowing granular products, which form multilamellar vesicles (MLVs) after the addition of water or after having contact with biological fluids *in vivo* [13, 14]. They had developed an alternative form of liposomes for drug delivery systems, which consisted of (i) water-soluble porous powder as a carrier and an organic solution of (ii) phospholipids as lipid phase and (iii) active pharmaceutical ingredients (APIs) which was coated on carrier. PLs have several advantages in comparison to conventional liposomes: in addition to increased encapsulation efficiency (EE) of hydrophilic substances, enhanced bioavailability or protection against degradation of the active substance in the gastrointestinal tract, also active targeting of cytotoxic substances in tumor issue could be mentioned [15, 16]. Current studies with [6]-gingerol PLs show increased bioavailability *in vivo* and an improved antitumor effect of the model substance [17]. Furthermore, PLs procedures are one of the most widely used and cost-effective methods for producing liposomes. It is easy to distribute, transfer or store PLs because of their availability as dry powder. In pharmaceutical technology, there are various techniques for preparation of PLs like fluidized bed method, coating technology, spray drying, lipid film deposition method, or supercritical anti-solvent method [18].

The aim of this work was to develop proliposomal formulations and corresponding liposomes. The focus was on a formulation suitable for large-scale production of PLs using the coating method. In addition, the spray drying process was investigated as production method. Moreover, one main topic was the development of a proliposomal formulation with good reconstitutability to generate small MLVs and a high EE. Fenofibrate and ibuprofen were selected as model drugs representing poorly soluble compounds according to Biopharmaceutics Classification System (BCS) class II.

The first part of this work presents the theoretical background of liposomes and PLs. Different classes of liposomes, preparation techniques of liposomes and PLs as well as methods applied for the characterization of liposomes are described.

The second part of this work deals with the manufacturing of liposomes *via* round bottom flask method by modifying different formulation parameters in order to investigate the resulting effect on liposomal size, polydispersity index (PDI) and zeta potential (ZP). Furthermore, the liposomal stability should be improved *via* pH variation.

The third part describes the development of PLs using the coating method. We investigated the influence of different types, surface and size of various material species (water-soluble and insoluble carrier) on liposomal size. In addition, the comparison with conventional round bottom flask method and stability studies are discussed. Microscopic studies using polarized light microscopy or cryo-transmission electron microscopy (cryo-TEM) were performed as tools for liposomes' existence. The release of fenofibrate out of proliposomal formulation was examined. The most suitable formulation of PLs containing fenofibrate was figured out *via* Design of experiments (DoE) and produced in scale-up manufacturing process. Besides, tablets containing PLs were manufactured with characterization of formed liposomes.

The second method of manufacturing of PLs was spray drying. Microparticulated mannitol was produced varying different parameters for the spray drying process as core carriers of PLs preparation. The spray dried PLs size were characterized as well as the liposomes with regard to used lipids and particle size of the carriers.

At the end of this work, the overall and integral conclusion of the coating method and spray drying process with a closer look on future perspectives is outlined.

2 THEORETICAL BACKGROUND

2.1 Classification of liposomes

Liposomes are spherical, self-closed colloidal particles with a diameter range from 20 nm to several microns, typically consisting of phospholipids and cholesterol. They are formed by one or several concentric bimolecular layers in the form of vesicles. **Figure 1** shows the structure of one bilayer with the polar head groups of phospholipids directed to the aqueous phase and two hydrophobic chains. Hydrophilic substances (for example doxorubicin hydrochloride in Doxil®/Caelyx® [19]) are encapsulated in the aqueous core whereas hydrophobic components are located between the hydrophobic chains of the bilayer.

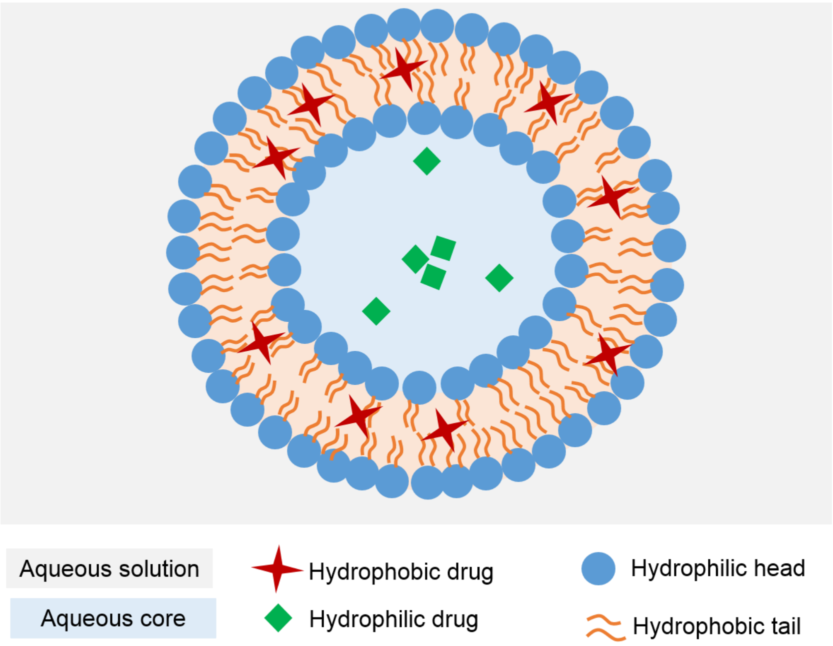

Figure 1: Liposome vesicle bilayer with encapsulated hydrophilic and hydrophobic substances. The figure is adapted from [20].

The size of the vesicles determines circulation half-life of liposomes and influences, next to the number of bilayers, the EE of drugs within liposomes. Depending on size and structure, liposomes are categorized in different classes which are summarized in **Table 1** [3, 21].

Table 1: Overview of different liposomal types. The size can range from 20 nm to about several micrometers. The vesicles can vary in shape.

Type of liposomes		Size range	Schematic drawing
MLV	Multilamellar vesicle	500 nm - 5000 nm	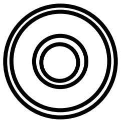
MVV	Multivesicular vesicle	> 1000 nm to several µm	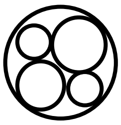
GUV	Giant unilamellar vesicle	> 1000 nm	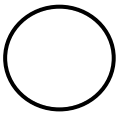
OLV	Oligolamellar vesicle	100 nm - 500 nm	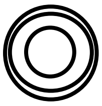
LUV	Large unilamellar vesicle	200 nm - 800 nm	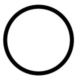
SUV	Small unilamellar vesicle	20 nm - 100 nm	

Besides these ”simple” types of vesicles, liposomes can be classified in terms of composition and mechanism of intracellular delivery [9]:

A) Conventional liposomes can be negatively charged or be without charge. They can contain cholesterol and have no surface modification. A schematic structural overview is shown in **Figure 2**. The density of charge on the surface can influence the mechanism and extent of liposome-cell interactions. Straubinger *et al.* have shown that negatively charged liposomes are absorbed in cells by coated-pit endocytose [22]. A liposomal drug release based on the pH-value is achieved using pH-sensitive liposomes. These are stable at physiological conditions (pH 7.4) but release the aqueous content under acidic conditions because of destabilization and the adoption of fusogenic properties [23]. Their structure can be equated with that of conventional liposomes.

B) Liposomes carrying antibodies attached to their surfaces are referred to as immunoliposomes. They are able to allow active tissue targeting through binding to tumor cell-specific receptors. The use of such generally speaking monoclonal antibody modified liposomes ranges from specific drug delivery to cancer cells to gene therapy or to molecular imaging [24]. The existence of two binding sites (antigen-binding fragments, Fab) on the molecule can be advantageous.

C) Long-circulating liposomes (PEGylated liposomes, stealth liposomes) contain a modified surface that is grafted with poly(ethylene glycol) (PEG) or other polymers (for example glucuronide derivatives or monosialoganglioside GM1) resulting in a longer circulation time up to several hours in the blood while reducing mononuclear phagocyte system (MPS) uptake. This modification prevents the entrapment of liposomes in the RES when their targets are tumor tissues and leads to a passive accumulation in the target tissue by reason of extravasation through the leaking vascular system of the cells [10, 25]. Since small liposomes tend to be retained in the blood without degradation, reticuloendothelial system (RES) targeting *via* liposomes is easily achieved.

D) Theranostic liposomes are nanoparticles which combine therapeutic and diagnostic tools. A typical theranostic system would contain a nanoparticle, a targeting element, an imaging component and a therapeutic compound [26]. Many studies have shown effective diagnostic imaging and therapeutic delivery of encapsulated drugs *in vivo*, especially in various forms of cancer [27, 28].

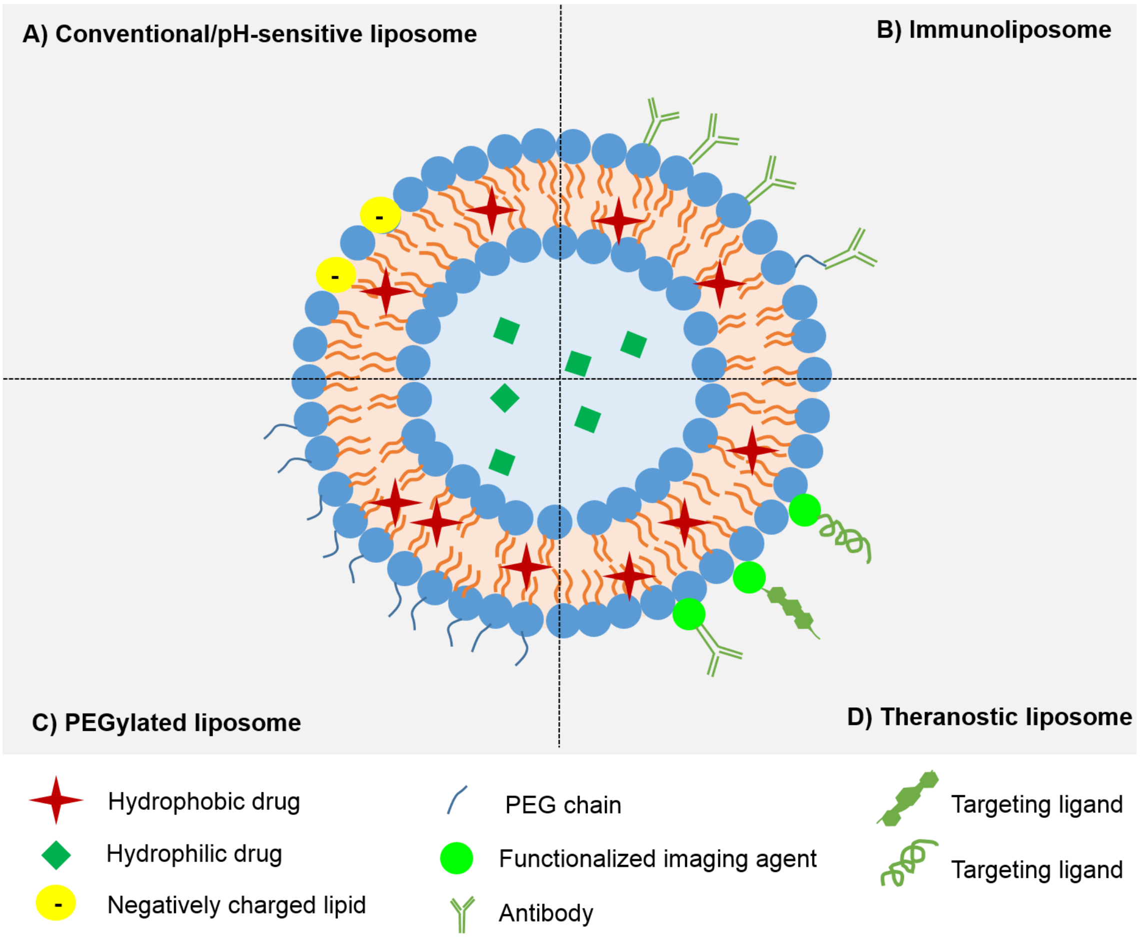
A) Conventional/pH-sensitive liposome
B) Immunoliposome
C) PEGylated liposome
D) Theranostic liposome
Hydrophobic drug
Hydrophilic drug
-
Negatively charged lipid
PEG chain
Functionalized imaging agent
Antibody
Targeting ligand
Targeting ligand

Figure 2: Schematic overview of different liposomal drug delivery systems adapted from [26]. A) Conventional/pH-sensitive liposome; B) Immunoliposome; C) PEGylated liposome; D) Theranostic liposome.

2.2 Classical preparation techniques of liposomes

Thin film hydration

Thin film hydration (round bottom flask method or hand shaken method) is the most widely used preparation method for the production of liposomes. Bangham *et al.* were the first who described this well-established technique in 1965 [29]. Here, the lipids were dissolved with or without drug in an organic solvent which is removed under reduced pressure by a rotary evaporator. The lipid film is hydrated adding an aqueous solution. The lamellae swell and grow into thin lipid tubules but are not detached from the wall of the round bottom flask. Only mechanical agitation (*e.g.* shaking, swirling, vortexing or pipetting) results in broken lipid tubules and the exposed hydrophobic edges are closed. This leads to the formation of MLVs [30].

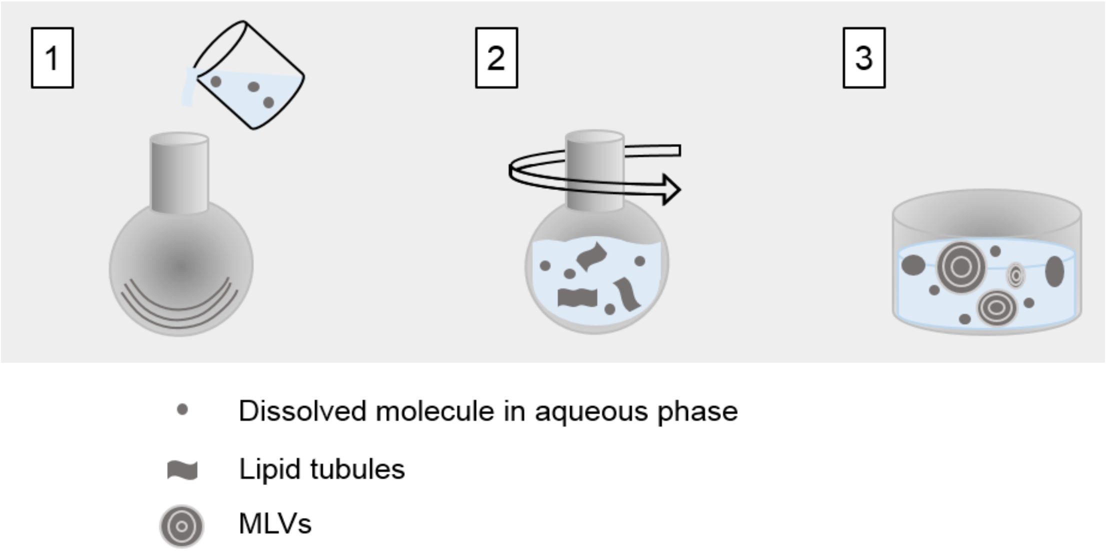

Figure 3: Schematic overview of the three MLVs' formation stages using hand shaken methods.
1: Addition of an aqueous phase to a dried thin lipid film; 2: Swelling and peeling of the lipid film under vigorous agitation; 3: Milky suspension of equilibrated MLVs. The figure is adapted from [30].

Solvent dispersion methods

Liposomes produced by reverse-phase evaporation (REV) consist of a large internal aqueous space and show a high EE. This special technique was introduced by Szoka and Papahadjopoulos in 1978 [31]. Inverted micelles are formed, *i.e.* small water droplets are stabilized by a phospholipid monolayer and dispersed in an excess of organic solvent. Such micelles are produced upon sonication of a mixture of an aqueous buffer (containing the water soluble molecules for the encapsulation) and an organic phase (solubilizing the amphiphilic phospholipids). The organic solvent is removed slowly under reduced pressure while inverted micelles are transformed into the viscous state and a certain gel state. At a critical point, the gel collapses and some of the inverted micelles disintegrate. The phospholipids' excess results in the formation of generally speaking unilamellar vesicles [30, 32, 33].

Batzri and Korn were the first who established the ethanol injection method [34]. Lipids were dissolved in ethanol and injected in a huge excess of buffer forming a characteristic opalescence of colloidal dispersion. On the one hand, the method is rapid and chemical degradation of the lipids is avoided [35]. On the other hand, the technique results in a heterogeneous size distribution, liposomes are very dilute and the removal of the alcohol is not easy to handle, since ethanol forms an azeotropic mixture with water. The low amounts of ethanol can as a result cause the inactivation of biologically active macromolecules [32, 34].

Another technique which is based on injection of an organic phospholipid solution (diethyl ether or ether-methanol mixture) into an aqueous solution is the so-called ether injection (solvent vaporization) method. The procedure temperature is about 55 °C to 65 °C whereas the pressure is reduced. This results in a removal of the solvent (ether). The heterogeneity of the vesicle size distribution and the exposure of high temperature are the limiting factors of this technique [36, 37].

Detergent depletion

The detergent depletion is a very mild treatment of producing liposomes achieved by (i) dilution, (ii) gel filtration, (iii) absorption or (iv) dialysis [38, 39]. After complete removal of the detergents, a mixture of micelles forms homogenously shaped liposomes [30]. Schurtenberger *et al.* described an increase in micellar size and polydispersity after dilution of the aqueous micellar solution. Since the system is diluted beyond the mixed micellar phase boundary, a spontaneous transformation from polydisperse micelles to monodisperse vesicles occurs which is followed by dialysis [40]. Gel filtration is used in the studies of Brunner *et al.* as detergent removal technique. Adding sodium cholate to a dispersion of lecithin in water results in the formation of small mixed micelles. The micellar solution is given on a Sephadex column. The micelles are finally separated from the low molecular weight (MW) substances including detergent monomers by percolation [41]. Quantitative selective adsorption was first described by Holloway [42]. The mixed micelle solution is shaken or twirled with beaded organic polystyrene detergent adsorbers (Bio-Beads SM2 or XAD-2 beads) or inorganic materials (zeolithes). This technique allows the removal of detergents with low critical micelle concentration (CMC) values *i.e.* not only monomers like dialysis or gel filtration. However, lipids are not adsorbed [30].

Freeze-dried rehydration

Freeze-drying is chosen as method for dehydration to obtain freeze-dried rehydration vesicles (FRVs) (**Figure 4**). Preformed vesicles were lyophilized bringing the lipid bilayers and the API into close contact. Therefore, a high entrapment efficiency can be achieved during rehydration which must be done carefully in order to rehydrate the liposomes. Small portions of the aqueous phase are pipetted successively on the sample immediately after disconnecting the flask from the lyophilizer. In general, the total rehydration volume must be smaller than the starting volume of liposomal dispersion [30]. This type of dehydration-rehydration vesicles was developed by Kirby and Gregoriadis [43].

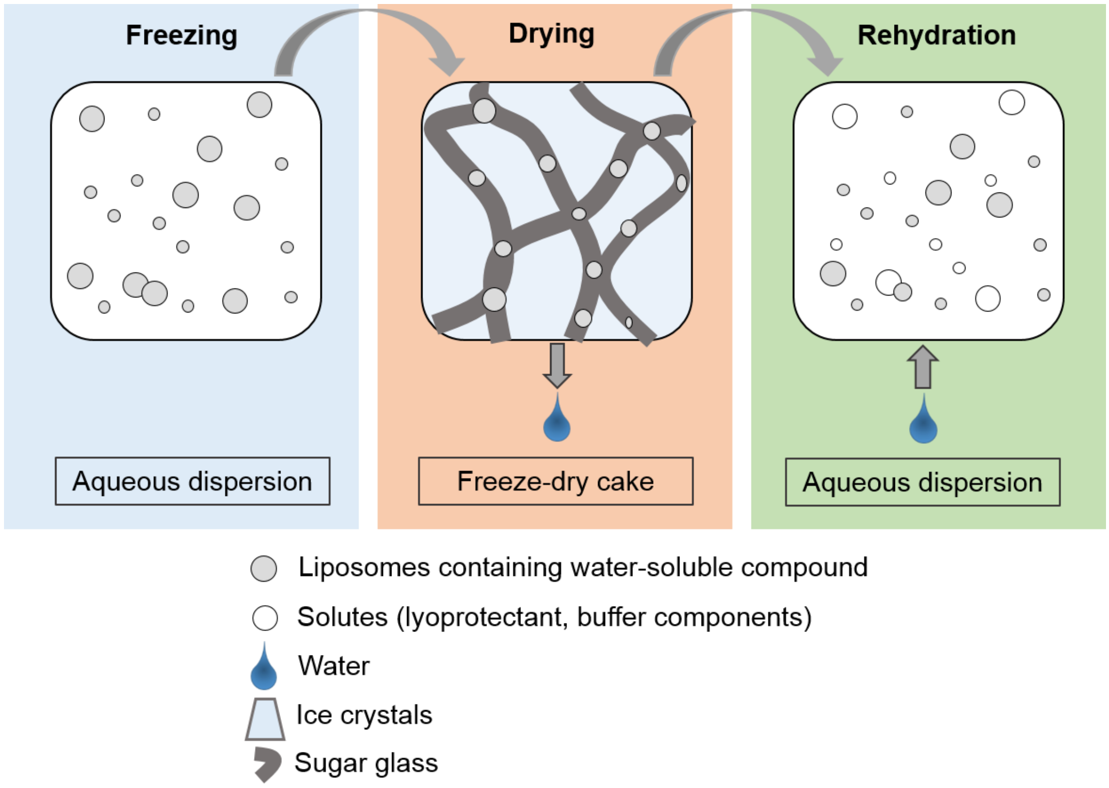
Freezing
Drying
Rehydration
Aqueous dispersion
Freeze-dry cake
Aqueous dispersion
Liposomes containing water-soluble compound
Solutes (lyoprotectant, buffer components)
Water
Ice crystals
Sugar glass

Figure 4: Formation of FRVs. During freezing ice crystals are formed with a concentrate of the remaining solutes (lyoprotectants like disaccharides) and the liposomes. Lyoprotectants effect the glass formation and interact with the phospholipids. In the second step, drying, the ice is being sublimated and the water content in the amorphous, porous structure is being reduced. The sugar glass serves as a protectant for the liposomes against damage by crystal formation and fusion processes [30].

2.3 Techniques to control liposomal size and size distribution

The major reason for homogenization of liposomes is size reduction and the achievement of a narrow size distribution. Additionally, there can also be mentioned that the macroscopic appearance of a preparation can be improved by this technique or the physical stability in terms of sedimentation or floating is enhanced [30]. This chapter discusses various techniques to control liposomal size.

Sonication

One simple, timesaving method to reduce vesicle size is the sonication of liposomal dispersions. It is not necessary to increase the temperature of the sample above the phase transition temperature (T_m) because the acoustic energy results in local heating and high-energy input. The induced pressure burst the larger MLVs which can be either unilamellar or multilamellar in composition [44]. The sonication time plays a major role in size determination of the liposomes. The smallest radius described for phosphatidylcholine (PC) vesicles, independent of the phospholipid hydrocarbon chain length, is in the range of 10.25 ± 0.55 nm [45]. There are two techniques for sonication: the first one uses a sonication tip which is directly immersed into the liposomal dispersion [46]. The disadvantage of this method is the existence of tip material (*i.e.* metal particles) in the sample which has to be removed by centrifugation afterwards. [47].The other possibility is the direct contact of a tube or beaker with dispersion into a bath sonicater [44, 48].

Membrane extrusion

Extrusion is a reproducible process for preparing monodisperse unilamellar liposomes which shows substantially increased EE [49-54]. In general, a lipid suspension is pushed several times through a polycarbonate membrane with a defined pore size. Due to shear forces it is possible to generate small unilamellar vesicles (SUVs) from preformed MLVs. There is no need to remove organic solvents or detergents from the final products. Many different kind of lipid species and mixtures are suitable for extrusion [55, 56]. Olson *et al.* described extrusion of the liposomal dispersion through a 0.2 µm membrane which results in a homogenous size distribution with a vesicle mean diameter of 0.27 µm [57]. Ong *et al.* also reported an increase in vesicle sizes compared to the pore sizes of less than 0.2 µm. The reverse effect is shown with bigger pores (0.2 µm and above) which results in a mean diameter of liposomal sizes smaller than that of the membranes [58]. This phenomenon can be elucidated *via* the elastic behavior of liposomes [59]. The chosen temperature of the liposomal dispersion has to be above T_m. Apart from that, the polycarbonate membrane breaks up. However, membrane extrusion technique is limited to small batch sizes.

High pressure homogenization

Homogenizers can be used for (i) transferring blends of solid lipid and buffer into SUVs (one-step method) [60], (ii) homogenizing preparations during injection of organic lipid solutions into the aqueous phase [61] or, of course, (iii) homogenizing preformed liposomes (MLVs) [62]. There are different types among the homogenizers depending on geometry of interaction devices. Torchilin and Weissig distinguish between three categories [30]:

- High pressure machines with a ring-shaped gap valve *e.g.* French Pressure Cell; **Figure 5 A** [47, 63]:

  The press uses an external hydraulic pump to drive a piston in a larger cylinder containing the aqueous suspension of lipid. After that, the sample is forced under high pressure (up to 275 and 138 MPa, respectively, depending on setup) through a needle valve. The throughput is up to 11.4 ml*min^{-1} and a volume of 3.7 and 35 ml, respectively can be used as batch size. The liquid is exposed to shear stress and decompression resulting in homogenization of the vesicles. The main components of a French Pressure Cell are made of stainless steel to avoid contamination of the samples [30].
- High pressure machines with an interaction chamber where two fluid streams collide *e.g.* Microfluidizer M110; **Figure 5 B** [64]:

  The pump feeds the liposomal dispersion through the micro-channels within the interaction chamber. By increasing the speed of the product flow, high shear and impact forces are created. This results in homogenous vesicles in size and shape. The product exits the interaction chamber and can be recycled for additional processing [65].

- High shear mixers like Ultra-Turrax® [66]:

  This technology is based on the rotor-stator principle. Here, the rotor is moved at high peripheral speed (*e.g.* 5000 rpm for 15 min at 21 °C). The rotation produces suction, which sucks the medium into the rotor and presses it outwards through the teeth of the stator. Therefore, this high shear process treatment leads to vesicles of preferable small sizes.

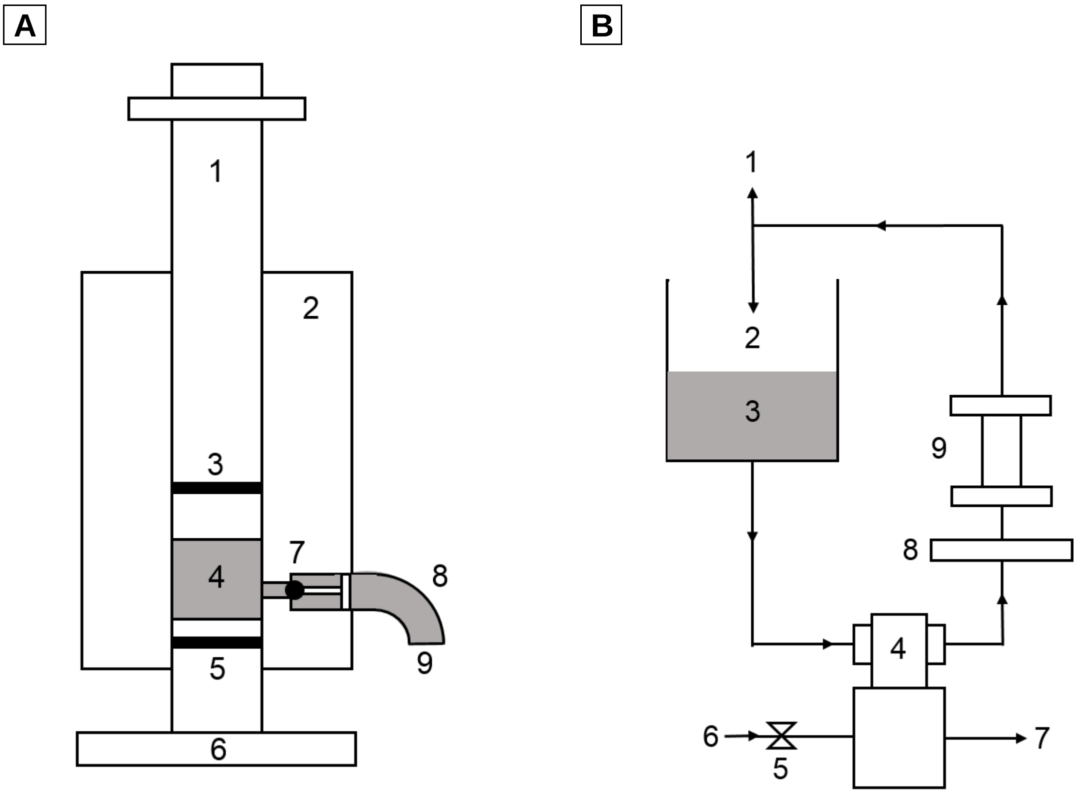

Figure 5: Schematic drawing of (**A**) French Pressure Cell and (**B**) Microfluidizer M110 modified from [67, 68]:
(**A**): (1) piston; (2) cell-body; (3), rubber O-ring; (4) sample compartment; (5) rubber O-ring; (6) closure plug; (7) nylon ball; (8) pressure relief valve; (9) outlet.
B: (1) product exit; (2) product recycle; (3), sample reservoir; (4) pump; (5) regulator; (6) air in; (7) air out; (8) filter; (9) interaction chamber.

2.4 Drug loading of liposomes

A major challenge for all encapsulation methods of active compounds is to improve the EE of drugs in vesicular forms. Hydrophilic drugs with a logP value smaller than 1.7 can be incorporated inside aqueous vacuoles. However, lipophilic substances (logP > 5) have to be encapsulated in the outer part of the vesicle, the lipid bilayer. Passive and active trapping are the two common methods to promote drug loading into liposomes.

Hydrophilic substances like antibiotics, proteins and sugars are entrapped in the core during liposome formation *via* passive drug loading [69]. This can be achieved by (i) mechanical dispersion methods like sonication or homogenization (see chapter **2.3**), (ii) solvent dispersion methods like ether/ethanol injection or (iii) detergent removal methods (see chapter **2.2**) [32]. Due to the larger internal volume, large unilamellar vesicles (LUVs) and MLVs can encapsulate more API in comparison to SUVs. Nevertheless, the MLVs' EE is limited by tight packing of the concentric lamellae and the small aqueous space between them. In summary, the passive drug encapsulation technique shows rather low EE, a relatively high loss rate due to non-encapsulated drug, as well as rapid *in vivo* drug leakage of bilayer-permeable drug-species [20].

The lipid bilayer is a natural barrier for charged, ionized molecules, whereas non-charged, lipophilic molecules can pass through. Using active drug loading, *i.e.* after vesicle formation it is possible to overcome this drawback. The two following procedures deal with active loading techniques of drugs into liposomes.

Remote loading procedure

The remote loading procedure, also known as pH gradient method, describes the drug loading using a pH gradient (inside acidic) and potential difference across the liposomal membrane ($\Delta\psi$) [70]. Creating an uptake in response to the pH value is achieved by the production of liposomes at acidic conditions with a pH value of about 4 (*e.g.* sodium citrate) and the subsequent adjustment of the external pH to a value of 7 or higher (**Figure 6**). Thereby, the equilibrium between the non-charged, neutral penetrating base (B_{out}) and the charged component (BH^+) is shifted to the non-charged molecule. The base diffuses through the bilayer ($B_{out} \rightarrow B_{in}$) by following the concentration gradient. Inside the liposomes, the protonation of the base occurs due to the low pH value. In consequence, the concentration gradient is maintained over the bilayer, since the concentration of the non-protonated form is constantly kept low inside the vesicles [71, 72]. It is important, that the process temperature is above T_m while performing the pH gradient method [73].

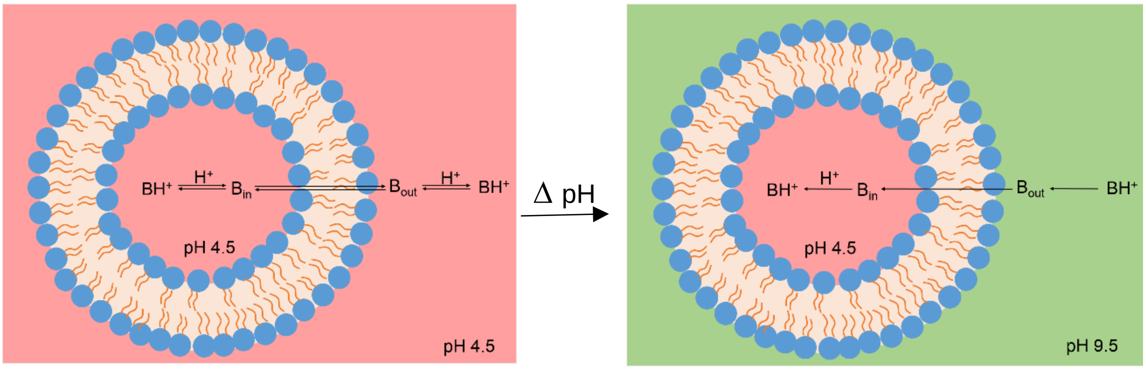

Figure 6: Entrapping of a water soluble base (B) by pH gradient method, adapted from [72].

The antibiotic drug daunorubicin which has basic properties by containing amine functions (logP value: 1.73; pK_a of the amine: 8.46), is encapsulated in DaunoXome®. This formulation is produced by using an ammonium sulfate ($(NH_4)_2SO_4$) method for generating the pH gradient. The counter ion sulfate (SO_4^{2-}) stabilizes the gradient due to its low membrane permeability. This results in an improved retention of the anthracycline drug due to salt formation of complexes with the SO_4^{2-}-ion. Daunorubicin accumulates within the liposomes and forms gel-like precipitates owing to the decreased limit of solubility in the presence of SO_4^{2-}-ions [74]. In consequence, the liposomes have a high shelf stability in terms of retaining the entrapped drug. **Figure 7** represents the process occurring during drug loading using the $(NH_4)_2SO_4$ method [75].

The calcium acetate procedure is based on the same principle. Due to different permeability coefficients, the calcium ions remain inside the liposomes and acetic acid molecules behave as proton shuttles. This leads to a pH gradient for entrapping weak amphiphilic, acidic molecules [76]. Another possibility for loading liposomes depending on pH gradients is the use of ionophores like potassium (K^+) [77]. Bally *et al.* described the accumulation of safranin and other active lipophilic cations in response to a K^+ diffusion potential (interior negative) across the large unilamellar vesicle membrane [78].

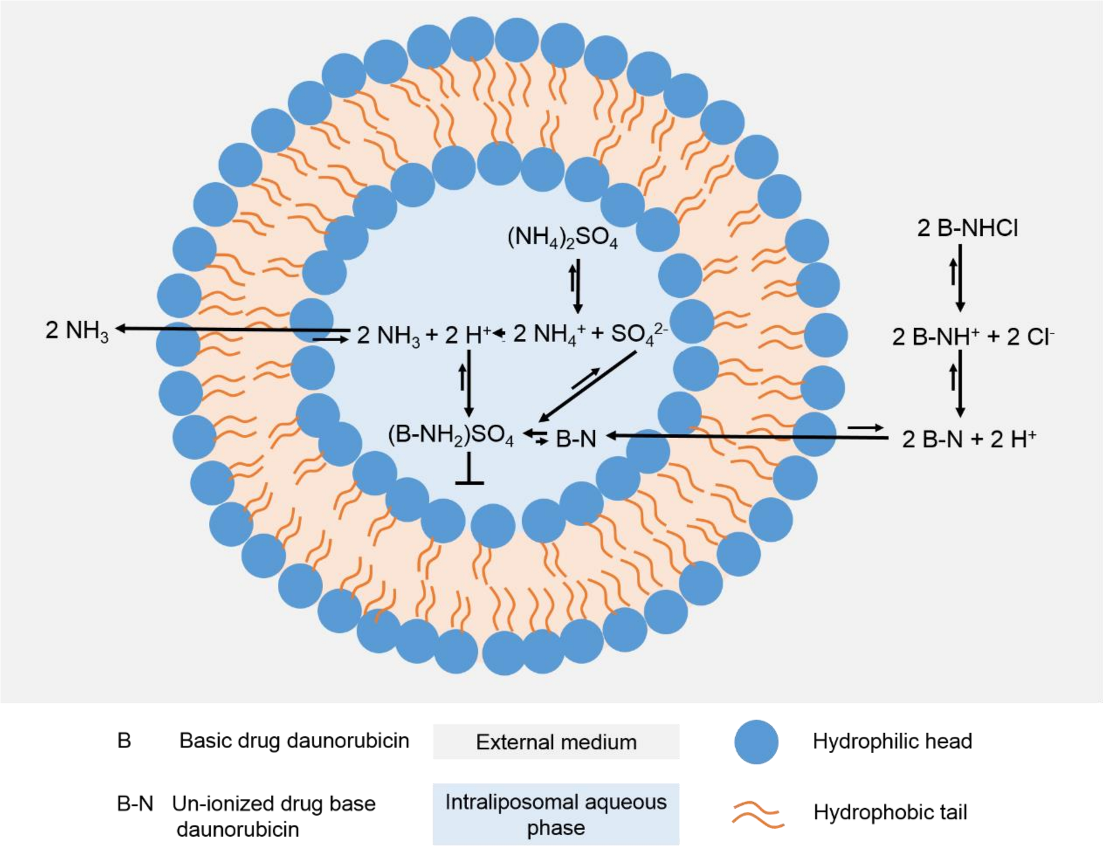
$(NH_4)_2SO_4$
$2\ NH_3$
$2\ NH_3 + 2\ H^+ \leftarrow 2\ NH_4^+ + SO_4^{2-}$
$(B\text{-}NH_2)SO_4$
B-N
2 B-NHCl
$2\ B\text{-}NH^+ + 2\ Cl^-$
$2\ B\text{-}N + 2\ H^+$
B
Basic drug daunorubicin
B-N
Un-ionized drug base daunorubicin
External medium
Intraliposomal aqueous phase
Hydrophilic head
Hydrophobic tail

Figure 7: Remote loading of amphipathic weak bases like daunorubicin (B) into liposomes using an ammonium sulfate ($(NH_4)_2SO_4$) gradient. The concentration of $(NH_4)_2SO_4$ in the liposomes is 1000-fold bigger compared to the extraliposomal medium. The entrapment occurs because of un-ionized drug base's (B-N) ionization and formation with the intra-liposomal counter ion sulfate (SO_4^{2-}). Schematic overview adapted from [75].

Freeze-thawing-technique

This method uses a sequence of rapidly freezing and slowly thawing processes for a liposomal suspension [32]. Here, the distance between the liposomal layers increases because of ice crystal growth which leads to formations of lacunas. As a result, better drug permeation is feasible and the liposomal volume increases. LUVs are created because of the fusion of SUVs [20]. The resulting EE is in a range of 25 to 30 % [79]. The rest of the drug solution is outside the vesicles and has to be removed *via* dialysis, for example. The disadvantage of this technique is a high drug loss and suboptimal lipid-to-drug ratios.

2.5 Liposome components

2.5.1 Phospholipids

As main component of cell membranes, phospholipids have the characteristics of good biocompatibility and amphiphilicity. Due to the latter property, they have emulsifying, wetting and self-assembling characteristics. Phospholipids, for example, can stabilize emulsions [80], enhance the hydrophilicity of hydrophobic drugs because of their surface-active wetting properties coating them on the surface of microcrystals [81], and form liposomes as drug carrier systems [82]. Phospholipids consist of two hydrophobic, non-polar fatty acyl chain tails and a hydrophilic, polar phosphorus head which are linked to alcohol. According to the type of alcohols, they can be classified into two types: glycerophospholipids (glycerol molecule) and sphingomyelins (sphingosine molecule). Glycerophospholipids differ in the head group, length and saturation of hydrophobic fatty acid side chains, the type of bonding between the aliphatic parts and glycerol backbone, and the number of aliphatic chains (**Figure 8**). The head group can vary (abbreviated with ‘R’) and is a differentiator between phospholipids. **Table 2** summarizes the different chemical structures of glycerophospholipids [83].

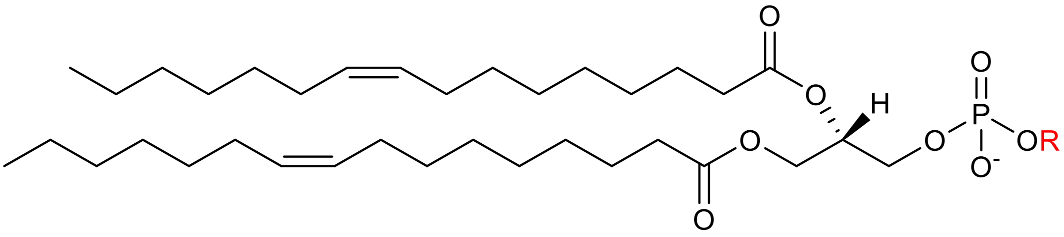

Figure 8: Chemical structure of an ester glycerophospholipid with two palmitoleic acid as fatty acid chains with a variable rest ‘R’.

Table 2: Overview of the commonly used structural formulas of phospholipids. 'R' marks the different relevant head groups [84]. R_1 and R_2 in the structural formula of cardiolipin (CL) can represent two fatty acid chains palmitic acid (16:0).

Phospholipid	R
Phosphatidylcholine (PC)	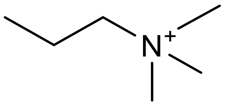
Phosphatidylethanolamine (PE)	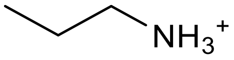
Phosphatidylserine (PS)	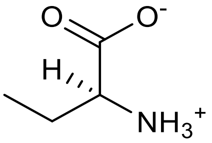
Phosphatidic acid (PA)	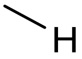
Phosphatidylinositol (PI)	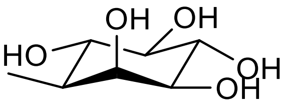
Phosphatidylglycerol (PG)	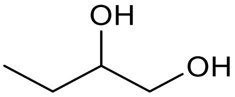
Cardiolipin (CL)	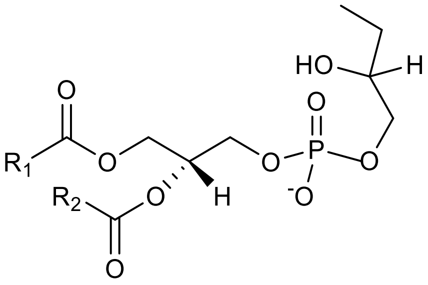

At their T_m, the phospholipids can be present in two different lipid physical states and undergo reversible, cooperative and thermotropic gel-to-liquid crystalline phase transition (**Figure 9**). The gel state is described as the ordered solid gel phase at a temperature less than the phase transition. All phospholipid hydrocarbon chains are in all-*trans* configurations. They are arranged perpendicularly to the plane of the bilayer resulting in a near ideal anisotropy of the acyl chains. The average area per phospholipid is therefore given with a value of

4.0 - 4.5 nm^2 and a maximum bilayer thickness of 5.0 - 5.5 nm [85, 86]. An increase in temperature above the T_m gives the liquid crystalline state with long-range order. The bilayer structure is preserved due to electrostatic interactions of the polar head groups of the phospholipids and hydrophobic interactions of the acyl chains. By reason of improved mobility of fatty acids, the cross-sectional area increases (6.0 – 7.0 nm^2), whereas the thickness decreases (4.0 - 4.5 nm) [85]. Consequently, the liquid crystalline state shows an increased permeability and this phase occurs in almost all biological membranes [61, 87]. Liposomes composed only of phospholipids have a low T_m and a tendency to leakage of the encapsulated drug molecules during storage. Because of this, bilayer additives like α-tocopherol or cholesterol are added to lipid formulations [88].

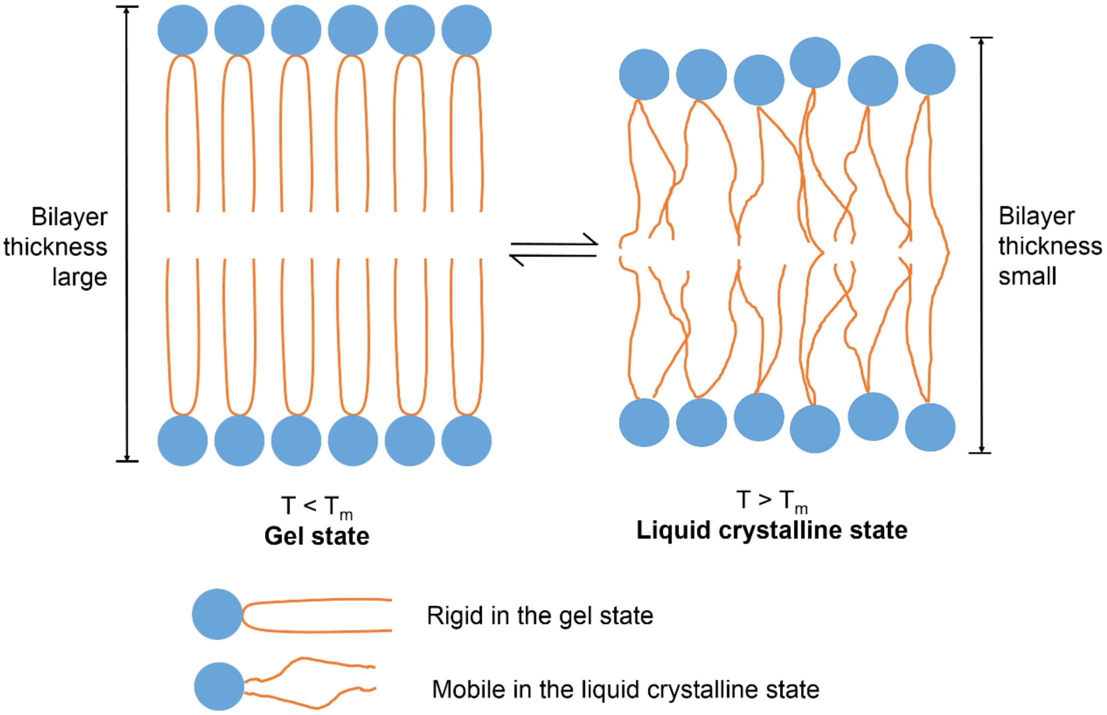
Bilayer thickness large
Bilayer thickness small
T < T$_m$
Gel state
T > T$_m$
Liquid crystalline state
Rigid in the gel state
Mobile in the liquid crystalline state

Figure 9: Schematic overview of the reversible gel-to-liquid crystalline phase transition. The drawing also shows the amphiphilic behavior *i.e.* the polar head group and the hydrophobic tail [86].

2.5.2 Role of cholesterol

Steroid cholesterol (**Figure 10**) plays a strategic role in liposomal composition and has a substantial influence on liposomal stability and on *in vitro* drug release. The content of cholesterol in liposomal formulations is an important variant in the liposomal structure which could control the stoutness [89]. When cholesterol is integrated in the bilayer phase, the hydroxyl group is placed beside the carboxyl groups of the phospholipids' ester linkages affecting the overall membrane properties. Several studies on the use of cholesterol as stabilizer show that its insertion into the membrane can (i) improve vesicle resistance to aggregation [90], (ii) reduce drug incorporation efficiency [91], (iii) create space between the fatty acid chains of the phospholipids [92] and (iv) change the fluidity of intravesicle interactions for increased stability and help to preserve the lipid bilayer structure under extreme shear stress [93]. The saturation limit for cholesterol which can be incorporated into the bilayer phase upon reconstitution is approximately 50 mol % [94, 95].

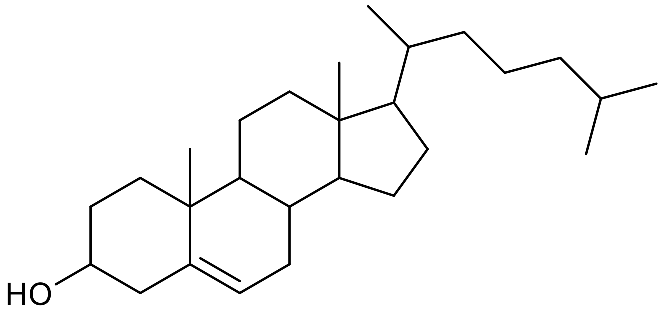

Figure 10: Chemical structure of cholesterol. The polycyclic alcohol belongs to the group of sterols, classified as lipid.

2.6 Characterization of liposomes

The *in vivo* and *in vitro* behavior of liposomes is determined by their chemical and physical characteristics. Thus, the choice and availability of suitable methods establishing these features is essential. All analyses require (i) dissolution, (ii) solubilization and (iii) extraction of the liposomal components. They need to be complete and non-selective to assay each component. Furthermore, the quality control is complex due to the supermolecular nature of the liposomal system [30]. **Table 3** summarizes various quality control assays of liposomal formulations.

Table 3: List of various aspects to be examined as quality control characteristics of liposomal formulations from development of research product to commercial product [30].

Basic characterization assays	Methodology
pH	pH meter
Osmolarity	Osmometer
Trapped volume	Measure of intra-liposomal aqueous phase
Phospholipid concentration	Lipid phosphorus content, High-performance liquid chromatography (HPLC), enzymatic assay
Phospholipid composition	Thin-layer chromatography (TLC) (combined with the Bartlett method), HPLC
Phospholipid acyl chain composition	Gas chromatography (GC)
Cholesterol concentration	Enzymatic assay, HPLC
Residual organic solvents and heavy metals	Nuclear magnetic resonance spectroscopy (NMR), GC, pharmacopeial protocols
$[H]^+$ or ion gradient before and after remote loading	Fluorescent indicators, Erythrocyte sedimentation rate (ESR) indicators, $[^{31}P]$NMR, $[^{19}F]$NMR, intra-liposomal concentration

Chemical stability	**Methodology**
Phospholipid hydrolysis	High-performance thin-layer chromatography (HPTLC), HPLC
Non-esterified fatty acid concentration	HPLC or enzymatic assay
Phospholipid acyl chain autoxidation	Conjugated dienes, lipid peroxides, thiobarbituric acid (TBA) reactive species, and fatty acid composition (GC)
Cholesterol autoxidation	TLC, HPLC
Antioxidant degradation	TLC, HPLC
Physical characterization	**Methodology**
Appearance	Pharmacopeial protocols (visual inspection)
Vesicle size distribution	
Submicron range	Dynamic light scattering (DLS), microscopy, gel extrusion chromatography, turbidimetry
Micron range	Coulter counter, light microscopy, Laser diffraction (LD) and light obscuration
Zeta potential	Electrophoretic mobility
Percentage of free drug	Gel exclusion chromatography, ion exchange chromatography, precipitation by polyelectrolyte, (ultra)centrifugation
Microbiological assays	**Methodology**
Sterility	Pharmacopeial protocols
Pyrogenicity (endotoxin level)	Pharmacopeial protocols

2.6.1 Chemical analysis of liposomal components

The Bartlett assay

The Bartlett assay defines a colorimetric determination of inorganic phosphate (PO_4^{3-}) using molybdate-containing reagents to yield a blue-colored product. First, the phospholipids are destroyed with perchloric acid to inorganic phosphate which forms phospho-molybdic acid after addition of ammonium molybdate. Phospho-molybdic acid is being reduced in the presence of 4-amino-2-naphtyl-4-sulfonic acid at 100 °C and forms a blue colored complex. The phospholipid content can be determined colorimetrically at $\lambda = 830$ nm [30, 96]. Worth and Wright described the reaction of quaternary ammonium salts or amines of lecithin or PC with phospho-molybdic acid to a water insoluble salt. It is extracted subsequently into chloroform for colorimetric determination of nitrogenous phospholipids at $\lambda = 680$ nm [97]. Another possibility of analyzing phospholipids is the complex formation with ammonium ferrothiocyanate (Stewart assay) [98].

Enzymatic reactions

Phospholipids can be hydrolyzed by the enzyme phospholipase D and thus release free choline. The free choline is oxidized to a betaine aldehyde using choline oxidase which results in the formation of betaine and hydrogen peroxide. The enzyme peroxidase mediates the oxidative coupling of phenol and 4-aminoantipyrine in the presence of generated hydrogen peroxide. A quinoneimine dye is formed and measured at $\lambda = 505$ nm [99, 100]. The enzymatic assay is also available for cholesterol determination [101].

HPLC analysis of (phospho)lipids

A disadvantage of enzymatic reactions and the Bartlett assay is that only the total lipid content can be determined and no specific composition of individual components is obtained. High-performance liquid chromatography (HPLC) analysis allows for qualitative and quantitative composition of the individual phospholipids. To perform HPLC analysis of a mixture of (phospho)lipids like PC, phosphatidylglycerol, phosphatidylethanolamine, phosphatidylserine, phosphatidic acid, sphingomyelin and cationic lipids, an amino (NH_2) phase column can be used [102, 103]. The separation is based on differences in head groups as well as on large modifications in acyl chains [30]. Oswald *et al.* developed a HPLC method as a tool for assessing targeted liposomal components. It was possible to track all compounds during each step of preparation, *e.g.* during the purification or coupling of ligands. Furthermore, the method gives evidence about the correct concentration of lipids which is important for functionalized liposomes' coupling reactions [104].

2.6.2 Physical characterization of liposomes

Size determination of liposomes

There are several techniques for the suitable determination of liposomal size and size distribution. These include types of microscopy techniques [105], size-exclusion chromatography (SEC) [106] or field-flow fractionation (FFF) [107]. The most common method is dynamic light scattering (DLS), also known as photon correlation spectroscopy (PCS) [108]. DLS determines Brownian motion of particles in solution or suspension and relates this to the size of the particles. The larger they are, the slower the Brownian motion is and *vice versa*. For calculating the size of a particle *d(H)*, the translational diffusion coefficient *D* is used in the following Stokes-Einstein equation (**Equation 1**) [109].

$$\mathrm{d(H)} = \frac{\mathrm{k} \times \mathrm{T}}{3 \times \pi \times \eta \times \mathrm{D}}$$

Equation 1

T is the absolute temperature, *η* the dynamic viscosity and *k* the Boltzmann's constant. The diameter measured is referred to as hydrodynamic diameter of a sphere, which has the same *D* as the particle. Next to the particle size, also the surface structure, the types of ions and their concentration in the medium control the diffusion speed.

Zeta potential measurements

Like size determination of liposomes, the ZP uses the same measurement principle, DLS. It is defined as the potential at the boundary of the slipping plane of an electric double layer around a charged particle, also known as the surface of hydrodynamic shear [110]. The Doppler frequency shift of the light which is scattered by the liposomes moving in an electric field, deduces the liposomal velocity. As a result, the ZP can be calculated from the electrophoretic mobility by the Henry equation:

$$U_E = \frac{2 \times \varepsilon \times z \times F \times (\kappa \times \alpha)}{3 \times \eta} \qquad \textbf{Equation 2}$$

U_E describes the electrophoretic mobility, ε is the dielectric constant, z is the ZP, η is the viscosity of the medium and the term $F \times (\kappa \times \alpha)$ is Henry's function which depends on the electric double layer thickness $\frac{1}{\kappa}$ and the particle radius α.

The ZP of liposomes plays a role in stabilizing liposomes against aggregation or fusion and in the interaction between liposomes and charged drugs. Furthermore, it has an influence on the liposomal *in vivo* behavior [30].

Determination of percentage capture

An essential parameter is the measurement of material entrapped inside liposomes. Especially for (i) long-term stability tests, (ii) initial stages of new formulation's development or (iii) new preparation technique designs, a method to quantify the fraction of liposome-associated material is necessary. In the following, three ways of determination are listed [30]:

- Leakage through phase separation:
  Lipophilic compounds may phase separate from liposomal bilayers. One possibility to determine the percentage capture is the use of light microscopy. With its use, amorphous precipitate or crystals in liposomal dispersions can be identified. Another possibility to separate liposomes and precipitate from each other is the measurement of drug content per mol phospholipid in the

supernatant after 10 - 30 sec centrifugation or the extrusion through a polycarbonate filter with pore sizes smaller than 0.1 µm.

- Leakage by membrane penetration:

  The free water-soluble compounds are estimated via ultracentrifugation followed by quantification of free drug in the supernatant. However, a potential drawback of this method is the leakage of drug during centrifugation and dilution which is often necessary. An alternative is the use of a minicolumn centrifugation method [111] and the utilization of protamine-induced aggregation of unilamellar liposomes [112, 113].

- Measurement of liposomal contents:

  The addition of liposomal dispersion to ethanol or its mixing with 10 % Triton X-100 can degrade the liposomes and release the liposomal content. Here, sufficiently clear solutions can be directly measured spectrophotometrically.

2.7 State of the art of liposomal formulations

2.7.1 Approved liposomal formulations

In 1995, Doxil® was introduced as the first successful milestone in liposome-based products to the U.S. market [114]. The formulation contains doxorubicin and HSPC, cholesterol, PEG-2000-DSPE as lipid components. It is used for the treatment of patients with ovarian cancer and AIDS-related Kaposi's sarcoma after the failure of prior systematic chemotherapy or intolerance to such therapy [115]. Besides the use in cancer therapy, medicinal products containing liposomal formulations with the indications fungal infections, pain therapy, immunotherapy and photodynamic therapy have been launched on the market since then (**Figure 11**).

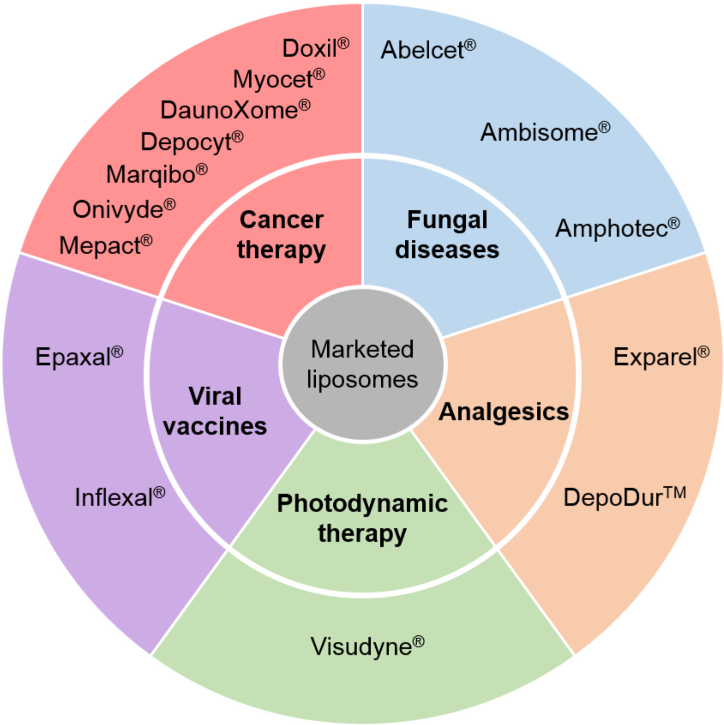
Marketed liposomes
Cancer therapy
Doxil®
Myocet®
DaunoXome®
Depocyt®
Marqibo®
Onivyde®
Mepact®
Fungal diseases
Abelcet®
Ambisome®
Amphotec®
Analgesics
Exparel®
DepoDur™
Photodynamic therapy
Visudyne®
Viral vaccines
Epaxal®
Inflexal®

Figure 11: Therapeutic areas covered by liposome-based products [115].

Table 4 summarizes 15 approved liposomal products including the year of approval, the way of application, the API, the lipid composition as well as the precise indication. Three exemplary liposomal drugs are elucidated hereafter:

Onivyde® is a product from Merrimack Pharmaceuticals and was approved in 2015. Combined with leucovorin and 5-fluorouracil, the pharmaceutical is indicated for metastatic pancreatic cancer after gemcitabine-based therapy. It is applied as a liposomal injection which forms unilamellar lipid bilayer vesicles with a mean diameter of 110 nm. The vesicles are composed of the topoisomerase inhibitor irinotecan hydrochloride and the lipids DSPC, cholesterol and MPEG-2000-DSPE [115]. As preparation procedure, a novel method described as intra-liposomal drug stabilization technology is chosen. The API is encapsulated into long circulating liposome-based nano-vesicles. Polymeric or nonpolymeric highly charged anions and intra-liposomal trapping agents *i.e.* sucrose octasulfate or polyphosphate are needed for the manufacture. The formulation has a high drug-to-lipid ratio that means more than 800 g irinotecan per mol of phospholipid. This corresponds to a final molar ratio of drug-to-phospholipid of 1.36:1 or 109 000 drug molecules per particle [116]. A randomized, open-label clinical trial NAPOLI-1 showed a survival of 6.1 months on average for patients with metastatic pancreatic adenocarcinoma whose cancer had progressed after the treatment with gemcitabine-based therapy consuming leucovorin/fluorouracil with Onivyde® [117]. Sigma-Tau Pharmaceuticals developed the sterile, preservative-free lipid complex suspension Abelcet® in 1995. Abelcet® is used to treat invasive fungal infections caused by *candida* or *aspergillus* species of patients who do not tolerate therapy with conventional amphotericin B (amphotericin B-sodium-deoxycholate complex). The liposomal formulation lowers the nephrotoxicity of the antifungal medication and consists of two lipids (DMPC/DMPG-ratio of 7:3) which form in combination with the API ribbon-like structures [115, 118]. Even though the concentration of amphotericin B is high (25 to about 50 mol % [119]), it is immediately released into the system following infusion. There are pharmacokinetic studies showing the deposition in the RES [120].

Doxil® is a nano drug delivery system based on PEG-ylated liposomal technology originally developed by Sequus Pharmaceuticals, USA. Indicated for advanced ovarian cancer, multiple myeloma and HIV-associated Kaposi’s sarcoma, the formulation is composed of phospholipids (HSPC, cholesterol, PEG 2000-DSPE) with high T_m [121]. A pilot clinical trial study on 15 cancer patients reported a 4 to 16 times higher concentration of doxorubicin in the tumor issue compared to free (unencapsulated) doxorubicin [122]. Furthermore, the cardiotoxicity, a side effect of free doxorubicin treatment, is reduced because encapsulated doxorubicin is not bioavailable at cardiac muscle cells and the myocardium [123].

Table 4: Overview of approved liposomal clinical products (in alphabetic order). The summary is taken from [115].

Product name (Approval Year)	Admin-istration	Active agent	Lipid composition	Indication
Abelcet® (1995)	Intravenous (i.v.)	Amphotericin B	DMPC, DMPG	Invasive severe fungal infections
Ambisome® (1997)	i.v.	Amphotericin B	HSPC, DSPG, cholesterol	Presumed fungal infections
Amphotec® (1996)	i.v.	Amphotericin B	Cholesteryl sulphate	Severe fungal infections
DaunoXome® (1996)	i.v.	Daunorubicin	DSPC, cholesterol	AIDS-related Kaposi's sarcoma
Depocyt® (1999)	Spinal	Cytarabine	DOPC, DPPG, cholesterol, triolein	Neoplastic meningitis
DepoDur™ (2004)	Epidural	Morphine sulfate	DOPC, DPPG, cholesterol, triolein	Pain management
Doxil® (1995)	i.v.	Doxorubicin	HSPC, cholesterol, PEG 2000-DSPE	Ovarian, breast cancer, Kaposi's sarcoma
Epaxal® (1993)	Intramuscular (i.m.)	Inactivated hepatitis A virus	DOPC, DOPE	Hepatitis A
Exparel® (2011)	i.v.	Bupivacaine	DEPC, DPPG, cholesterol, tricaprylin	Pain management
Inflexal® V (1997)	i.m.	Inactivated hemaglutinine of influenza virus strains A and B	DOPC, DOPE	Influenza
Marqibo® (2012)	i.v.	Vincristine	SM, cholesterol	Acute lymphoblastic leukemia
Mepact® (2004)	i.v.	Mifamurtide	DOPS, POPC	High-grade, resectable, non-metastatic osteosarcoma
Myocet® (2000)	i.v.	Doxorubicin	Egg PC, cholesterol	Combination therapy with cyclophosphamide in metastatic breast cancer
Onivyde® (2015)	i.v.	Irinotecan	DSPC, MPEG-2000-DSPE	Combination therapy with fluorouracil and leucovorin in metastatic adenocarcinoma of the pancreas
Visudyne® (2000)	i.v.	Verteporphin	DMPC, egg PC	Choroidal neovascularisation

2.7.2 Liposomal formulations in clinical use

Many new liposomal formulations for the management of various diseases are under phases of clinical trial investigations. **Table 5** summarizes liposomal formulations which are currently investigated in clinical trials (status 2017).

Table 5: Overview of formulations under clinical trials for phase I to III, taken from [115]. Products are listed alphabetically for each clinical phase.

Product name	Admin-istration	Active agent	Lipid composition	Indication
		Phase I		
2B3-101	i.v.	Doxorubicin	Glutathione PEGylated liposomes	Solid tumors
Alocrest	i.v.	Vinorelbine	SM/cholesterol (OPTISOME^{TM})	Breast and lung cancers
ATI-1123	i.v.	Docetaxel	Protein stabilizing liposomes (PSL^{TM})	Solid tumors
Atu027	i.v.	PKN3 Small interfering ribonucleic acid (siRNA)	AtuFECT01	Pancreatic cancer
INX-0076	i.v.	Topotecan	Cholesterol, SM	Advanced solid tumors
INX-0125	i.v.	Vinorelbine tartrate	Cholesterol, SM	Advanced solid tumors
LEM-ETU	i.v.	Mitoxantrone	DOPC, cholesterol, cardiolipin	Various cancers
LiPlaCis	i.v.	Cisplatin	The lipid composition of the LiPlasomes is tailored to be specifically sensitive to degradation by the sPLA2 enzyme	Advanced solid tumors
Liposomal Grb-2	i.v.	Antisense oligodeoxynucleotide growth factor receptor bound protein 2 (Grb-2)	Unknown	Hematologic malignancies
MCC-465	i.v.	Doxorubicin	DPPC, cholesterol, maleimidiated palmitoyl phosphatidyl ethanolamine; immunoliposomes tagged with PEG and the F(ab')2 fragment of human monoclonal antibody GAH	Metastatic stomach cancer

Product name	Admin-istration	Active agent	Lipid composition	Indication
Phase I				
MTL-CEBPA	i.v.	CEBPA siRNA	SMARTICLES® liposomal nanoparticles	Liver cancer
SGT-53	i.v.	p53 gene	Cationic lipids complexed with plasmid Deoxyribonucleic acid (DNA) encoding wild-type p53 tumor suppressor protein	Various solid tumors
TKM-080301	Hepatic intra-arterial	PLK1 siRNA	Unique lipid nanoparticle (LNP) technology (formerly referred to as stable nucleic acid-lipid particles or stable nucleic acid lipid particle (SNALP))	Neuroendocrine tumors
Phase II				
Aroplatin™	i.v.	Platinum analogue *cis*-(*trans*-R,R-1,2-diaminocyclo-hexane) bis (neodecanoato) platinum (II)	DMPC, DMPG	Metastatic colorectal cancer
Atragen	i.v.	All-*trans* retinoic acid	DMPC, soybean oil	Hormone-resistant prostate cancer, renal cell carcinoma and acute myelogenous leukemia
EndoTAG®-1	i.v.	Paclitaxel	DOTAP, DOPC	Breast and pancreatic cancers
LEP-ETU	i.v.	Paclitaxel	DOPC, cholesterol, cardiolipin	Cancer
LE-SN38	i.v.	Irinotecan’s active metabolite	DOPC, cholesterol, cardiolipin	Advanced colorectal cancer
Liposomal Annamycin	i.v.	Semi-synthetic doxorubicin analogue Annamycin	DMPC, DMPG	Relapsed or refractory acute myeloid leukemia
OSI-211	i.v.	Lurtotecan	HSPC, cholesterol	Ovarian, head and neck cancer
S-CKD602	i.v.	Potent topoisomerase I inhibitor	Phospholipids covalently bound to mPEG	Cancer
SPI-077	i.v.	Cisplatin	Soybean PC, cholesterol	Lung, head and neck cancer

Product name	Admin-istration	Active agent	Lipid composition	Indication
Phase III				
Arikace™	Aerosol delivery	Amikacin	DPPC, cholesterol	Lung infections
Lipoplatin™	i.v.	Cisplatin	DPPG, soy PC, MPEG-DSPE lipid conjugate and cholesterol	Non-small cell lung cancer
Liprostin™	i.v.	Prostaglandin E-1 (PGE-1)	Unknown	Restenosis after angioplasty
Stimuvax®	s.c.	Tecemotide	DMPG, DPPC, cholesterol	Non-small cell lung cancer
T4N5 liposomal lotion	Topical	T4 endonuclease V	Egg lecithin	Xeroderma pigmentosum
ThermoDox®	i.v.	Doxorubicin	DPPC, Myristoyl stearyl PC and DSPE-N-[amino(polyethylene glycol)-2000)	Hepatocellular carcinoma and also recurring chest wall breast cancer

Liposome-entrapped mitoxantrone Easy-to-Use (LEM-ETU) is a formulation listed under phase I trials developed by NeoPharm’s NeoLipid for the treatment of leukemia, breast, stomach, liver and ovarian cancer. It consists of the lipid components DOPC, cholesterol and CL [124, 125]. The negatively charged co-lipid cardiolipin is responsible for electrostatic interactions with the loaded moiety of the API. This phenomenon results in higher drug loading compared to other liposomal formulation [126].

DOTAP and DOPC are the ingredients of the cationic lipid complexed paclitaxel (EndoTAG®-1) which is used as vascular targeting agent [127]. The cationic liposomal vesicles interact with negatively charged endothelial cells required for tumor angiogenesis. These cells are negatively charged through lacking the glycocalix that is usually covering the endothelial cells. Paclitaxel targets the vascular cells. This results in negatively charged cells which impedes selective attachment and internalization of EndoTAG®-1. This mechanism prevents angiogenesis in the tumor and inhibits its growth. The product showed prolonged survival rates combined with gemcitabine in patients with pancreatic adenocarcinoma [115, 128].

The product Lipoplatin™ is currently under phase III trial investigations. It is a liposomal formulation that contains encapsulated cisplatin in liposome nanoparticles with an average diameter of 110 nm. Cisplatin is a DNA cross-linking agent. DPPG, soy-PC, MPEG-DSPE lipid conjugate and cholesterol are the included liposomal components of the membrane [115]. The renal toxicity, peripheral neuropathy, ototoxicity, myelotoxicity as well as nausea and asthenia were reduced under the treatment of liposomal cisplatin. Furthermore, the efficacy to cisplatin was enhanced [129]. Lipoplatin^{TM} is used in combination with gemcitabine in pretreated advanced pancreatic cancer [130]. The European Medicines Agency (EMA) authorizes orphan drug status to the latter product for this indication [115].

2.8 Preparation techniques of proliposomes

2.8.1 Lipid film deposition method

In 1986, Payne *et al.* [13] were the first who described this original method for the preparation of PLs. A film of lipid and drug is deposited onto a porous water-soluble carrier using a modified rotary evaporator. The evaporator is equipped with a mixing unit for the powder blend and a thermocouple to control the powder bed temperature. An aliquot of an organic solution (volatile) of drug and phospholipids is introduced onto the powder bed under vacuum. Thus, no overwetting occurs at any time. As soon as a free-flowing powder matrix is obtained, this procedure is repeated which is followed by a sieving step [131]. The carrier material should have a high surface area and porosity for supporting the lipids in film formation and enables high surfactant to carrier mass ratio [132]. Sorbitol [13], maltodextrin, microcrystalline cellulose (MCC), magnesium aluminum silicates or mannitol [14] are possible carrier materials.

The successive addition of the lipid drug solution results in a discontinuous process. Xu *et al.* developed a modification of the conventional lipid film deposition method dispersing the carrier material in the organic solution of drug and lipid in the flask of the rotary unit under vacuum evaporation. This led to a continuous and time saving process with a uniform lipid distribution [15].

2.8.2 Fluidized bed method

Fluidized bed method is suitable for large-scale production of PLs. The principle is based on particle coating technology which is defined by a frequent, repeated, thin application of droplets on to the presented substrate in an environment of high heat transfer (**Figure 12**) [133]. It is possible to use many different types of carrier, both crystalline powder and nonpareil beads, the latter are seal coated creating a smoother surface and smaller liposomes after hydration. The organic solution of phospholipid and drug is sprayed through a nozzle on the carrier material. By applying vacuum, the organic solvent is removed [132]. This method allows a cost-effective, well established processing and the use of different cores and coating materials.

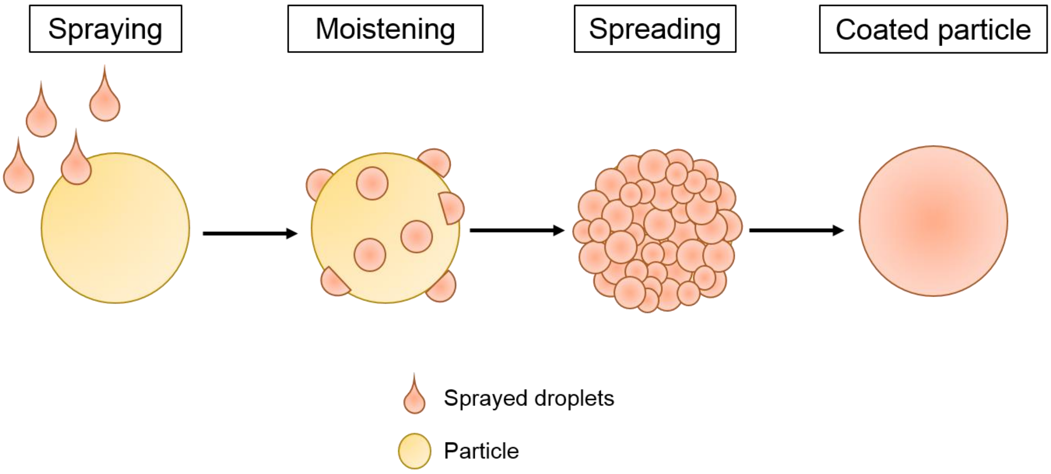

Figure 12: Principle of particle coating technology adapted from [133]. First, the coating suspension is sprayed on to the carrier and moistens it. Subsequently, the droplets are distributed on the surface of the particle and a closed film is formed.

2.8.3 Spray drying method

Spray drying process stages

Spray drying is one of the most important processes producing powders out of solutions, suspensions or emulsions. The method is not only limited to aqueous solutions, but is also applicable for non-aqueous systems like ethanol or methanol to prepare particles. Spray drying is often used to create uniform particles in size and shape. The process itself is divided into five stages [134]:

- Atomization:

  The formation of an atomization into small droplets plays an important role in the spray drying process and the suitable atomizer has to be selected carefully. Its task is to atomize the liquid formulation into fine droplets and distribute them evenly in the drying gas. There are several types of atomizers working according to different physical principles: (i) rotary atomizers (utilization of centrifugal energy), (ii) pressure nozzles (utilization of pressure energy), (iii) pneumatic nozzles (utilization of kinetic energy) and (iv) sonic nozzles (utilization of acoustic/pulsation energy).
- Spray air contact:

  The position of the atomizer in relation to the drying air flow direction determines the spray droplet-air contact. The entry of the spray and hot air in drying chambers can be controlled by different flow chamber designs: (i) ‘co-current’, (ii) ‘counter-current’ and (iii) ‘mixed flow’.

- Drying of spray:

  Spray drying is a convective drying process in which the thermal energy of a drying gas is transferred to the atomized liquid. The solvent evaporates almost simultaneously on the surface of the droplet during atomization (moisture release). Encrustation takes place and the dry particle is formed. Various shapes and structures are possible, for example solid and spherical, hollow and spherical, cenospherical or disintegrated.
- Dried product separation:

  The so-called primary discharge of product takes place at the base of the drying chamber and finer particles are separated from the drying air flow (secondary discharge) in the particulate collection system (e.g. cyclone, bag filter, electrostatic precipitator). However, total dried product discharge occurs in the particulate collection equipment.
- Dried powder handling:

  Depending on its final use, the powder can be handled according to whether it is directly packed or needs additional treatment. This can be for example post drying, product cooling, conveying, dedusting or coating.

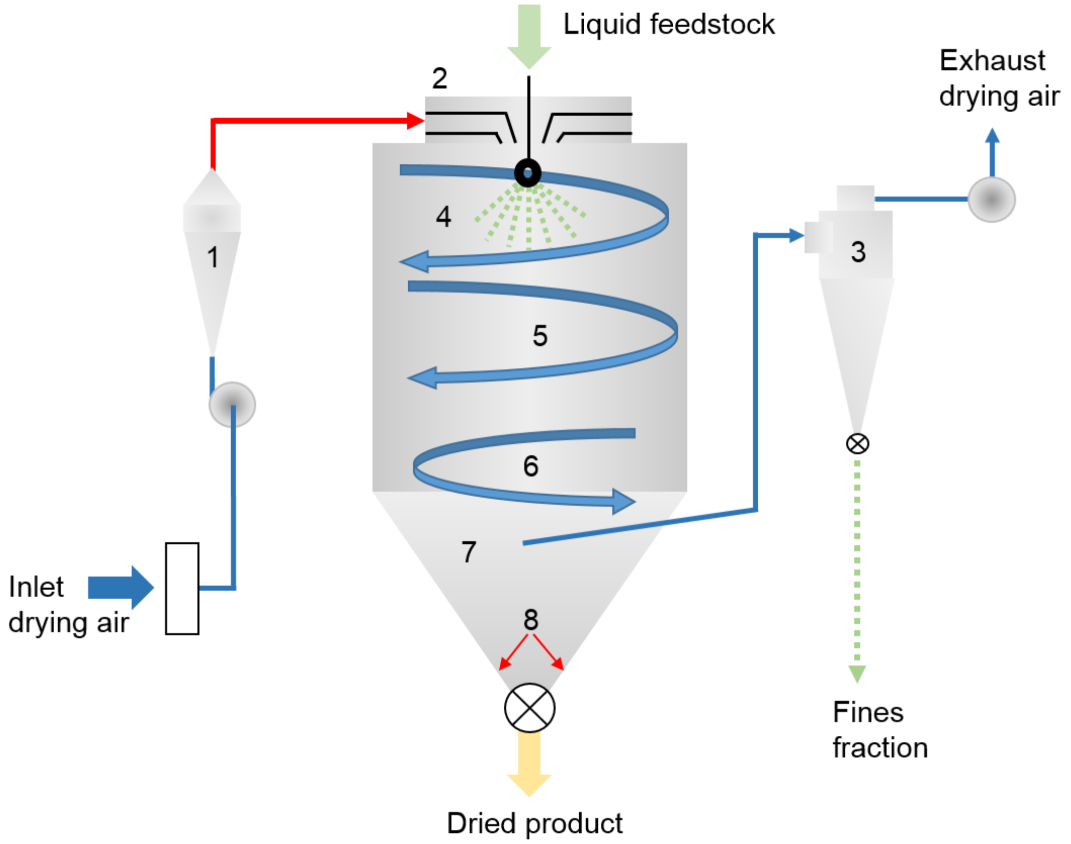

Figure 13: Schematic drawing of a basic spray dryer adapted from [134].
(1) air heater; (2) air disperser with atomizer; (3) dry particulate fines collector; (4) spray-air contact area; (5) swirling particle flow area; (6) particle separation area; (7) drying chamber; (8) powder slides down chamber wall.

Production of PLs by spray drying

For the production of PLs by spray drying, a liquid dispersion of a carrier which is suspended in a solution of the API and the lipids in an organic solvent is spray dried. Rojanarat *et al.* produced PLs *via* spray drying by using microparticulated porous mannitol powder as carrier material [135, 136]. The addition of stabilizing adjuvants like disaccharides, cyclic oligosaccharides and polyols protects the integrity of the drug and leads to an increase of the surface area of the lipids which results in an enhancement of the efficiency of hydration [137, 138]. Furthermore, the spray drying method can be easily scaled up for mass production of PLs [137, 138].

2.8.4 Lipid drug matrix method

The lipid drug matrix method was developed by Hiremath *et al.* and described the production of PLs without using a carrier material [139]. In the studies, they dissolved the drug exemestane and lipid followed by evaporation of the solvent and sieving to obtain a free flowing drug loaded proliposomal formulation. The prerequisite for this method is the solubility of all formulation components in the same solvent or solvent mixture and the subsequent removal by evaporation [140].

2.8.5 Supercritical anti-solvent method

The supercritical anti-solvent (SAS) method is widely used in the food industry because of (i) its lower residual solvents, (ii) simpler steps and (iii) mild operation temperatures [141]. It is also possible to prepare phospholipid powders [142-144] and to produce PLs [145]. For the procedure, supercritical carbon dioxide (SC-CO_2) is used which defines a fluid state of carbon dioxide (CO_2) above its critical temperature and pressure. The principle of the technique is based on bringing an organic solution in contact with SC-CO_2. During the mix of both components, SC-CO_2 is quickly dissolved in the organic solution which leads to precipitation of the dissolved substances due to antisolvent effect. Afterwards, SC-CO_2 extracts efficiently the organic solvent and enables the production of completely solvent-free products. The apparatus (**Figure 14 A**) is assembled with a sample delivery unit, a precipitation unit and a separation unit. A pump for CO_2 and another pump for the sample solution are the parts of the sample delivery unit. Additionally, the precipitation unit consists of a vessel with windows heated by an air bath. In the separation unit (including separator and wet gas meter), the organic solvent is separated from the SC-CO_2 because of lower pressure. The production procedure is as follows: CO_2 is transported from a CO_2 cylinder, cooled down by a refrigerator and subsequently pumped into a stabilization tank where CO_2 is preheated. Valve A is opened after the pressure and temperature of the view vessel reach the preset values. Meanwhile, valve C is adjusted to reach a constant pressure in the vessel. The liquid solution (*via* opened valve B) and CO_2 are sprayed in the vessel of the precipitation unit using a coaxial nozzle shown in **Figure 14 B**. The solution is sprayed through the inner tubule and CO_2 through the outside part of the nozzle. The substances dissolved in organic solvents reach supersaturation in a very short time as the solubility of the solutes in the organic solvent decreases significantly [146]. The PLs are precipitated in the vessel. When the solution is finished, valve B is closed and valve A is kept open for a few minutes to remove the residual solvent. Finally, valve A is closed while valve C is still open in order to depressurize the vessel at operating temperature. The PLs are collected on the filter at the bottom of the vessel and allow the formation of liposomal dispersion on hydration [132, 145].

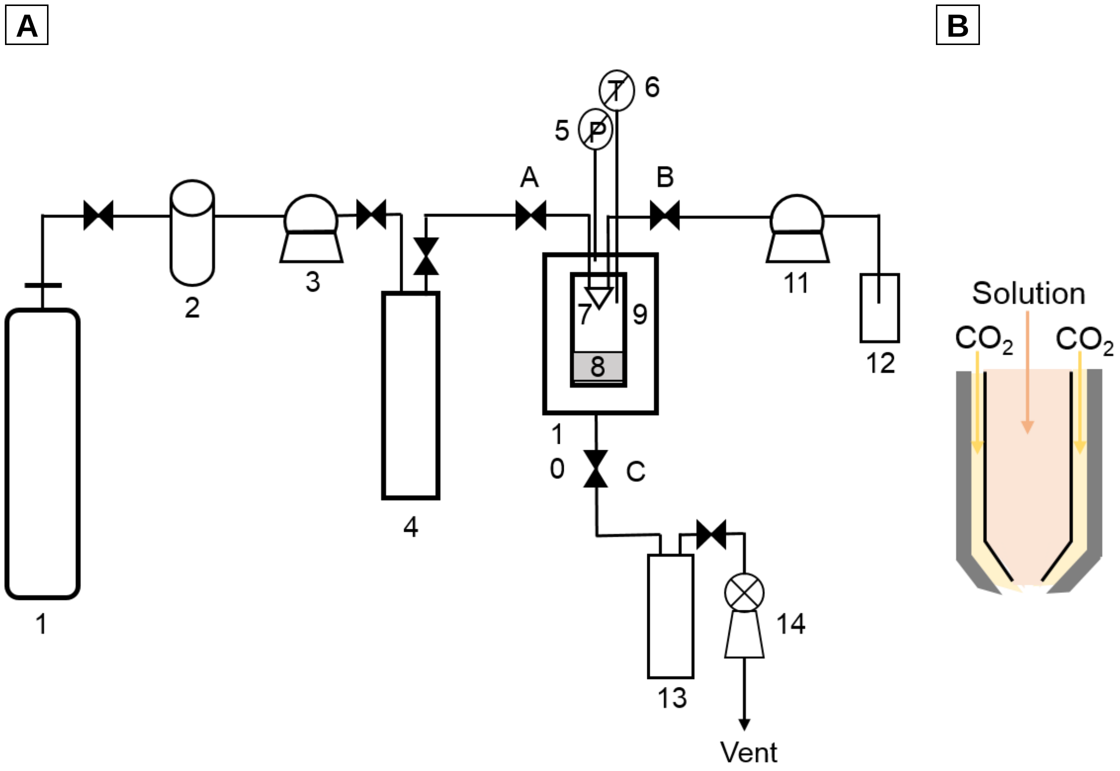

Figure 14: (**A**) Apparatus for preparing PLs by SAS method ((1) CO_2 cylinder; (2) refrigerator; (3) CO_2 pump; (4) stabilization tank; (5) pressure sensor; (6) temperature sensor; (7) nozzle; (8) filter; (9) view vessel; (10) air bath; (11) solution pump; (12) solution supply; (13) separator; (14) wet gas meter; (A) valve A; (B) valve B; (C) valve C) and (**B**) schematic drawing of coaxial nozzle, both adapted from [145].

2.8.6 Lyophilization method

Fei *et al.* reported a new type of lyophilization method to produce PLs: injection-homogenization-lyophilization method. An ethanolic solution of the drug breviscapine, lipid and surfactant was added to a solution of the cryoprotective agent mannitol and ethylenediaminetetraacetic acid (EDTA) at 37 °C. After the evaporation of ethanol, the mixture was homogenized, quickly frozen at - 20 °C and put in a freeze-drier to get a proliposomal formulation [140, 147].

2.9 Potential routes of application of proliposomes

There are various potential routes of application investigated for proliposomal formulations: (i) oral, (ii) transdermal, (iii) parenteral delivery and (iv) the application using a dry powder inhaler (DPI).

Because of the poor water solubility of APIs resulting in poor bioavailability, proliposomal oral formulations were developed to improve the bioavailability of poorly-soluble substances (for example zaleplon [14], indomethacin [148] or silymarin [149]). Vanić *et al.* developed proliposomal tablets by mixing spray dried PLs with different tableting excipients which form liposomes *in situ* during their dissolution. The system combines the possibility of encapsulating active ingredients by liposomes and increases, at the same time, the stability of the dosage form through the solid tablet formulation. In addition, it can also be used for the development of mucoadhesive delivery systems by mucoadhesive polymers, *e.g.* chitosan [150].

As major component of liposomes, phospholipids can be integrated containing skin lipids and improve the drug permeation in the skin maintaining hydration conditions. After application to mucosal membranes, liposomes formed out of PLs serve as a sustained release dosage form of the loaded drug [151]. They can vary the diffusion across the skin which results in an increased skin permeation. A study of Gupta *et al.* shows a proliposomal drug delivery system of aceclofenac eliminating side effects like gastrointestinal bleeding using transdermal way of application. The formulation contains lecithin which allows a far better permeation of the API into the skin [152]. Hwang *et al.* developed proliposomes composed of nicotine, sorbitol as carrier material and lecithin as liposome-forming lipid and evaluated the *in vitro* skin permeation of entrapped nicotine under occlusive conditions [151].

Proliposomal formulations are most suited for parenteral application than liposomes themselves because they have two significant advantages over them. First, parenteralia do not influence the intrinsic properties of liposomes during sterilization. Second, they can be stored in the sterilized solid state and hydrated directly before use [153]. If terminal sterilization *via* steam at 121 °C is chosen as sterilization method for liposomes, substantial degradation can occur due to lipid hydrolysis and the peroxidation of unsaturated lipids increases. A possible sterilization technique for the dry PLs is the γ-irradiation [154].

Rojanarat *et al.* developed a proliposomal powder containing the antibiotic isoniazid for the treatment of tuberculosis in a DPI formulation. Their studies showed no toxicity to respiratory-associated cells and no activation of alveolar macrophages to produce inflammatory cytokines or nitric oxide in amounts that could trigger a secondary inflammation. Furthermore, proliposomes containing isoniazid exhibited better antimycobacterial activity against *Mycobacterium bovis*-infected alveolar macrophages than the free drug [135].

Table 6: Overview of studies with PLs classified according to the way of application in alphabetical order [140]. The list is not exhaustive.
Definition of the color code: oral transdermal intravenous inhalative.

Drug	Lipid composition	Carrier	Method	References
Acetylsalicylic acid	Soybean lecithin, cholesterol, stearylamine	Effervescent granules	Lipid onto a carrier	[155]
Exemestane	DSPC, DMPC	-	Lipid drug matrix method	[139]
Glyburide	DSPC, egg PC, cholesterol, stearylamine	Nonpareil beads	Lipid onto a carrier	[156]
Indomethacin	Soybean lecithin, cholesterol, stearylamine	Effervescent granules	Lipid onto a carrier	[148]
Israpedine	HSPC, cholesterol	Mannitol	Lipid onto a carrier	[157]
Phenylbutazone	Soybean lecithin, cholesterol, stearylamine	Effervescent granules	Lipid onto a carrier	[155]
Progesterone	DMPC, soybean lecithin	MCC	Lipid onto a carrier	[158]
Raloxifen	HSPC, cholesterol, stearylamine, dicetyl phosphate	Mannitol	Lipid onto a carrier	[159]
Salmon calcitonin	Egg yolk PC	Sorbitol	Lipid onto a carrier	[131, 160]
Silymarin	PC	Mannitol	Lipid onto a carrier	[149]
Vinpocetine	Soybean PC, cholesterol	Sorbitol	Lipid onto a carrier	[15]

Drug	Lipid composition	Carrier	Method	References
Zaleplon	HSPC, cholesterol	Mannitol	Lipid onto a carrier	[14]
Aceclofenac	Soybean lecithin	Mannitol	Lipid onto a carrier	[152]
Nicotine	Egg lecithin	Sorbitol	Lipid onto a carrier	[151]
Adriamycin	Egg lecithin	Sorbitol	Lipid onto a carrier	[161]
Amphotericin B	DMPC, DMPG, egg lecithin, ergosterol	Sorbitol, sodium chloride	Lipid onto a carrier	[162]
Brevascapine	Egg yolk lecithin, cholesterol	Mannitol	Lyophilization	[147]
Ibuprofen	Soybean lecithin, cholesterol, stearylamine	Effervescent granules	Lipid onto a carrier	[163]
Methotrexate	Egg lecithin	Sorbitol	Lipid onto a carrier	[164]
Isoniazid	Soybean PC, cholesterol	Porous mannitol	Spray drying	[135]
Pyrazinamide	Soybean PC, cholesterol	Porous mannitol	Spray drying	[136]

3 MATERIALS AND METHODS

3.1 Materials

3.1.1 Active pharmaceutical ingredients

The APIs fenofibrate and ibuprofen are considered as class II drugs of the BCS [165]. They have low solubility and high permeability and were chosen as model substances for the formulation of pro-/liposomes.

Fenofibrate (2-[4-(4-chlorobenzoyl)phenoxy]-2-methyl-propanoic acid-1-methylethyl ester) is part of a class of amphipathic carboxylic acids, the fibrates. It is a lipid-modifying neutral prodrug of the active metabolite fenofibric acid (**Figure 15**) and used against hypercholesterolemia and hypertriglyceridemia. Fenofibrate operates as a peroxisome proliferator receptor alpha (PPARα) agonist which activates lipoprotein lipase. Furthermore, apoprotein C-III is reduced that increases lipolysis [166]. The activation of PPARα results in a reduction of triglycerides and a transportation of free fatty acid uptake, decrease in low-density lipoprotein (LDL) cholesterol and an increase in high-density lipoprotein (HDL) cholesterol concentrations [167]. The common doses of fenofibrate are 145 mg, 160 mg, 200 mg, and 250 mg (retarded).

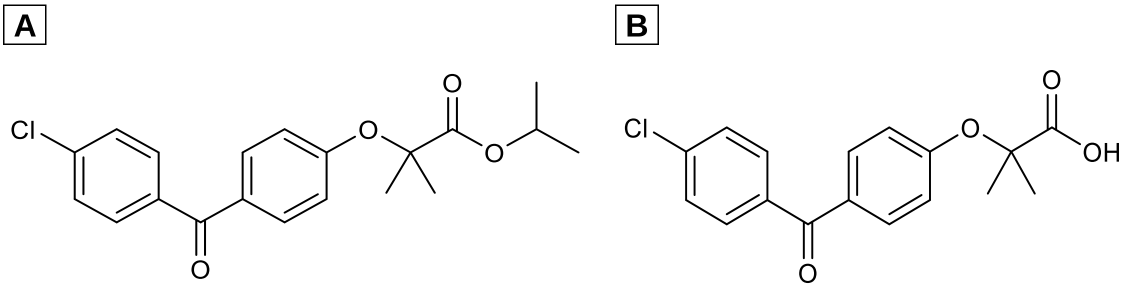

Figure 15: Chemical structure of (**A**) fenofibrate (prodrug) and (**B**) fenofibric acid (active metabolite).

Ibuprofen ((2*RS*)-1(4-(2-methylpropyl)phenyl)propanoic acid) was introduced in 1969 as a better alternative to Aspirin® [168] and is a nonsteroidal anti-inflammatory drug (NSAID) [169, 170]. This class is used for the treatment of pain, fever and inflammation [171]. It is a non-selective inhibitor of both isoforms cyclooxygenase-1 (COX-1), which is constitutively expressed and cyclooxygenase-2 (COX-2; expressed in inflamed tissue) which converts arachidonic acid to prostaglandin H_2 (PGH_2) [172, 173]. PGH_2 is converted by various cell specific isomerases and synthases to produce prostaglandins (PGD_2, PGE_2, $PGF_{2\alpha}$, PGI_2 as mediators of pain, inflammation and fever) and thromboxane A_2 (TxA_2 which stimulates platelet aggregation, leading to the formation of blood clots) [174]. Ibuprofen is supplied in common potencies of 200 to 800 mg and can be used for the following therapeutic applications: patent ductus arteriosus, rheumatoid and osteo-arthritis, cystic fibrosis, dental pain and dysmenorrhea, fever and headache [168].

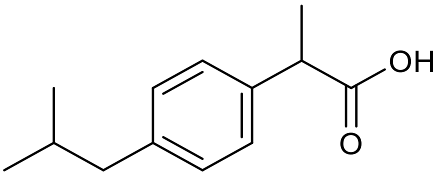

Figure 16: Structural formula of ibuprofen.

Fenofibrate and ibuprofen were commercially obtained as white, crystalline powders and used as received. The physical properties of both substances are listed in **Table 7**.

Table 7: Physical properties of fenofibrate and ibuprofen.

Property	**Value**		**Reference**	
	Fenofibrate	*Ibuprofen*		
MW	360.8 g*mol^{-1}	206.3 g*mol^{-1}	[175]	
Melting point	79-82 °C	75-78 °C	[175]	
Solubility in water	0.1 µg*ml^{-1} (25 °C)	86 µg*ml^{-1} (27 °C)	[176]	[177]
pK_a	-	4.9	-	[165]
logP	5.24	1.37 at pH = 7.4	[178]	[179]

3.1.2 Lipids

DSPC (1,2-distearoyl-*sn*-glycero-3-phosphocholine) is an uncharged lipid. It has a zwitterionic structure consisting of a monocationic trimethylammonium head group and two saturated hydrocarbon chains (18:0) as the lipophilic component of the molecule (**Figure 17**). The T_m of DSPC is 54.4 °C [180]. Most experiments in this work were performed using a mixture of DSPC-to-cholesterol in a molar ratio of 4:1. The same ratio of lipid (egg-PC based on a mixture of DMPC and DSPC) to cholesterol is used for a formulation containing ibuprofen. Investigations using environmental scanning electron microscopy (ESEM) showed an improved stability of the liposomes composed of the far mentioned lipids and increased prevention of agglomeration during hydration [91].

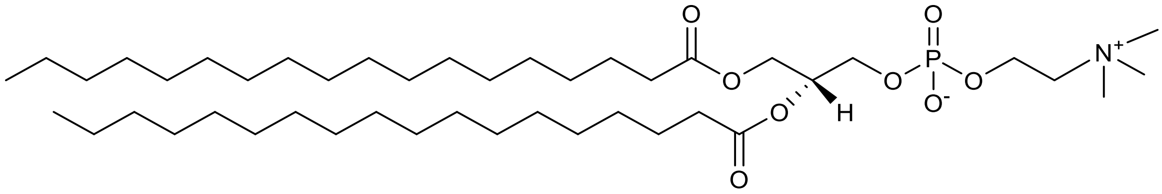

Figure 17: Chemical structure of DSPC.

DOTAP (1,2-dioleoyl-3-trimethylammonium-propane, chloride salt) is a cationic lipid. It is generally used together with a neutral helper lipid. It consists of a monocationic trimethylammonium head group and two unsaturated hydrocarbon chains, derived of oleic acid (18:1), as the lipophilic part of the molecule (**Figure 18**). The T_m is specified at $T_m < 5$ °C [181] by Regelin *et al*.

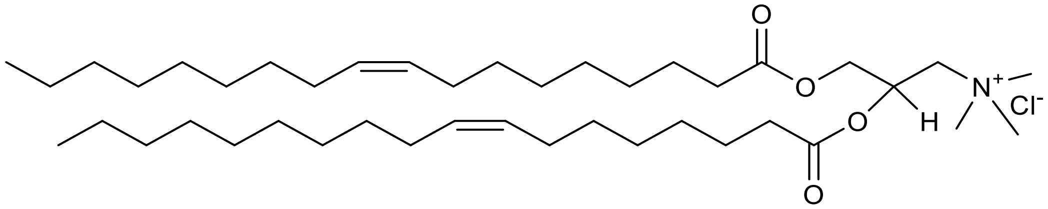

Figure 18: Chemical structure of DOTAP.

DMPG (1,2-dimyristoyl-*sn*-glycero-3-phospho-(1'-rac-glycerol); sodium salt) is an anionic phospholipid or rather PG containing saturated fatty acids (14:0) and an important component of bacterial membranes. The gel to liquid crystalline phase transition is at a temperature of 23 °C [182].

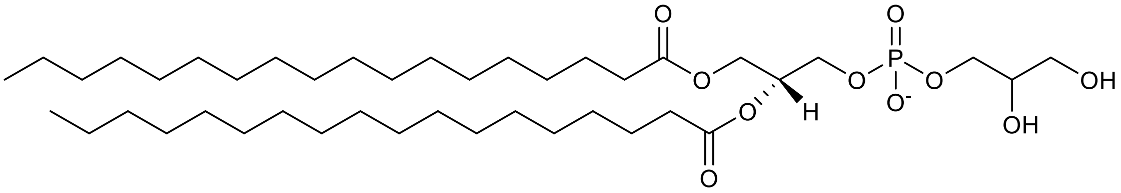

Figure 19: Chemical structure of DMPG.

Egg phosphatidylcholine (egg-PC) and hydro soy-PC (**HSPC**) belong to the group of PCs and are major components in biological membranes. The PCs used in this work derive from egg yolk and soybeans which are available at lower cost than the abovementioned phospholipids. DSPC as shown in **Figure 19** can be considered as a representative structure for the mixture of phospholipids in the natural lipids egg-PC or HSPC. The T_m of HSPC is described at approximate 53 °C and of egg-PC at - 7 °C [183, 184].

3.1.3 Excipients and reagents

Table 8 shows the used chemicals and equipment for the preparation and further processing of pro-/liposomes and the analyses performed in this work. Double distilled water from an all-glass apparatus (Destamat Bi 18 T, Heraeus Holding GmbH, Hanau, Germany) was filtered through a 0.1 µm regenerated cellulose (RC) membrane filter (Stedim Biotech S.A., Sartorius AG, Göttingen, Germany). All solutions were prepared freshly and stored in the refrigerator at 4 °C, if necessary.

Table 8: Excipients used for preparation and characterization.

Excipient/Reagent	Item number	Lot number	Supplier
Preparation of pro-/liposomes			
Chloroform	733.1	810831	Carl Roth GmbH & Co. KG, Germany
Cholesterol	8866.1	306233522	Carl Roth GmbH & Co. KG, Germany
DMPG-Na	67232-80-8	560200-2140090-01	Lipoid GmbH, Germany
DOTAP-Cl	4235-95-4	593500-2110001-01	Lipoid GmbH, Germany
DSPC	816-94-4	556500-2160333-01	Lipoid GmbH, Germany
Egg-PC (LIPOID E PC S)	97281-44-2	510800-2150090-02	Lipoid GmbH, Germany
Ethanol	9065.6	028266148	Carl Roth GmbH & Co. KG, Germany
HSPC (LIPOID S PC-3)	97281-45-3	525600-2170639-01	Lipoid GmbH, Germany
Methanol	7342.1	Various	Carl Roth GmbH & Co. KG, Germany
Encapsulated substances			
Fenofibrate	F0674	CWAPE-CC; CWAPE-EF	TCI Deutschland GmbH, Germany
Ibuprofen	5260	13105104	Caesar & Loretz GmbH, Germany

Excipient/Reagent	**Item number**	**Lot number**	**Supplier**
Spray drying excipients			
D-Mannitol	M4125	WXBB6836V	Sigma-Aldrich, Germany
Ethanol	9065.6	028266148	Carl Roth GmbH & Co. KG, Germany
α-Lactose monohydrate	61341	BCBT5292	Sigma-Aldrich, Germany
Carrier material			
Glass beads 0.1 mm	N029.1	11079101	Carl Roth GmbH & Co. KG, Germany
Globuli sacchari			
No 1 (800 – 1,600 µm)	08710	08710018	Hanns G. Werner GmbH & Co. KG, Germany
No 2 (1,250 – 2,000 µm)	08720	08720019	Hanns G. Werner GmbH & Co. KG, Germany
No 3 (1,600 – 2,400 µm)	08730	08731145	Hanns G. Werner GmbH & Co. KG, Germany
No 4 (2,000 – 2,800 µm)	08740	08740005	Hanns G. Werner GmbH & Co. KG, Germany
No 5 (2,500 – 3,300 µm)	08750	08750040	Hanns G. Werner GmbH & Co. KG, Germany
Tablettose® 80	13005001	L104314416A 552	Molkerei MEGGLE Wasserburg GmbH & Co. KG, Germany
Sucrose-Lactose Globuli (~ 1,250 µm)	08832	08832016	Hanns G. Werner GmbH & Co. KG, Germany
Transparent beads 1.5 mm	353	D630316A	Geotech International B.V., The Netherlands

Excipient/Reagent	**Item number**	**Lot number**	**Supplier**
Carrier material			
VIVAPUR® MCC Spheres			
100	9004-34-6	5110050523	JRS PHARMA GmbH & Co. KG, Germany
350	9004-34-6	5135042541	JRS PHARMA GmbH & Co. KG, Germany
1000	9004-34-6	5100050321	JRS PHARMA GmbH & Co. KG, Germany
Xylit Globuli (~ 1,250 µm)	08811	08811004	Hanns G. Werner GmbH & Co. KG, Germany
Tableting excipients			
AEROSIL® Type 200	5053	15170502	Caesar & Loretz GmbH, Germany
Magnesium stearate	2402	15305324	Caesar & Loretz GmbH, Germany
Tablettose® 80	13005001	L104314416A552	Molkerei MEGGLE Wasserburg GmbH & Co. KG, Germany
Talc Pharma G	991000	P140503682	C.H. Erbslöh GmbH & Co. KG, Germany
VIVAPUR® 301	-	6630140331	JRS PHARMA GmbH & Co. KG, Germany
VIVASOL®	74811-65-7	3201062074	JRS PHARMA GmbH & Co. KG, Germany

Excipient/Reagent	**Item number**	**Lot number**	**Supplier**
Buffer preparation			
Hydrochloric acid (1 N)	K025.1	1856117	Carl Roth GmbH & Co. KG, Germany
Potassium dihydrogen phosphate	P018.1	021164077	Carl Roth GmbH & Co. KG, Germany
Sodium hydroxide solution (1 N)	K021.1	1772394	Carl Roth GmbH & Co. KG, Germany
Laser diffraction			
Miglyol®812	3274	Various	Sigma-Aldrich, Germany
Sorbitane trioleate	3459	Various	Sigma-Aldrich, Germany
HPLC analysis			
Methanol	7342.1	Various	Carl Roth GmbH & Co. KG, Germany
Triton™ X-100	93426	BCBH2984V	Sigma-Aldrich, Germany

3.1.4 Further materials

An overview of the further materials used in this work is given in **Table 9**.

Table 9: Overview on further materials used in this work in alphabetical order.

Material	Item number	Lot number	Supplier
Al-crucibles	ME27331	-	Mettler Toledo, USA
Amicon Ultra-4 Centrifugal Filter Units (100000 NMWL)	UFC810024	R4CA41755	Merck Millipore, Germany
BRAND® counting chamber BLAUBRAND® Thoma pattern	BR718005-1EA	-	Sigma-Aldrich, Germany
Filter Supports 10 mm	610014	Various	Avanti Polar Lipids Inc., USA
Microscope Slides	0656	0754476	Carl Roth GmbH & Co. KG, Germany
Minisart® RC Syringe Filter 0.2 µm	1000005222	80299103	Sartorius AG, Germany
PC Membranes 0.1 µm	610005	Various	Avanti Polar Lipids Inc., USA
PC Membranes 0.4 µm	61007	Various	Avanti Polar Lipids Inc., USA
PC Membranes 0.8 µm	800284	145091	Avanti Polar Lipids Inc., USA
RC Membrane filter 0.2 µm	18407--47----N	-	Sartorius AG, Germany

3.2 Methods

3.2.1 Preparation of liposomes

Conventional liposomes were prepared by the round bottom flask method [59]. The lipids (DSPC-to-cholesterol in a molar ratio of 4:1) and an active ingredient (fenofibrate or ibuprofen) were weighed and dissolved in about 10 ml of ethanol. Organic solvents were removed using a rotary evaporator Heidolph VV 2000 equipped with a water bath Heidolph WB 2000 (both Heidolph Instruments GmbH, Schwabach, Germany), which was set to 65 °C. The vacuum pump Vario PC 3001 (Vacuubrand GmbH, Wertheim, Germany) was set to 300 mbar for 2 min followed by 150 mbar for another 4 min. The round bottom flask rotation speed was adjusted to 120 rpm. The lipid film was finally dried on the internal wall of the round bottom flask setting vacuum to 10 mbar for 1 h. The films were then rehydrated with an aqueous solution for 20 min in the rotating flask keeping the water bath at 65 °C. For some experiments, the carriers were added to the organic solution in the round bottom flask and enriched on the ground of the vessel.

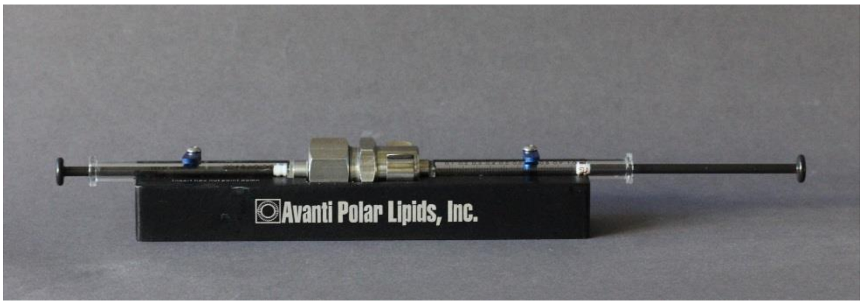

Figure 20: Avanti Mini-Extruder constructed of stainless steel and Teflon. Two polycarbonate membranes and filter supports are placed between two Teflon bearings and membrane supports. The heating block allows the extrusion of vesicles for lipids which have a transition temperature above room temperature.

The crude liposomal dispersion was extruded, in each case, 11 times through a 0.4 and afterwards a 0.1 µm polycarbonate membrane (Whatman® Nuclepore Track-Etch Membrane, Maidstone, UK) using a Mini-Extruder (**Figure 20**; Avanti Polar Lipids Inc., Alabaster, USA) to generate LUVs.

3.2.2 Preparation of proliposomes

3.2.2.1 Coating method

PLs were prepared by a coating method or modified fluidized bed method. A solution mixture of the lipids (DSPC-to-cholesterol molar ratio of 4:1) and the active ingredient fenofibrate or ibuprofen (5.36 / 10.71 / 16.07 mg*ml^{-1}) were sprayed at a controlled temperature (using a water bath; T = 55 - 65 °C) different types of carrier (**Table 8**, *Carrier material*). The solution was sprayed in several steps with a flow rate of 1 ml*min^{-1} with a peristaltic pump P-1 (Pharmacia BioTech, Uppsala, Sweden) using a 25 kHz ultrasonic nozzle (Sono-Tek Corporation, Milton, USA). The container was turned and also the carrier material was moved with a spattle to cover it all around. During coating the ethanol was removed at 55 °C. PLs were hydrated with water or phosphate buffered saline (PBS) buffer pH 7.4 (European Pharmacopeia (Ph.Eur.)) at 65 °C. In some instances, the crude liposomal dispersion was extruded subsequently, as per description in chapter **3.2.1**. PLs were stored at room temperature in the desiccator.

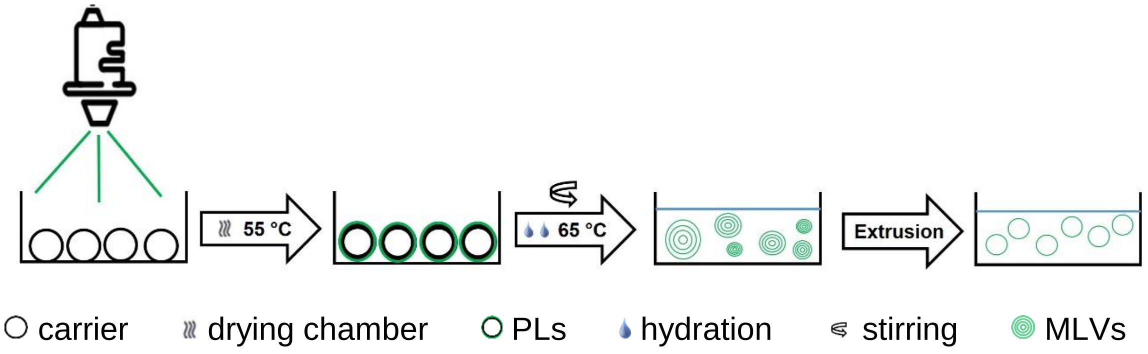

Figure 21: Schematic presentation of the experimental setup used for preparation of PLs by a coating method. Drying of the lipid film during coating was done at 55 °C and rehydration was performed while stirring with rehydrated water or PBS buffer at 65 °C for the lipid DSPC.

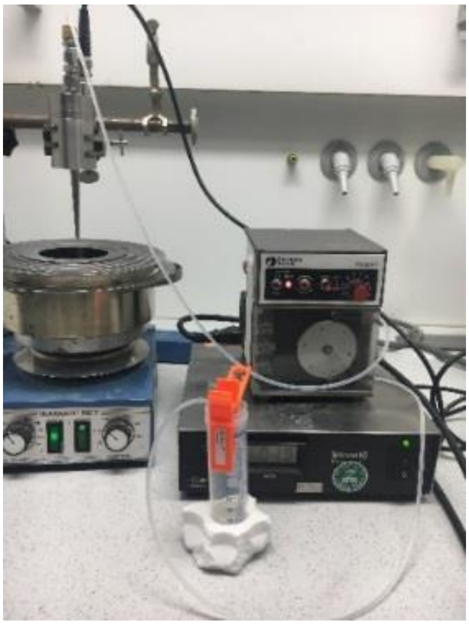

Figure 22: Experimental setup of proliposomal production in small scale.

3.2.2.2 Spray drying

Spray drying of PLs

Spray drying experiments with organic solvent were performed using a closed-loop Büchi Mini Spray Dryer B-290 (Büchi AG, Flawil, Switzerland) purged with nitrogen. Solvent was separated and recovered by condensation of solvent vapor from the drying gas using an inert Loop B-295 (Büchi AG, Flawil, Switzerland). The liquid feed, controlled by a ten-roll peristaltic pump (ISM597D, Ismatec®, Wertheim, Germany) was 3 ml*min^{-1} and pumped to the two-fluid nozzle. The spray dryer was heated to 110 °C T_{inlet} for about 30 min and then equilibrated by atomizing pure solvent (ethanol). T_{outlet} was in a range between 70 - 80 °C and an atomization flow rate of 700 L*h^{-1}. The organic solution was prepared analogously to the preparation technique in the chapter **Coating method** (**3.2.2.1**) and microparticulated mannitol (see section **Spray drying of microparticulated mannitol**) was added in concentration of 10 % or 1 % (w/w). The solution was put in the ultrasonic bath (SONOREX SUPER RK 106, BANDELIN electronic GmbH & Co. KG, Berlin, Germany) for 30 min before spray drying to remove agglomerates. Spray dried samples were directly collected in a 100 ml wide neck bottle (DURAN® GLS 80® laboratory bottle) and stored in a freezer at - 80 °C (Herafreeze, Heraeus Holding GmbH, Hanau, Germany).

Spray drying of microparticulated mannitol

Microparticulated mannitol was used as carrier for PLs produced by spray drying. The T_{inlet} and feed rates were varied. Configuration of the spray dryer is summarized in **Table 10**.

Table 10: Overview of spray drying parameters and settings.

Parameters	Settings
Spray dryer	Büchi Mini Spray Dryer B-290 (open loop)
Spray drying medium	10 % (w/w) mannitol solution
Nozzle type	Two-fluid nozzle; 2 bar
T_{inlet} / °C	90; 110; 130
T_{outlet} / °C	60 - 90
Feed rate / ml*min^{-1}	0.5 / 1 / 2 / 3

Spray freeze drying of mannitol

A laboratory scale spray freeze drying (SFD) apparatus was used as illustrated in **Figure 23**. A two-fluid nozzle (Büchi AG, Flawil, Switzerland) is suspended above a circular stainless steel bowl. The bowl was filled with liquid nitrogen (N_2), and after a short pause the solution was sprayed into the bowl using a peristaltic pump (ISM597D, Ismatec®, Wertheim, Germany) with a feed rate of 3 ml*min^{-1}. Mannitol solution of 10 ml with a total solid content of 10 % (w/w) was sprayed.

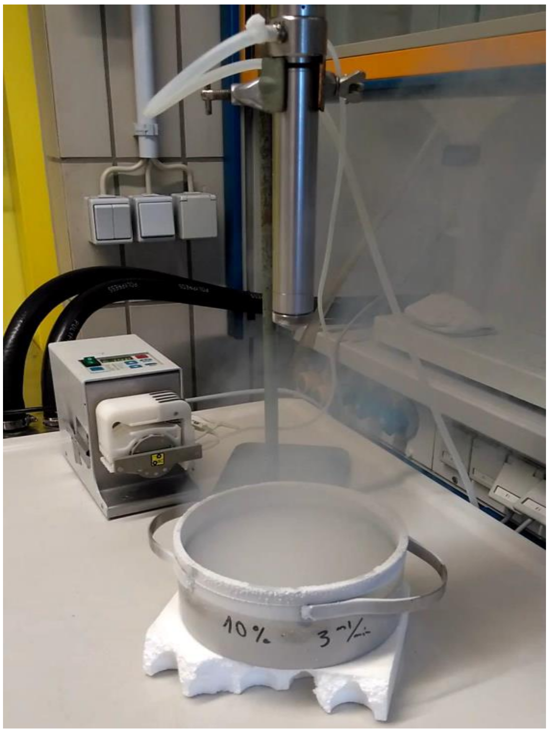

Figure 23: Schematic overview of lab scale SFD apparatus.

3.2.3 Characterization of liposomes

3.2.3.1 Laser diffraction

For determination of the size of the raw liposomal dispersion (MLVs) and particle size of the spray dried products a Mastersizer 2000 (Malvern Instruments Ltd., Worcestershire, UK) connected to a Hydro 2000S wet sample dispersion unit was used. For size measurement of the liposomes 2 ml of the suspension were pipetted in the Hydro cell with water and homogenized for 2 min stirring at 1750 rpm. Sample was added until the obscuration was in range (7 - 12 %). The analysis model "general purpose (spherical)" was chosen and three measurement cycles for each run were performed. After that all samples were treated with ultrasonic sound for one minute and three measurements afterwards. The d_{50}-value of the volume based size distribution was usually used for result evaluation. Dry powder samples were treated analogously and dispersed in a mixture of Miglyol® 812 and 1 % (V/V) Sorbitan trioleate (Span®) as wetting agent.

Default settings were used for dispersed material and the dispersion medium, *i.e.* "Default" (refractive index (RI) = 1.520), "Mannitol" (RI = 1.520), "Miglyol" (RI = 1.450) or "Water" (RI = 1.330).

3.2.3.2 Dynamic light scattering

Particle size distribution of the extruded liposomal dispersions were determined using a Zetasizer Nano ZS (Malvern Instruments Ltd., Worcestershire, UK). Z-average (intensity based mean particle diameter; Z-ave) and the dimensionless polydispersity index (PDI) were the parameters for characterization of the liposomal dispersions**. Table 11** shows the evaluation of PDI.

Table 11: Overview on arrangement of PDI values.

PDI	Arrangement
< 0.05	Highly monodisperse
0.05 - 0.2	Narrow size distribution
0.2 - 0.7	Slightly polydisperse
> 0.7	Very broad size distribution

Measurement of size and size distribution were performed in standard disposable PS cuvettes (Brand GmbH, Wertheim, Germany). The RIs and viscosities used for characterization of the different liposomal dispersions are shown in **Table 12**.

Table 12: Refractive indices and viscosities used for size distribution determination.

Solution	Refractive index	Viscosity / mPa*s	Dilution
Lactose in aqueous solution 10 % (w/V)	1.347	1.3000	100 µL (~ 2 droplets) in 3 ml aqueous solution
Phosphate buffer 7.4 (Ph.Eur.)	Default settings of “Water”		

Diluted liposomal dispersions were measured directly after preparation or tableting with subsequent extrusion. The measurement angle was 173° (non-invasive backscatter technique, NIBS) and the measurement temperature was usually set at 25 °C. Each sample was measured three times with a minimum of ten individual runs. Default settings of “Polystyrene latex” were assumed for the dispersed material (RI = 1.590, Absorption = 0.010).

3.2.3.3 Zeta potential determination

Determination of ZP in this work was performed in phosphate buffer 7.4 (Ph.Eur.), water or lactose solution 10 % (w/V). Measurement principle, settings and sample treatment were identical to the procedure as described in this chapter in the section ***Dynamic light scattering***. A volume of approximately 750 µL of the sample was filled in disposable folded capillary cells (DTS 1070, Malvern) using a standard 2 ml syringe (Injekt®, B. Braun Melsungen AG, Melsungen, Germany). The “General purpose” mode was used for data analysis to calculate the mean zeta potential and the zeta potential distribution.

3.2.3.4 Thoma cell counting chamber

Calculating the total number of liposomes per cubic millimeter (mm) is one of the important parameter to optimize the formulation composition. Therefore, PLs were hydrated with phosphate-buffered saline (pH 7.4, Ph.Eur.) and the number of vesicles formed per cubic mm was counted by optical micrometer using a BRAND® counting chamber BLAUBRAND® Thoma pattern (hemocytometer). The number of vesicles in 80 squares was counted at 20 x magnification using Olympus IMT-2 inverted Research Microscope, Tokyo, Japan and calculated according to **Equation 3** [185].

$$\text{Total number of liposomes per cubic mm} = \frac{\text{Total number of liposomes counted} \times \text{ dilution factor} \times 4000}{\text{Total number of squares counted}}$$

Equation 3

Figure 24 shows the method of counting the squares under the polarized light microscope. The vesicles (black labeled in the drawing) located on the left and upper dimension line (marked in red) were counted. The left square in the upper corner marks the starting point followed by meander-shaped counting method in direction of arrow. Two subsequent counting for one sample were performed and the difference between counted vesicles has to be less than ten counts.

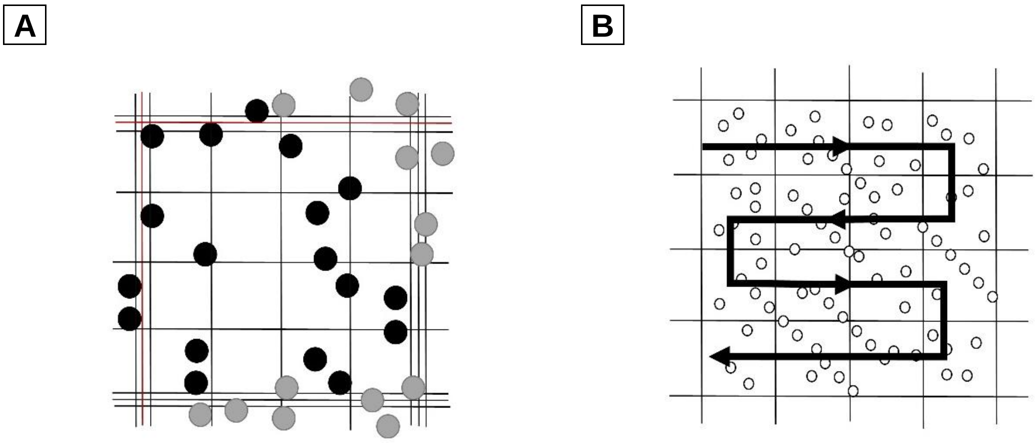

Figure 24: Schematic images of the (**A**) counted vesicles and counting delimination (vesicles marked in black; boundary marked in red) and the (**B**) counting direction of liposomes per cubic mm adapted from [186].

3.2.4 Encapsulation efficiency

The EE was determined using centrifugation. 2.5 ml of the raw liposomal dispersion were filled into the filter insert of Amicon® Ultra Centrifugal tubes (100,000 MWCO, Merck Millipore, Darmstadt, Germany) and centrifuged in a Hettich EBA 12 centrifuge (Andreas Hettich GmbH & Co.KG, Tuttlingen, Germany) for 90 min at 4,500 rpm (2,264 g). The sample was washed with buffer three times. Liposomes with API were not able to pass the regenerated cellulose membrane, whereas free active ingredient passes the membrane. Each component of the Ultra Centrifugal filter (filter unit, tube, lid) was weighed before use. The filtrate was measured UV-photometrically ($\lambda_{\text{Ibuprofen}}$ = 228 nm, $\lambda_{\text{Fenofibrate}}$ = 286 nm) with appropriate dilutions. The supernatant in the filter was dissolved in 2.5 ml ethanol, filtered through a 0.8 µm syringe filter and measured at UV-photometrically. The mass of API in the filtrate (m_{filt}) and in the supernatant (m_{sup}) are estimated in mg. **Equation 4** was used to calculate the EE.

$$\mathrm{EE}\ [\%] = \frac{m_{sup}\ [mg]}{(m_{sup} + m_{filt})\ [mg]} \times 100\ \% \qquad \textbf{Equation 4}$$

3.2.5 Release studies

600 mg of PLs were weighed into 10 ml glass sample vials and filled with 5,000 µl of release medium (PBS buffer 7.4 (Ph.Eur.)) which had been filtered through a 0.1 µm regenerated cellulose membrane filter (Stedim Biotech S.A., Sartorius AG, Göttingen, Germany). The samples were stirred at 500 rpm and conditioned to 37 °C (**Figure 25**). At specific time points (5 min, 10 min, 20 min, 30 min, 60 min, 90 min, 120 min, 180 min and 24 h) the sample was taken and subsequently filtered through RC membrane filter 0.2 µm. Samples were directly filled in HPLC vials.

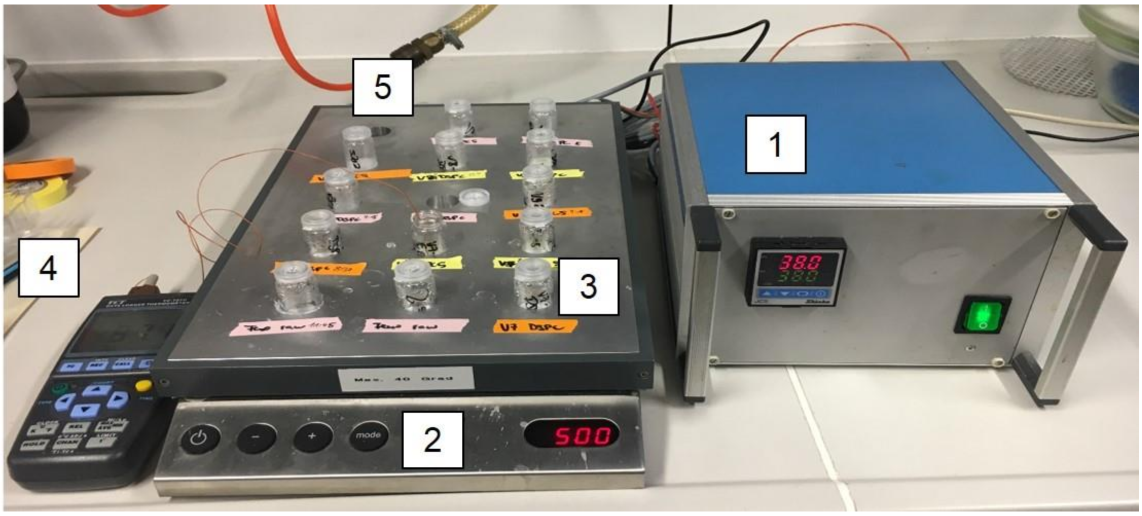

Figure 25: Release testing equipment consisting of (1) control unit, (2) magnetic stirring plate, (3) glass sample vials, (4) temperature control and (5) heating plate.

3.2.6 HPLC analysis

The quantification of fenofibrate was performed using HPLC system of Perkin Elmer, Waltham, USA. The configuration of HPLC equipment is described in **Table 13**.

Table 13: Configuration of HPLC system.

Component	Description
Autosampler	Flexar FX-UHPLC
Detector	UV/Vis Flexar FX UHPLC
Pump	Flexar FX-15 UHPLC
Software	TotalChrom Workstation 6.3.2

A Vertex Plus C18 Column (5 µm, 150 x 4.6 mm, KNAUER, Berlin, Germany) was connected to the HPLC system. As mobile phase a mixture (by volume) of 90 parts of methanol and 10 parts PBS buffer pH 7.4 (Ph.Eur.), 0.1 M was used. The flow rate was set to 1.0 ml*min^{-1} and the injection volume was 10 µL. Under these conditions the retention time for the fenofibrate peak, detected at λ = 286 nm, was about 9 min at a total run time of 20 min. Blank and standard solutions of fenofibrate were analyzed every time. Evaluation of the results was carried out by the comparison of the peak area based on the calibration in the range 5 - 500 µg*ml^{-1}.

3.2.7 Optical analysis

3.2.7.1 Polarized light microscopy

The liposomal form, the presence of crystals, as well as the shape of the vesicles were visualized by using an IMT-2 inverted Research Microscope (Olympus Corporation, Tokyo, Japan). A drop of the liposomal dispersion was pipetted on a microscope slide covered with a cover glass and observed at 40x magnification. Pictures were taken with a DS-Fi2 camera (5 MP, 12-Bit, Nikon GmbH, Düsseldorf, Germany) mounted on the microscope and the Nikon NISElements F and Axio Vision V4.2 imaging software (Carl Zeiss Vision GmbH, Aalen, Germany).

3.2.7.2 Scanning electron microscopy

Spray dried powders and PLs were imaged using scanning electron microscopy (SEM). An AMRAY 1810 T (Bedford, Massachusetts) and a CarlZeiss Gemini

Ultra55 (Carl Zeiss Microscopy GmbH, Jena, Germany) were used. Samples were fixed onto an aluminum sample stub (Model G301, Plano) with self-adhesive films and sputtered with gold in an argon atmosphere for 1 - 3 min (depending on sample and microscope type) at 5 kV and 20 mA in a sputter unit (Hummer JR Technics, Munich, Germany).

3.2.7.3 Transmission electron microscopy

Extruded liposomes were acquired with a CM300 UltraTWIN (Phillips, Eindhoven, Netherlands) for conventional transmission electron microscopy (TEM). The acceleration voltage was set at 300 kV and variable spot size. For cryo-TEM a CM30 (Phillips) device was utilized operating at 200 kV. Images were taken with a charge-coupled device (CCD) camera connected to a computer. The sample were prepared as follows:

- Procedure A (conventional TEM):
  6 µL of the diluted liposomal dispersion were pipetted on a TEM grid. The copper grid then was placed on a paper filter and the dispersion was sucked through the pores of the copper grid to the paper filter, leaving an appropriate amount of material on the surface of the copper grid. The sample was washed three times with 6 µL of water to remove soluble components. The droplet then was allowed to dry in a desiccator overnight at ambient temperature.
- Procedure B (cryo-TEM):
  The samples were prepared by depositing 5 µL of the diluted sample solution onto carbon-coated copper grids, 300 mesh, and air dry the grids. Cryo-TEM samples were prepared by the use of a Vitrobot (FEI, Eindhoven, Netherlands) and glow discharged using an Elmo Glow Discharge Cleaning System (Cordouan Technologies, Pessac, France) operating at 0.5 mbar for 2 min and Quantifoil grid (Quanitfoil Micro Tools GmbH, Großlöbichau, Germany). The sample was refrigerated in a LN2 cooling holder (- 175 °C) (Gatan Inc, Pleasanton, USA) during examination.

3.2.8 Characterization of dried powder samples using X-Ray diffraction

Wide-Angle-X-Ray diffraction (WAXD) was used for the characterization of the physical state of spray dried powder samples utilizing a Philips X'Pert X-Ray diffractometer (PANalytical, Almelo, The Netherlands). The acceleration voltage was set to 40 kV and the anode current to 40 mA. Measurements were performed at ambient temperature under nitrogen atmosphere. Powders were prepared on a stainless-steel sample holder (indentation width: 2.0 mm) and the surface was smoothened using a microscope slide. Samples were measured in the range of $2\theta = 0.5° - 40°$ (step size 0.02°, time per step 1 sec) with a wavelength of 0.1542 nm.

3.2.9 Tableting

Tablets were produced with an EK0 single punch tablet press machine (Korsch AG, Berlin, Germany) using 13 mm flat punches. All substances (**Table 14** summarizes the type and amount of each used excipient for tableting) were sieved through a 300 µm sieve. The excipients for tableting (proliposomal powder or filler for placebo tablets, binder and disintegrant) were blended in a Turbula® mixer Type T2C (Willy A. Bachofen AG Maschinenfabrik, Muttenz, Switzerland) at 50 rpm for 5 min. The free-flowing agent, release agent and lubricant were mixed separately in the same manner. Both containers were combined and blended again for 10 min. The tablets' mass was set to 250 ±10 mg and hardness > 30 N. Tablet mass was evaluated using an analytical balance (Sartorius AG, Göttingen, Germany), tablet hardness was determined using a Tablet Hardness Testing Instrument PTB311E (Pharma Test Apparatebau AG, Hainburg, Germany).

However, a comprehensive characterization in accordance with Ph.Eur. was not possible due to small batch size of the proliposomal granules.

Table 14: Overview of applied excipients for tableting.

Function of excipient	Type of used excipient	Amount / %
Filler	Tablettose® 80 or proliposomal granules	66.0
Binder	VIVAPUR® 301	25.0
Disintegrant	VIVASOL®	3.0
Lubricant	Magnesium stearate	1.8
Release agent	Talc	3.6
Free-flowing agent	Aerosil® Type 200	0.6

3.2.10 Stability

Freshly prepared PLs were filled into clear vials (SUPELCO, Sigma Aldrich, Germany) and stored at 40 °C (conditioning cabinet CO_2-Auto-Zero, Heraeus Holding GmbH, Hanau, Germany). The liposomal size, PDI and ZP were measured at the beginning of the long-term stability experiment. Samples were retested after 8 and 24 weeks regarding liposomal size after extrusion, PDI and ZP.

3.2.11 Design of experiments approach

To investigate the optimal formulation of PLs for large-scale production in detail a statistical design of experiments was generated using MODDE® Pro 12.0.1 software package (Umetrics, Malmö, Sweden). A full-factorial screening design with seven factors varying at two levels was chosen to identify the most appropriate formulation of PLs with regard to liposomal size, ZP and EE.

3.2.12 Scale-up production of proliposomes

A conventional lab scale drum coater, the mini-coater GMPC I (Glatt®, Binzen, Germany) was used to show and confirm the feasibility of the coating method with conventional, well established coating technique. **Table 15** summarizes the process parameters. Nylon tights were put over the drum to avoid loss of carrier material through the wholes of the perforated drum. 100 g of carrier material were given in the drum, equilibrated at ~ 65 °C T_{inlet} and afterwards coated with ethanolic lipid solution. Pump rate was calculated avoiding explosive atmosphere. For exact composition of the formulation see chapter **4.2.11 Scale-up of proliposomal preparation**.

Table 15: Overview of coating parameters.

Process parameter	Value
Process air flow / Nm^3*h^{-1}	35
Drum speed / min^{-1}	14
Inlet temperature / °C	65
Outlet temperature / °C	~ 45
Pump speed / $g*min^{-1}$	5.5
Spraying air pressure / bar	1.3
Wide air pressure / bar	1.6

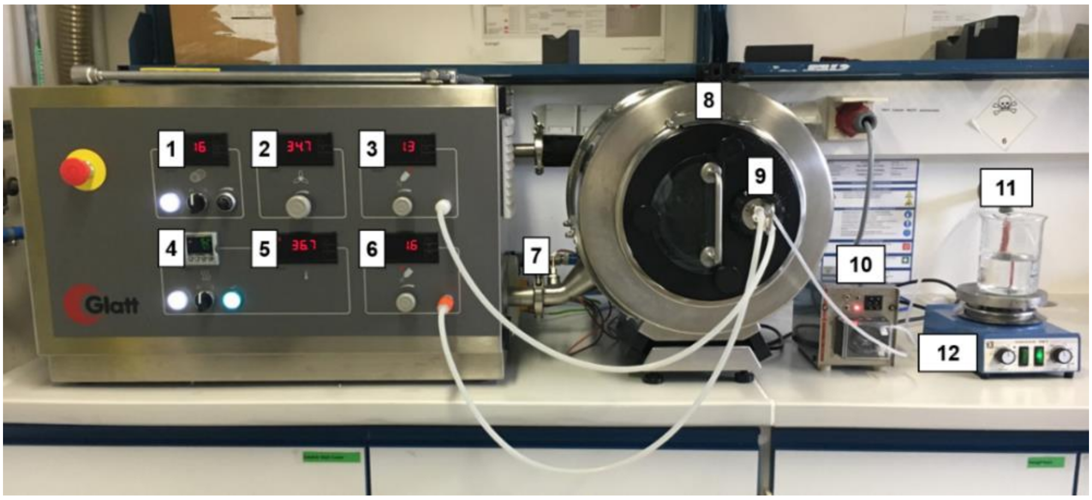

Figure 26: Coating equipment consisting of control units of (1) drum speed, (2) process air flow, (3) spraying air pressure, (4) inlet temperature, (5) outlet temperature, (6) wide air pressure and (7) temperature sensor, (8) drum, (9) three fluid nozzle, (10) pump, (11) ethanolic lipid solution as well as (12) magnetic stirrer.

4 RESULTS AND DISCUSSION

In this first section the manufacture of liposomes applying the conventional round bottom flask method was investigated. After complete drying of the lipid films various techniques for homogenization on size reduction of the liposomes were evaluated in terms of vesicle size and zeta potential.

4.1 Investigation of various techniques for homogenization of liposomes manufactured with the round bottom flask method

The first part of this chapter describes the conventional preparation of liposomes using the round bottom flask method with subsequent extrusion of the dispersion. These investigations provide a basis for the characterization of the liposomes and can act as comparison for the results of the liposomes produced with the coating method (see chapter **4.2 Production of proliposomes using coating methods**). Different reconstitution parameters were chosen in order to investigate the effects on liposomal size, PDI and ZP and show the limitations of this established method. Furthermore, the physical stability of liposomal dispersion was tested by variation of the pH-value.

4.1.1 Variation in sample treatment by filtration, ultrasonic sound and vortexing

Liposomal formulations were prepared *via* round bottom flask method using DSPC and cholesterol in an equimolar molar ratio of 5 to 5 mM (in total 10 mM). A placebo batch was compared with one sample preparation including ibuprofen in an equimolar molar ratio of lipid-to-cholesterol-to-API (1:1:1). The vesicles were reconstituted in a lactose solution 10 % (w/w) and extruded 11 times through a

0.4 µm and 0.1 µm membrane in a further step. After extrusion, several techniques to enhance homogenization of the liposomal size were used. Therefore, three different treatments and combinations were chosen: (i) filtration (fil) through a 0.2 µm RC membrane, (ii) ultrasonic sound (us) for 5 min and (iii) vortexing (vortex) with maximum power for 20 sec. Extruded liposomal dispersions were stored over two days in the fridge at 4 °C. **Table 16** gives an overview of the variations in sample treatment after extrusion.

Table 16: Combinations of performed experiments using different sample treatment.

Variation	Fil	Us	Vortex
1	x	-	-
2	x	x	-
3	x	x	x
4	-	x	-
5	-	x	x
6	-	-	x

Figure 27 shows the liposomal size and PDI for the placebo (**A**) and the API batch (**B**). The grey marked line in the background marks the liposomal size of the untreated liposomal dispersion after extrusion (value between 370 and 390 nm after two days). For the placebo batches a size reduction for all samples was observed after two days. At t = 0 h the Z-ave was > 300 nm and after 48 h at a value of ~ 300 nm. The PDI showed more fluctuations within a range higher than 0.2, which indicated a more polydisperse state. The smallest effect if any on a decrease in size was shown after stirring the samples with the vortex. After one day there was substantial in size increase of up to 475 ± 59 nm (398 ± 7 nm after 48 h). Similar behaviour on the liposomal size measured was observed after a slight increase after 24 h for the fil, fil + us, fil + vortex, us and us + vortex samples, which all gave a reduction in size to ~ 300 nm after 48 h after initially showing a slight increase in size. The combination of all three pre-treatment methods

(fil + us + vortex) showed a tendency to have the biggest influence on liposomal size. At t = 0 h as well as after two days the smallest liposomal size of <300 nm was reached.

However, the liposomes with incorporated API resulted in a more uniform and smaller vesicle size of ~ 250 nm over the whole two days. The presence of drug substance in the aqueous medium which might result in smaller vesicles due to smaller curvature radiuses. The calculated results of the PDI (= ~ 0.2) revealed a rather narrow size distribution for the API batch when compared to the higher PDI values of the placebo samples.

For both formulations, the placebo as well as API batch, Z-ave was increased compared to treated samples of the reference batch (marked with grey area).

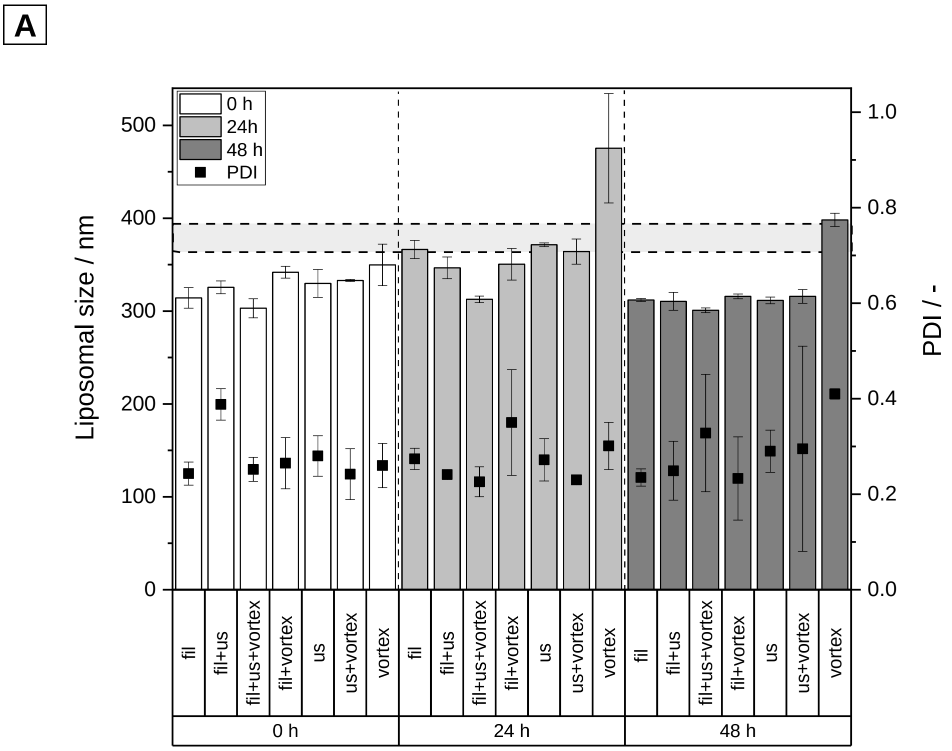

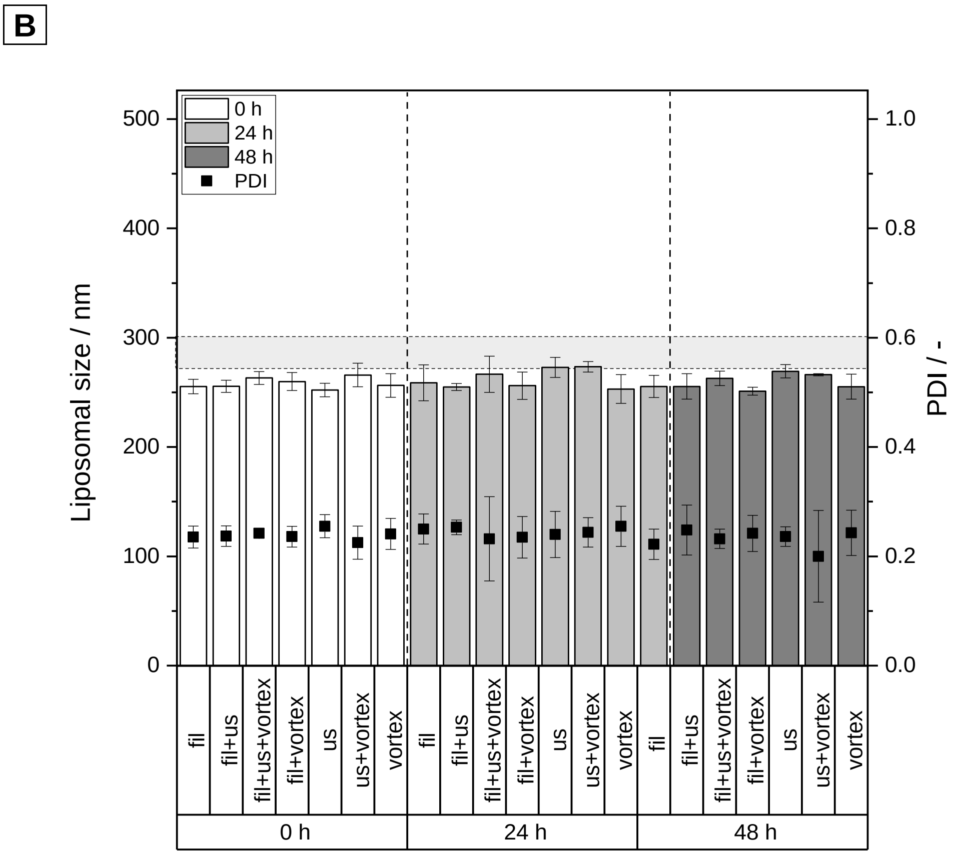

Figure 27: Liposomal size after different sample treatments (fil, us, vortex) for (**A**) placebo and (**B**) API batch (n = 3; 2σ). As reference, the untreated liposomal dispersions were in a range of 360 to 400 nm for the placebo batch and 280 to 300 nm for the batch containing ibuprofen (see grey areas). The observation period was 48 h.

The values for the ZP of the liposomal dispersions for the individual treatments at t = 0 h, t = 24 h and t = 48 h are depicted in **Figure 28**.

For the placebo batch the ZP showed an almost identical value for all samples approximately at each measurement point. At t = 0 h the ZP was at a value of ~ - 7 mV, after t = 24 h and t = 48 h at a value of ~ - 17.5 mV. This might indicate a stabilization of the liposomal dispersions over the time period of two days. However, the samples treated with fil + vortex behave differently and show lower ZP values. For the API batch (**B**), a similar behaviour of ZP could be observed in comparison to the references (marked with black lines). Like the placebo batches there was a tendency of lowering vales for the ZP over 48 h, although the effect was less pronounced (~ - 9 mV to - 12 mV). With respect to the ultrasonic treatment of the API batch, an increase in absolute values of ZP as seen with the placebo dispersion was expected. Nevertheless, no significant changes in ZP were observed (0 h: - 8.02 ± 0.38 mV; 24 h: - 7.8 ± 0.76 mV; 48 h: - 8.30 ± 0.69 mV).

Also Dimitrios and Antimisiaris [187] observed an increase in ZP over 24 h while incubating liposomal formulations. Additionally, a remarkable difference in ZP-values between empty liposomes *versus* API incorporated SUVs was observed. Deviations in ZP may result in the oriented changes of PC head groups at liposomal surfaces [188]. This phenomenon also contributed to the negative surface potential might be the result of the choline group plane lying below the phosphate group plane.

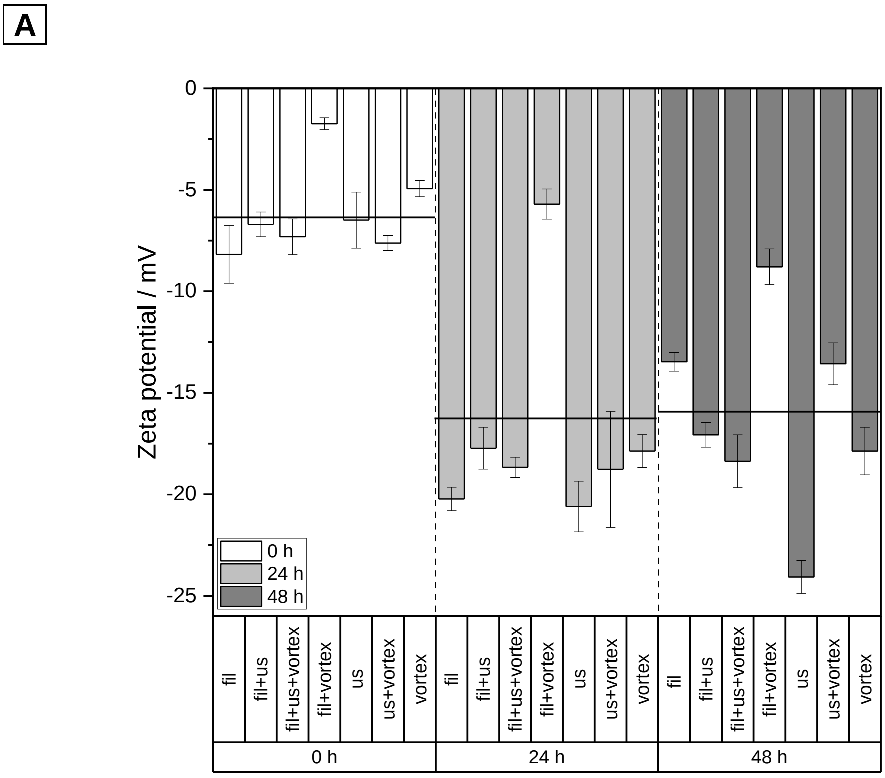

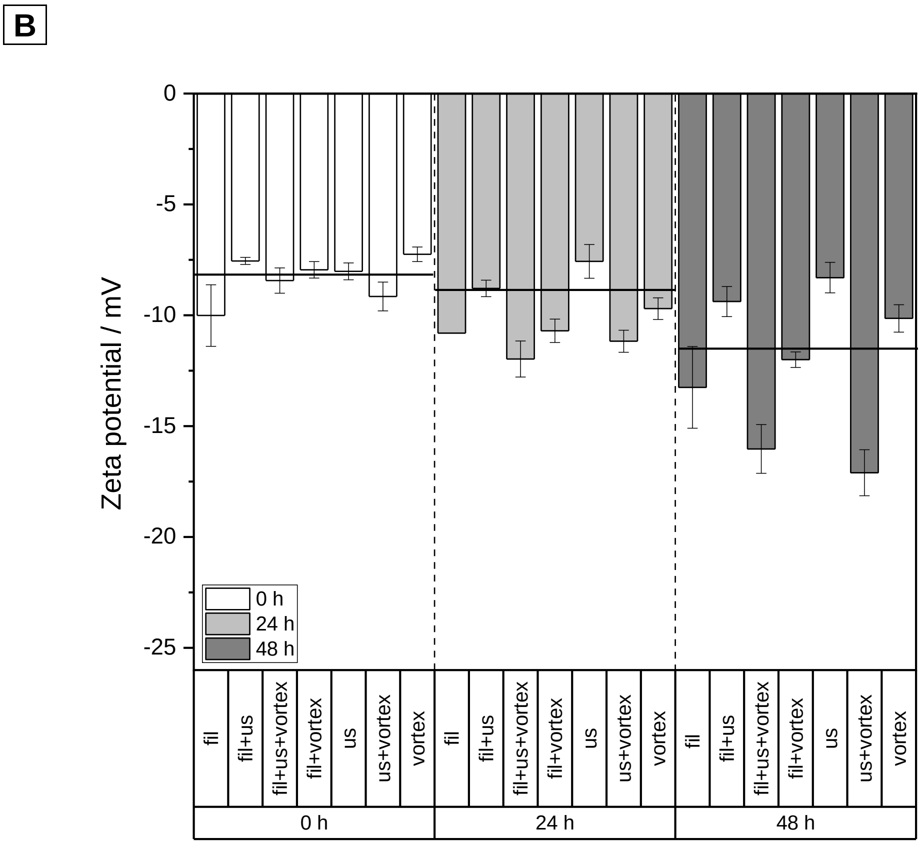

Figure 28: ZP of liposomal dispersions of (**A**) placebo and (**B**) API batch (n = 3; 2σ). As reference, untreated liposomes with and without API are indicated as black lines.

In summary it was possible to decrease the liposomal size slightly varying pre-treatment methods. The rather slight decrease may be attributed to the initially already low size. The most effective seemed to be the combination of fil + us + vortex (noticeable at placebo batch). Already at t = 0 h the smallest vesicle size was reached as well as after two days. In contrast vortexing only had the lowest effect. Regarding the API batch all the results of the pre-treated samples were below the untreated reference dispersion. After two days an increase in ZP was observed for both (placebo and API) which indicated in addition to the decrease in liposomal size a stabilization of the pre-treated liposomal dispersions.

4.1.2 Improvement of liposomal stability *via* pH variation

Objective of this section was the investigation of acidic or basic conditions (pH variation) on the stability of the liposomes, tested *via* photomicrographs and measurements of liposomal size, PDI and ZP. According to Zhang *et al.* [189], not only temperature but also pH level has an effect on the extent of hydrolysis of phospholipids and therefore on the shelf-life of liposomes. Preparation of vesicles containing ibuprofen was introduced by Mohammed *et al.* [91] and performed according to the method described in chapter **3.2.1**. Two different types of reconstitution media were used: (i) water or (ii) 10 % (w/V) aqueous lactose solution. Subsequently, the produced batches were extruded. **Table 17** shows an overview of the pH values and temperatures measured of the raw liposomal dispersion (reference) as well as after addition of acid, *i.e.* 0.1 M hydrochloric acid (HCl) or base, *i.e.* 1 M sodium hydroxide (NaOH), respectively. For DLS measurements, a volume of 10 µL acid or base was pipetted into 2 ml extruded sample and the pH was measured subsequently. Three measurement times were chosen: directly after production, after 24 h and 48 h.

Table 17: Different pH values of raw liposomal dispersion before and after addition of acid or base, respectively. Water and lactose solution (10 % (w/V)) were both used as rehydration media.

	Samples	**pH value / -**	**Temperature / °C**
Water	Reference	4.81	22.6
	1 M NaOH	10.84	22.7
	0.1 M HCl	3.65	22.6
Lactose solution	Reference	4.42	22.6
	1 M NaOH	10.59	23.0
	0.1 M HCl	3.66	22.7

Agglomeration, the appearance and form of the lipid vesicles as well as potential crystallization of ibuprofen were examined using polarization microscopy. Exemplary pictures of the crude liposomal dispersions after rehydration without any extrusion steps are presented in **Figure 29**. After extrusion liposomes were not detectable because of the size distribution in the nanometer range. The photomicrographs show large MLVs which show a size from 10 µm up to 20 µm due to vesicles' accumulation. Arrows in image **A**, which was taken from the reference batch, indicate agglomeration of the liposomes. Several vesicles lay closely together, touch each other and form agglomerates. By addition of acid or base, no changes in the shape of the liposomes could be observed. Image **B** shows a picture of liposomal dispersions rehydrated with water and after addition of HCl. A decrease in pH value resulted in a lower tendency to agglomeration and liposomes were mostly present as individual vesicles. A similar effect could be observed after addition of NaOH (image **C**), where most of the vesicles observed were not agglomerated.

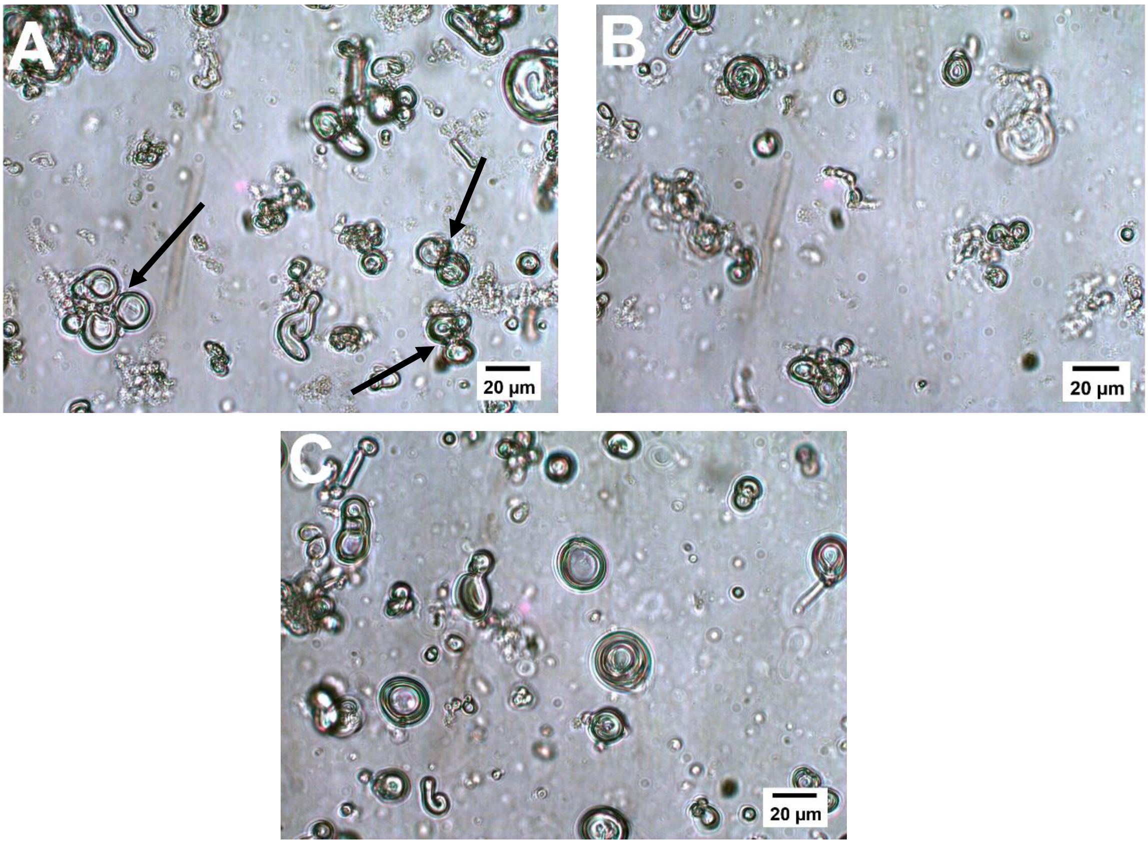

Figure 29: Photomicrographs of raw liposomal dispersions taken before extrusion with 40x magnification.
(**A**) Reference with water as reconstitution media showing accumulation of the liposomes (indicated by black arrows). (**B**) Liposomal dispersion rehydrated with water after addition of HCl. (**C**) Liposomal dispersion rehydrated with 10 % (w/V) lactose solution after addition of NaOH.

An overview of the Zetasizer measurements during a time frame of three days after extrusion is depicted in **Figure 30**. For the reference batch liposomal size was increased than those for the dispersions after addition of HCl or NaOH. The liposomal size increased from 300 - 320 nm during the period of three days when using water as reconstitution medium. This might be a result of the formation of agglomerates of fusion of the liposomes. Furthermore, the PDI was clearly above a value of 0.2 which is typical for MLVs. Liposomes containing lactose as reconstitution medium showed a larger vesicle mean diameter (~ 400 nm) initially, after 24 h the size levelling out to a value of ~ 370 nm over the period of two days. By adding acid or base to the solution, liposomes became more uniform in size with a diameter from 225 - 250 nm. The PDI of 0.2 for all alkaline or acidic samples indicates a nearly monodisperse size distribution for these samples. Formulations containing lactose solution resulted in smaller liposomal sizes (~ 200 nm) compared to those which were rehydrated with water-based solutions (~250 nm) despite of increased PDIs.

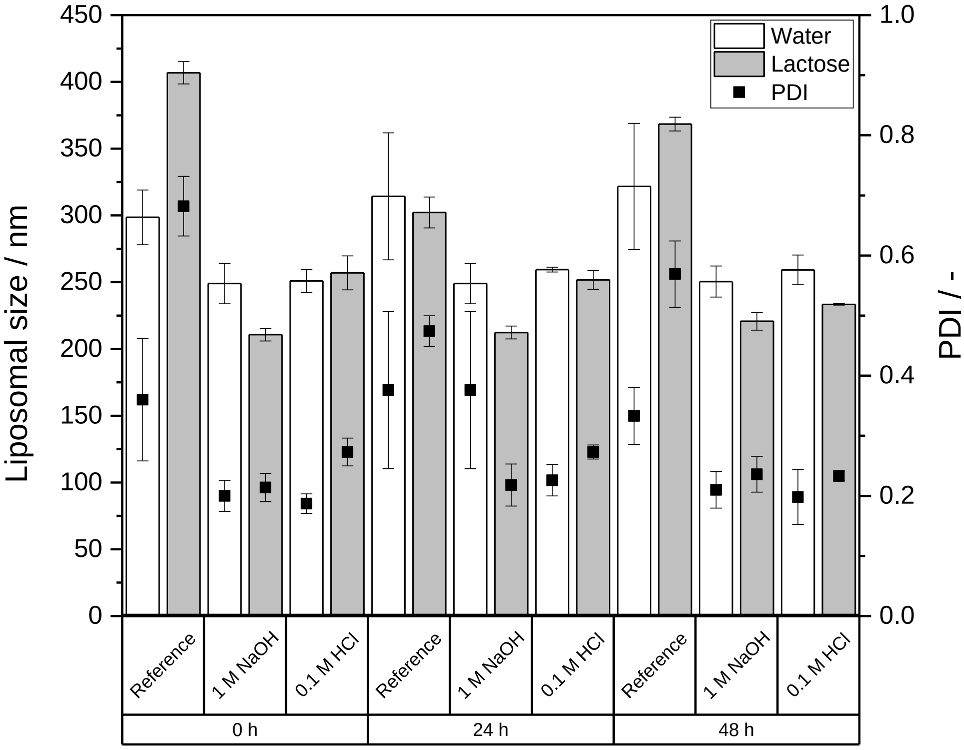

Figure 30: DLS measurements of liposomal dispersions (i) without any change of pH value (reference) and after addition of (ii) 1 M NaOH and (iii) 0.1 M HCl. In one case water was used for reconstitution, in the other case lactose solution (10 % (w/V)) (n = 3; 2*σ*).

The addition of HCl or NaOH had an unequivocally effect on the ZP values measured. In both cases a higher value of ZP was measured, indicative of higher repulsive forces between the vesicles (**Figure 31**). After addition of HCl, the ZP had a value of ~ 21 mV for water and ~ 17 mV for lactose solution as reconstitution media. This means a doubling of ZP in contrast to the reference batch with ZP of ~ 10 mV and 1 mV for water and lactose, respectively and thus higher stability of the liposomal dispersions over the time period. At lower pH level, the phosphate groups of DSPC could be protonated and hydrogen bonds might be formed by reacting with neighboring phospholipids molecules [190]. Electrostatic repulsion between choline groups, which were protonated because of the zwitterionic nature of the molecule DSPC might be another reason for improved stability [191]. In contrast, ZP became negative (- 30 mV to - 22 mV) after addition of NaOH. Consequently, the characteristic carboxylic acid group of ibuprofen (pK_a = 4.4) was deprotonated which resulted in a negative charged functionality. No substantial changes in ZP could be observed within two days.

These results confirm substantial effects of the pH-value on the liposomes formed. After rehydration the raw dispersions initially indicated the formation of large MLVs with a size range up to several µm. Furthermore, a tendency for agglomeration was observed using polarized light microscopy, which was reversible after addition of NaOH or HCl. As the liposomal size of the alkaline or acidic batches was reduced a reversible accumulation of vesicles could be expected. The reduced agglomeration was reflected in higher absolute values of ZP as well as smaller liposomal sizes after extrusion as well.

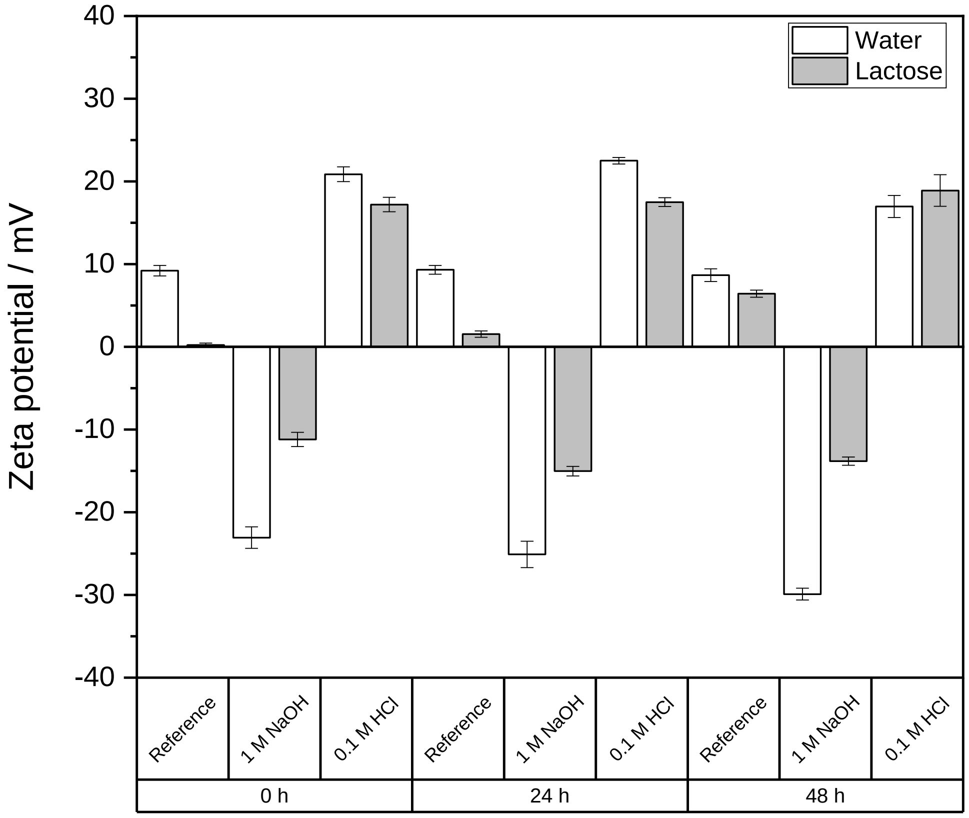

Figure 31: Zeta potential of liposomal dispersions (i) before (reference) and after addition of (ii) base (1 M NaOH) or (iii) acid (0.1 M HCl), respectively (n = 3). Rehydration was performed using water or lactose solution 10 % (w/V) as media (n = 3; 2*σ*).

4.2 Production of proliposomes using coating methods

The focus of the second part of this thesis was set on the production of PLs by a modified coating method for (i) lab scale and therefore the established (ii) scale-up using a design of experiments (DoE) approach. Microscopic studies proved the presence of vesicles after reconstitution of the PLs. Furthermore, liposomes were characterized performing stability as well as release studies. The subsequent processing of the proliposomal powders to tablets was investigated as well.

4.2.1 Characterization of carrier materials

A conventional, well established coating method which was modified for lab scale production was chosen. An ethanolic solution of the lipids DSPC or egg-PC and cholesterol (4:1; in sum 600 mg of lipids in 28 ml ethanol with a carrier-to-lipid ratio of 10:1) was sprayed with an ultrasonic nozzle onto carrier material in a bin, which was heated up to 55 °C for efficient evaporation of the organic solvent. The spraying process was performed for approximately 5 min alternately with the drying step. Conditions were applicable to common coating devices. At the beginning, the carriers used were characterized by (i) the different types of materials, (ii) carrier size and (iii) their surface before and after coating.

4.2.1.1 Comparison of different material species of carrier

Different types of carrier with water-soluble or water-insoluble properties were screened and are listed in **Table 18**:

Table 18: Overview of the carrier used ordered by water-solubility and water-insolubility, respectively; GHP: Globuli Homeopathic Pharmacopoeia.

Name	Type of material	Pieces per g	Size / µm
	Water-soluble		
GHP 1	Sucrose	470-530	800-1,600
GHP 2	Sucrose	220-280	1,250-2,000
GHP 3	Sucrose	110-130	1,600-2,400
GHP 4	Sucrose	70-90	2,000-2,800
GHP 5	Sucrose	40-50	2,500-3,300
Suc-lac	Sucrose-lactose	200-220	1,250
Xyl	Xylitol	200-220	1,250
	Water-insoluble		
MCC1000	MCC	-	1,000-1,400
MCC350	MCC	-	355-500
MCC100	MCC	-	100-200
Beads 1.5	Lucent glass	-	1500
Beads 0.1	Glass	-	100

XRD measurements of the different solid carriers (**Figure 32**) were performed in order to investigate the raw material and to exclude the presence of impurities (*e.g.* binder). The large sucrose spheres were pulverized (plv.) with a rough mortar and pestle to enable a correct filling of the sample holder. Crystalline sucrose was treated analogously. The diffraction pattern of GHP 4 plv. and GHP 5 plv. agree well with those of sucrose plv. Larger crystals were given for raw sucrose which results in much higher peak intensity. XRD confirms the crystalline nature of all samples investigated.

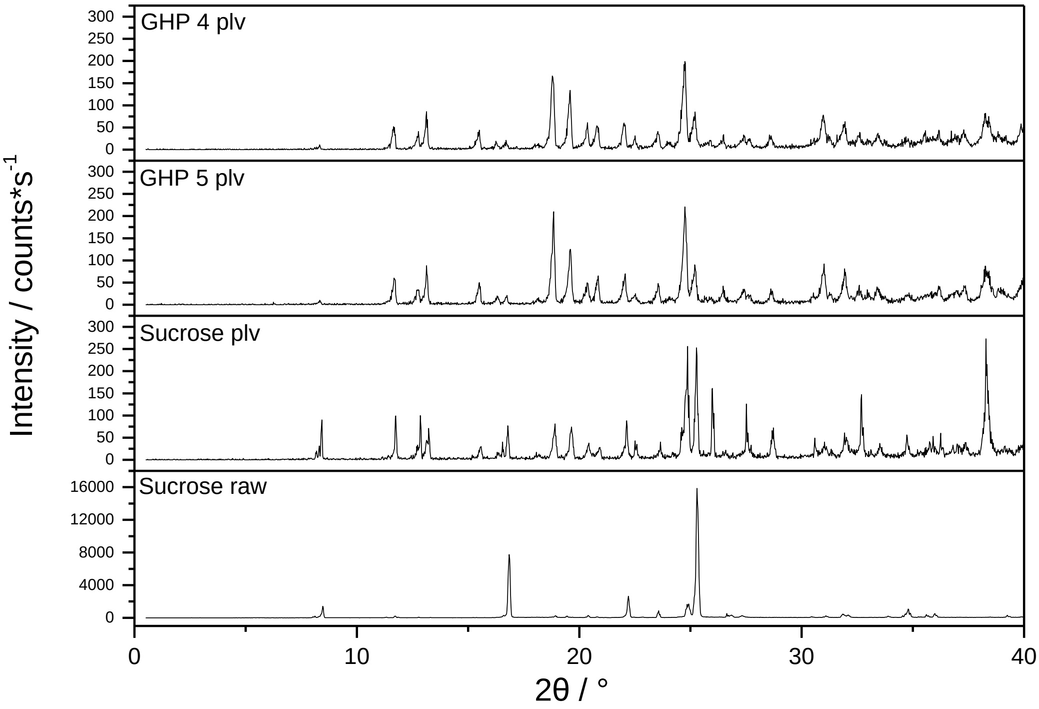

Figure 32: WAXD of crystalline sucrose and samples of pulverized (plv.) water-soluble carrier materials.

4.2.1.2 Carrier surface analysis before and after coating

Before coating, the surface of the carrier made of sucrose had a sensory matt and whitish turbid look (**Figure 33 A**). In contrast, PLs based on the same material, developed a smooth, wax like to oily appearance. Egg-PC created a more glossy surface with sticking tendency of PLs (**B**). Kumar et. al. observed aggregation of beads coated with egg-PC which could be due to the low T_g of the lipid [156]. However, PLs covered with the lipid DSPC looked more tarnished and showed better flowability of the spherical particles after removal of the solvent (**C**).

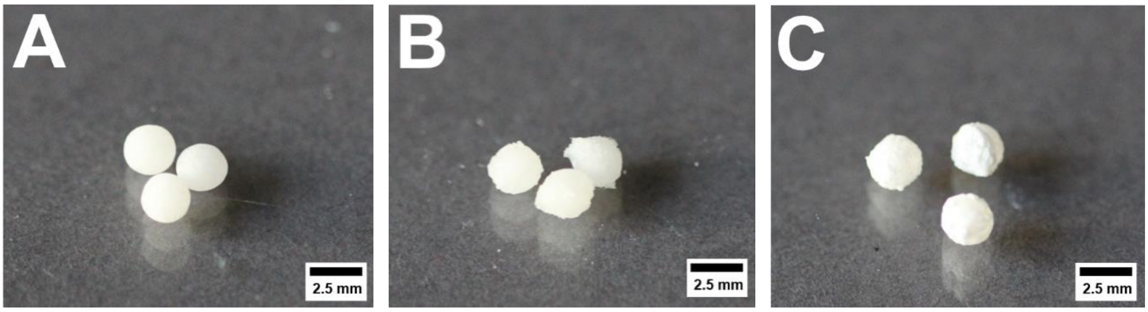

Figure 33: Pictures of the carriers before coating as well as PLs after layering processes. (**A**) GHP 5, (**B**) GHP 5 coated with egg-PC and fenofibrate, (**C**) GHP 5 coated with DSPC and fenofibrate.

Figure 34 shows SEM micrographs of the carrier and PLs, respectively, which were taken before and after coating. The lipid coating was clearly recognizable comparing image **A** to **B**. It can be seen that the surface texture of the raw carrier based on sucrose is rough, highly convoluted and irregular as seen in SEM images **E** or **I**. For the water-insoluble carrier MCC (**M**/**N**) and the glass beads (**K**/**L**) the surface structure was not that rough but more regular.

The appearance of the produced PLs was smooth since a uniform lipid layer on the carriers was formed, confirming the applicability and effectiveness of the deposition of lipids using the coating method. There might be a filling effect of lipid on the irregular surfaces in the initial state. Comparing the lipids used, the layers of PLs coated with DSPC (**D**) were more cracked than those of the PLs coated with egg-PC (see chapter **4.2.6 Effect of lipid species on size and number of liposomes**). This film seemed to be smoother and more superficial (**H**; **J**). Comparing water-soluble and water-insoluble carrier there were no difference in the visual appearance of PLs. The spraying characteristics of the lipids was comparable. Nevertheless, the water-soluble carrier showed visually a better coating behavior on their surface with better adhesion of the lipid covers. Blazek-Welsh and Rhodes [192] took SEM images of proniosomes based on the water-soluble carrier material maltodextrin. They developed niosomes out of the precursor, which represent vesicle systems similar to liposomes loaded with amphiphilic or lipophilic drugs. Furthermore, they predicted the quality (*i.e.* dosing or carrier amount) of niosomes based on SEM-imaging. The appearance of niosomes correlated with coarse, broken structures on the surface of proniosomes.

Water-soluble

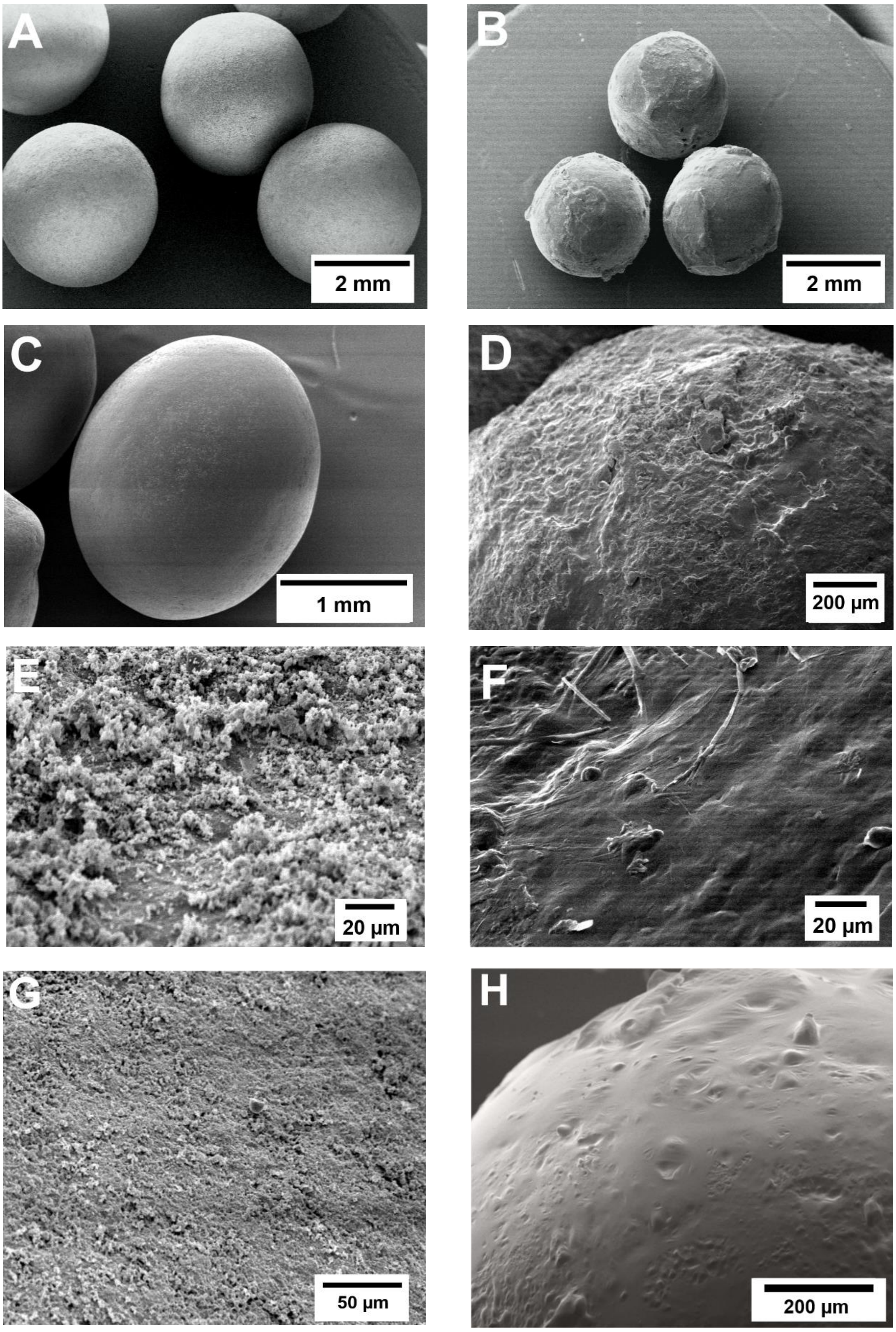
A
2 mm
B
2 mm
C
1 mm
D
200 µm
E
20 µm
F
20 µm
G
50 µm
H
200 µm

Water-soluble

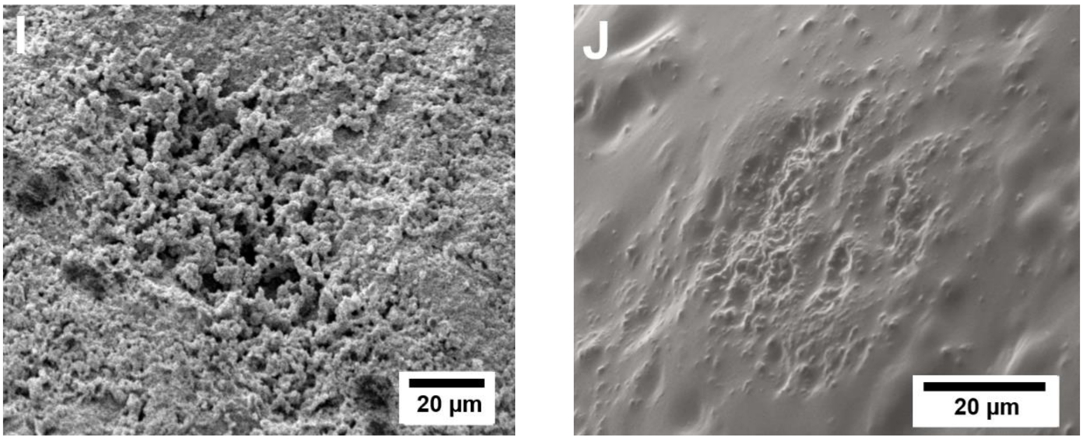

Water-insoluble

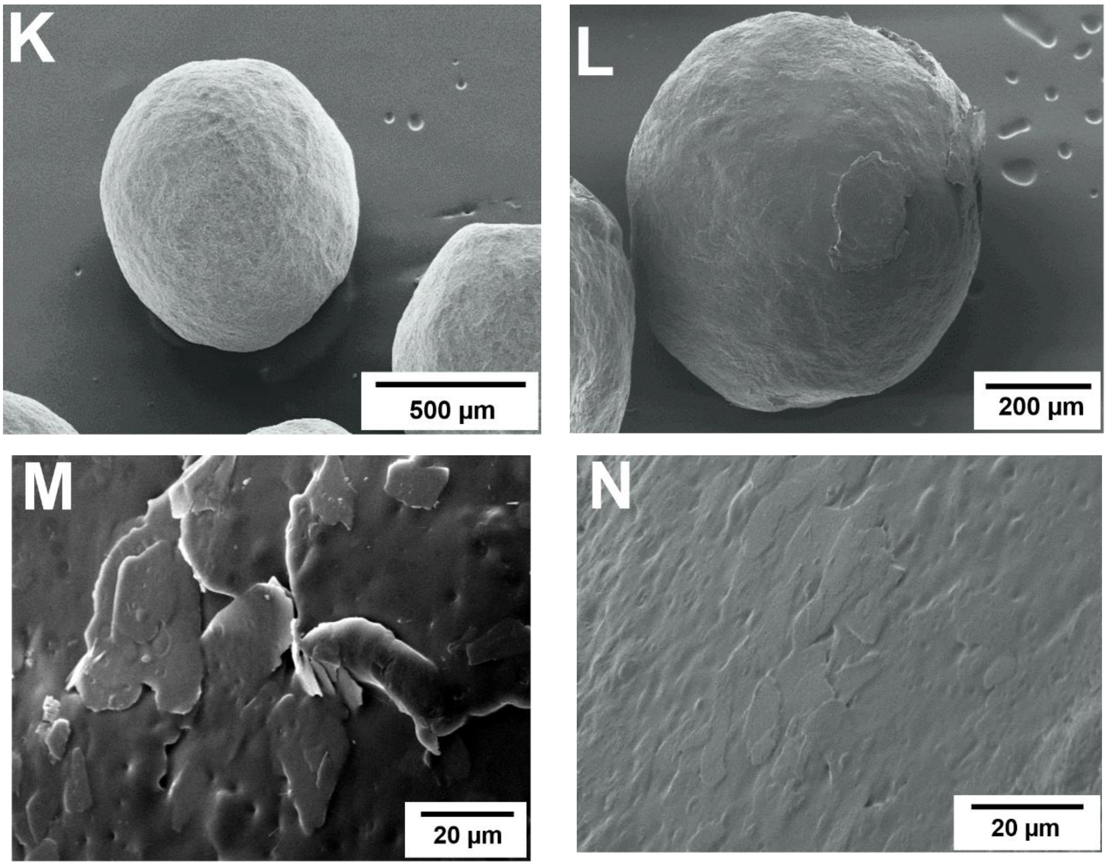

Figure 34: Surface structure of carrier material before and after coating with lipid solution of DSPC (B, D and F) and egg-PC (H, I), so-called PLs.
(**A**) GHP 4 raw 15x, (**B**) GHP 4 coated 14x, (**C**) Xyl raw 40x, (**D**) Xyl coated 100, (**E**) GHP 5 raw 1000x, (**F**) GHP 5 coated 1000x, (**G**) GHP 5 raw 500x, (**H**) GHP 5 coated 250x, (**I**) GHP 5 raw 1000x, (**J**) GHP 5 coated 1000x, (**K**) glass beads raw 1.5 mm 50x, (**L**) glass beads 1.5 mm coated 70x, (**M**) MCC1000 raw 1500x, (**N**) MCC1000 coated 1500x.

4.2.2 Microscopic studies using polarized light microscopy and (cryo-) TEM as tool for proof of liposomes

The formation of liposomes out of PLs manufactured with the coating method was verified using cryo-TEM and polarized light microscopy. Besides that, a control of the measured extruded vesicles' size was performed by cryo-TEM.

Polarized light microscopy was used as first microscopic analysis technique to check the presence of vesicles in the raw liposomal dispersions (see **Figure 35**). Bibi *et al.* [193] achieved an imaging of liposomes using amongst others polarized light microscopy, too. Size and vesicle morphology were confirmed *via* observation using a microscope. Challenges like poor vesicle formation or aggregation could be easily observed. The polarization microscope offers an easy and quick way to confirm the presence of liposomes by visibility of Maltese crosses.

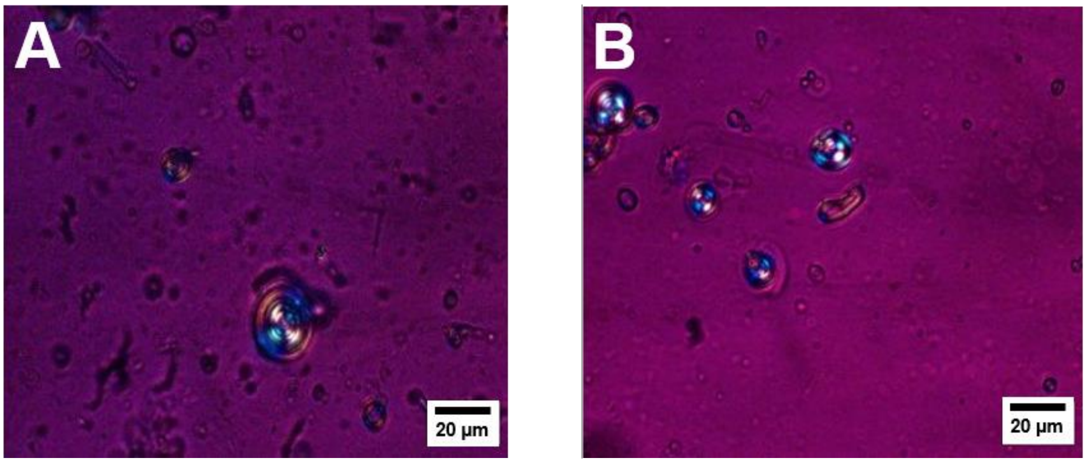

Figure 35: Polarized light microscopy. These are images obtained using a 40x magnification *via* brightfield with a polarizer. (**A**) Sucrose was used as carrier for these PLs. (**B**) The water-insoluble MCC served as carrier material. In both cases, liposomes could be clearly identified through the presence of Maltese crosses by a polarizer.

Secondly, TEM was used as analytical tool to image formed liposomes. Two liposomal dispersions without any extrusion step were examined under the microscope. The first one was chosen as reference batch (produced *via* round bottom flask method) as tool for proof of the presence of vesicles. The second batch contained liposomes formed out of PLs, which were manufactured using the coating method as described in chapter **3.2.2 Preparation of proliposomes**. The lipids' composition of both formulations was identical: DSPC and cholesterol were dissolved in ethanol in a DSPC-to-cholesterol ratio of 4:1. Two round shaped circles were observable under the microscope. The inner circle showed a darker appearance whereas the outer, bigger circle is illustrated less intensively. As the liposomes were used without extrusion step the size of the liposomes was in accordance (several microns) with the vesicle size observed using polarized light microscopy. Even though, the TEM technique is not the method of choice to depict liposomes. Rrepresentative TEM images of liposomes were taken and referenced in other publications (Roy *et al.* [194]). Roy *et al.* observed a spherical morphology and the existence of the bilayer for LUVs (100 nm - 400 nm in dependence to pH value) in formulations with DPPC+DPPG, soy-PC and cholesterol. Image **C** (**Figure 36**) indicates also a bilayer and the imaging of vesicles is comparable to those of Roy *et al.*: a spherical morphology with a circle rich in contrast and a clearer ring all around.

For a better understanding of the bilayered structure and the formation of ULVs, cryo-TEM served as often used technique for depiction of numerous, complex biological structures formed by amphiphilic molecules in aqueous solutions [195, 196]. Cyo-TEM images depicted in **Figure 37** represent a blank formulation (**A** - **D**) using DSPC and cholesterol as lipids and sucrose (~2000 µm; GHP 3) as carrier. The liposomal dispersion was extruded in a well-known manner and clearly shows the existence of liposomes formed out of PLs. The pictures indicate a quite monodisperse batch with a majority of spherical unilamellar vesicles, whereas SUVs and LUVs could be seen. Furthermore, some MVV with diverse vesicles into one another were noticeable. Liposomal size, as obtained from cryo-TEM measurements, were found to be comparable to those determined by DLS (~ 150 nm) (see chapter **4.2.3**). Cryo-TEM images **E** and **F** specify a sample with the same lipid and carrier composition containing fenofibrate in a concentration of 10.7 mg*ml^{-1}. Here, a higher number of liposomes could be found on the image although these liposomes were manufactured the same way. The fenofibrate containing liposomes showed much more polydisperse appearance when observed in the cryo-TEM. As fenofibrate is a lipophilic drug substance it could be incorporated in the lamellar bilayers which could even result in layers composed with more API than membrane lipids. A higher number of vesicles was indicated. Unfortunately no conclusion on the EE can be drawn for the cryo-TEM pictures since the contrast is too low. Almgren *et al.* [197] also observed the phenomenon of vesicles which appear double-walled (**D**). However, they showed invaginated single-wall structures. Such structures were studied by Regev and Khan [198] who wanted to understand the self-aggregation behavior of double-tailed quaternary-type surfactant systems.

These microscopic studies clearly show proof on the existence of liposomes both for the raw dispersions derived from the coated PLs and the dispersions obtained after extrusion.

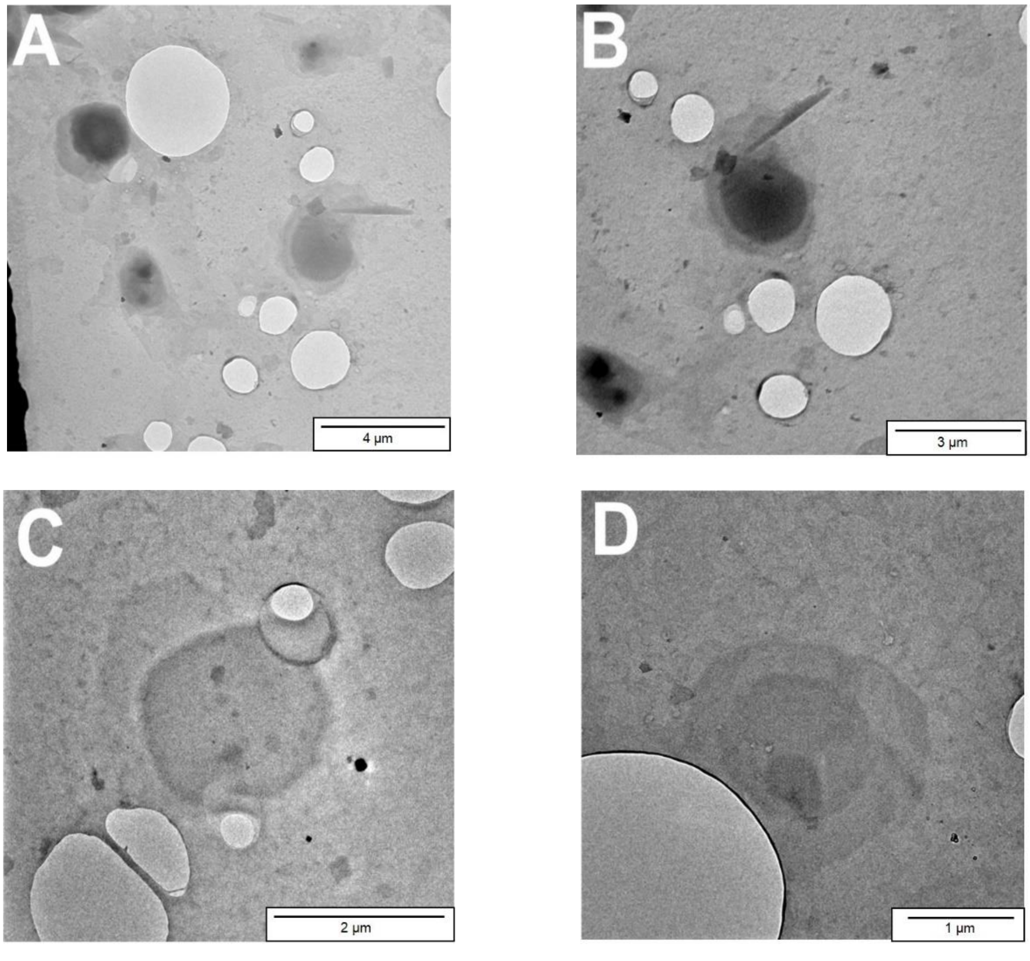

Figure 36: TEM images of liposomal dispersions without any extrusion step.
(**A**-**B**) Liposomal dispersion made *via* round bottom flask method as reference for liposomes' existence. (**C**-**D**) Sample of PLs with an identical lipid composition as the reference batch but manufactured using the established coating method.

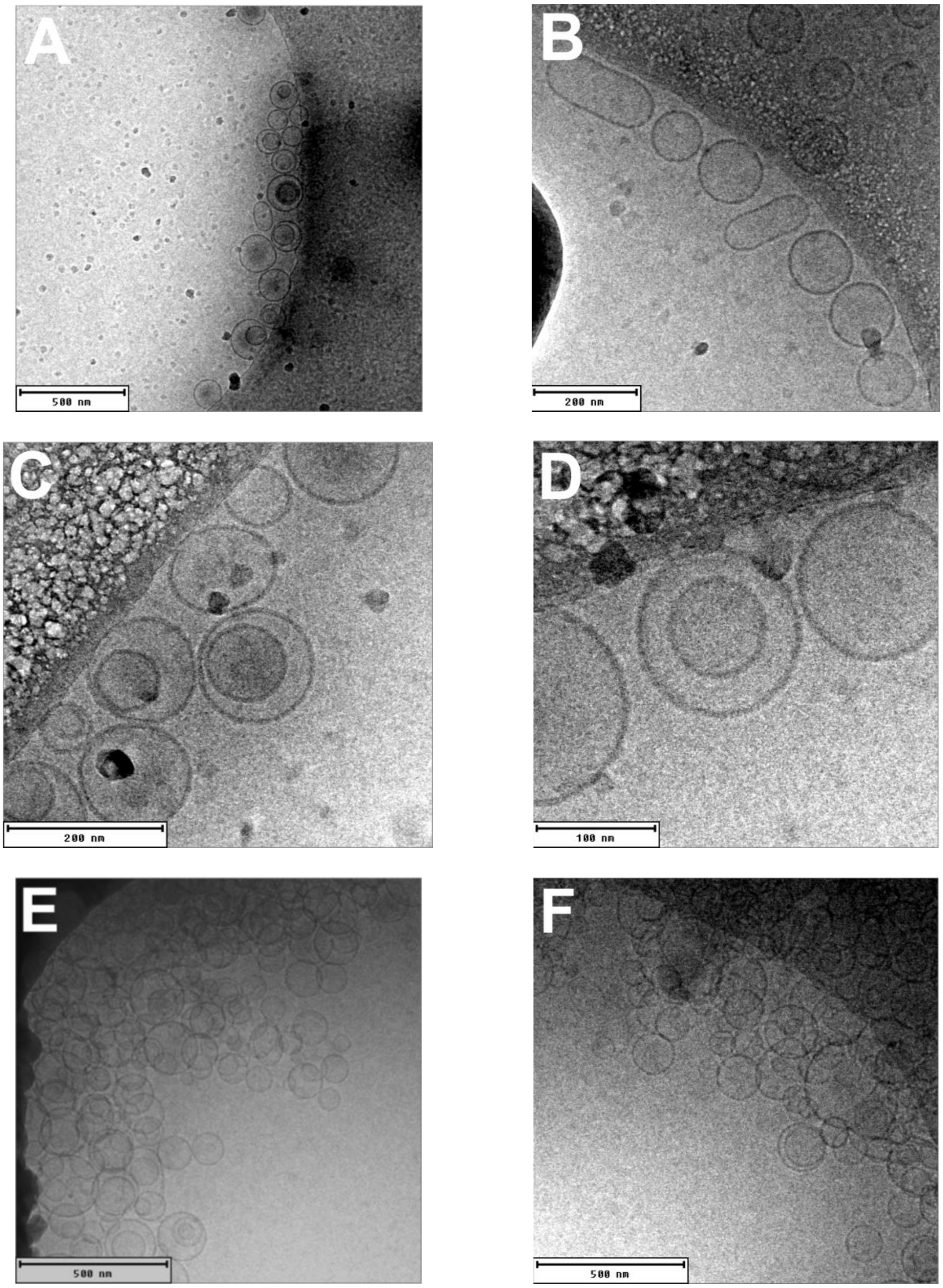
A
500 nm
B
200 nm
C
200 nm
D
100 nm
E
500 nm
F
500 nm

Figure 37: Cryo-TEM images of two extruded liposomal dispersion formed out of PLs. (**A**-**D**) depicting blank formulations that were composed of DSPC/cholesterol as lipids and GHP 3 as carrier. (**E**-**F**) Formulations containing fenofibrate as drug.

4.2.3 Characterization of liposomes before and after extrusion in comparison with conventional round bottom flask method

After reconstitution of proliposomes consisting of both, water-soluble and water-insoluble carriers, the crude liposomal dispersions were investigated regarding liposomal size, PDI and ZP. The same analytical tools were applied after 11 extrusion steps and results were compared with the conventional round bottom flask preparation method. One additional step of the formulations containing water-insoluble carriers was the decantation of the insoluble material after formation of liposomes.

The size of crude liposomes produced with water-insoluble carriers was comparable to the size results yielded by the round bottom flask method (~ 8 µm). They are depicted in stripped columns in **Figure 38**. Graph **A** shows the d_{50}-values of the volume-based size distribution for vesicles made of PLs with water-insoluble carriers. Water-soluble carriers are shown in graph **B**.
A clear trend was observed: the use of smaller water-insoluble carriers also favored the formation of slightly smaller vesicles (**A**) whereas with larger water-insoluble carriers noticeably larger vesicles could be formed. All formulations with water-insoluble carriers showed a larger vesicle size than the reference batch using the round bottom flask method. The insoluble carrier material made of glass beads might show more similar properties to the round bottom flask because there is also no simultaneous dissolution process. Slightly bigger liposomes were prepared using water-soluble carriers with a mean diameter of ~ 9 µm (**B**). All formulations are larger than those shown in graph **A**. Additionally, all formulations with water-soluble carriers resulted in larger vesicle size than the reference formulation (round bottom flask method). The effect of carrier size on the size of the liposomes seemed to be inverted in contrast to water-insoluble batches. Carrier materials of sucrose with a size of ~ 2400 µm and 2900 µm (GHP 4 and GHP 5) gave the impression to be more suitable to form liposomes in a size range of the comparative round bottom flask method. When comparing different sugar carriers with the same carrier size of ~ 220 µm *i.e.* sucrose (GHP 2), xylitol (xyl) and sucrose-lactose (suc-lac) there might be an effect of the sugars' solubility (sucrose: 2000 mg*ml^{-1}; xylitol: 650 mg*ml^{-1}; sucrose-lactose: 520 mg*ml^{-1}). The carrier material with the portion

of lactose might result in a lower solubility. Therefore, it can be concluded that the better the solubility of the water-soluble sugar the smaller the vesicles formed.

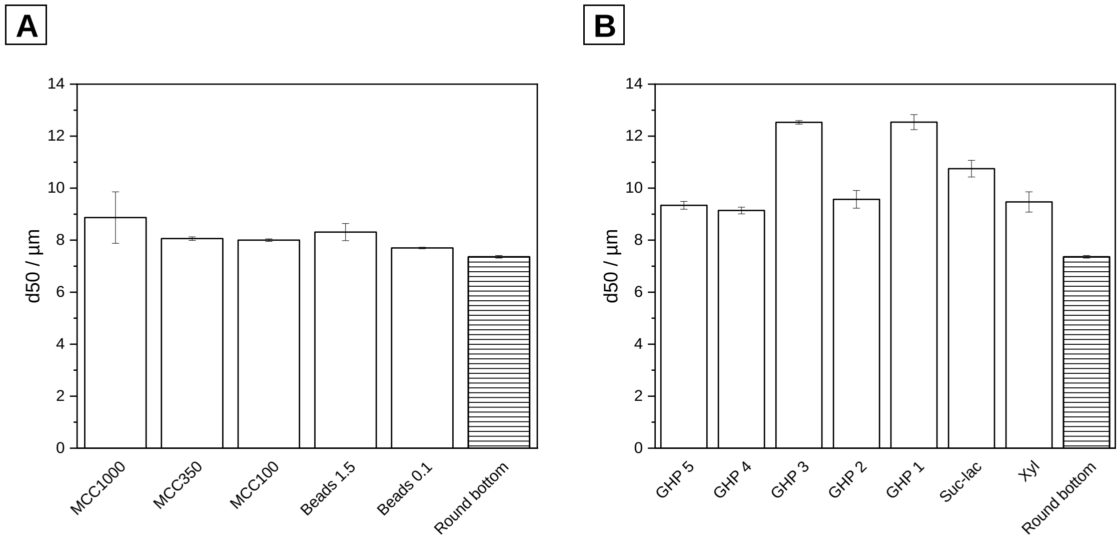

Figure 38: D_{50}-values of the volume-based size distribution (n = 3, 2σ). All samples were treated with ultrasonic sound for one minute. Striped columns indicate the production of liposomes *via* round bottom flask method.
(**A**) Liposomal size (d_{50}-value) of vesicles made of PLs with water-insoluble carrier. (**B**) Overview of d_{50}-value of liposomes using different kind and sizes of water-soluble carrier in comparison to the conventional round bottom flask method.

Figure 39 shows the results of the DLS measurements after extrusion for both, water-soluble carrier type (**B**) like sucrose, sucrose-lactose and xylitol and water-insoluble (**A**) as MCC beads. The first extrusion step through a 0.4 µm polycarbonate membrane of the three MCC batches resulted in a decrease in vesicular size (430 nm - 380 nm): the smaller the carrier size, the smaller also the Z-ave measured. Additionally, the liposomes showed increased diameter sizes compared to the vesicles formed *via* round bottom flask method. This tendency was also observed for the glass beads' batches (beads 1.5 mm/beads 0.1 µm). With a PDI higher than 0.2, a polydisperse size distribution of extruded dispersions can be started. Furthermore, a certain irregularity for the water-insoluble batches could be observed. This might be the result of potential carrier left overs in the liposomal dispersion which have been separated by decantation. After extrusion through a 0.1 µm membrane, the vesicles increased in size compared to the membrane's pore size and reached values of about 150 nm. For all batches, the

PDI was in an acceptable range higher than 0.2 and represented a polydisperse size distribution. Additionally, after the second extrusion step there was less cloudiness of the liposomal suspension, which might be an indicator for the retention of the carrier particles. The formulations using water-soluble carriers all showed vesicles with a size of 260 - 300 nm, well below the membrane pore size of the 400 nm membrane. All samples showed smaller sizes than the reference batch extruded (round bottom flask method). After the second extrusion step, accomplished liposomes had a size of 150 nm and a excellent PDI < 0.1. Ong *et al.* [58] reported on this phenomenon. They prepared vesicles that increased in size compared to the pore size of less than 0.2 µm. On the contrary, samples with bigger pores (0.2 µm and above) resulted in a smaller mean diameter of liposomal sizes in comparison to the one of the membranes. This can be explained by a given elasticity of the liposomes [59]. Carrier roughness could also influence liposomal size. Additionally, proliposomal formulations manufactured according to the coating method showed the same results after extrusion treatment as observed for the conventional production technique. There is no limitation for the proliposomal batches which makes it very easy to treat them in the same manner as already shown for extruded liposomes produced *via* round bottom flask method.

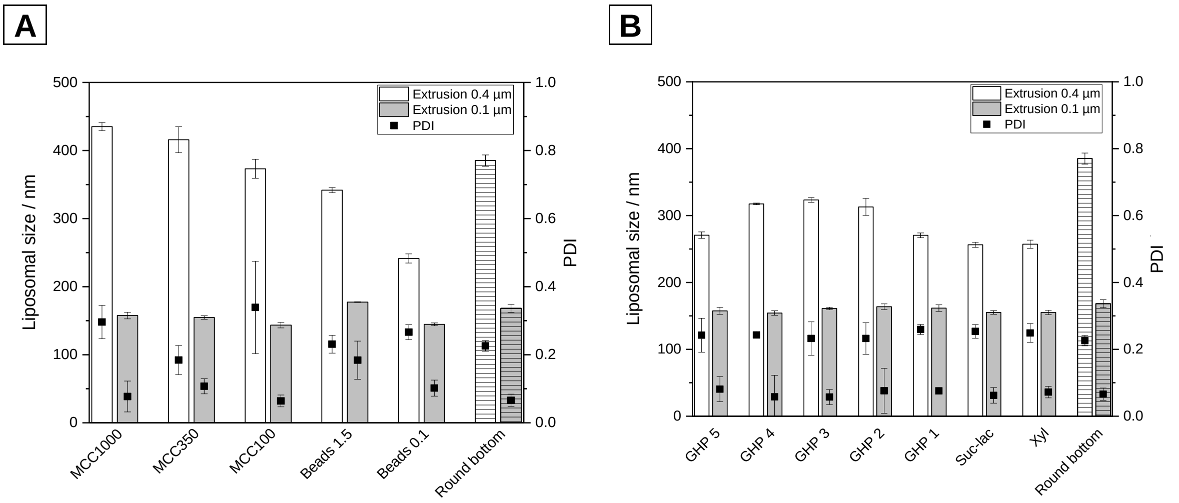

Figure 39: Vesicular sizes after liposomal extrusion with a 0.4 µm and a 0.1 µm polycarbonate membrane filter. Vesicles were prepared out of PLs containing (**A**) water-insoluble and (**B**) water-soluble carriers (n = 3, 2σ).

ZP measurements are presented in **Figure 40**. This analytical variable is often used as key tool in order to understand dispersion and aggregation processes for liposomal applications [199]. In general, there is a correlation between ZP and liposomal size of untreated samples. This effect is explained for the batches using sucrose as carrier material: liposomes formed from GHP 3 and GHP 1 have the lowest ZP with a value of - 6 mV but favor the formation of relatively large vesicles of about 12 µm. Compared to sugar-based formulations like sucrose batch with a carrier size of 1200 µm (GHP 1), the sucro and xyl batches showed the same tendency. However, many preparation procedures like extrusion using shear forces aim to form smaller vesicles that involve less aggregation trends and consequently higher ZP values. Furthermore, with increased ZPs, increased storage stability of the dispersion is guaranteed. Dispersions with ZP levels > |30| mV are considered to have a good stability, with values > |60| mV the optimum for appropriate electrostatic stabilization is reached [200]. The formulations in this study were in a range of - 6 mV to - 19 mV which could indicate a limited flocculation The ZP can easily be influenced by the selection of phospholipids, *i.e.* the addition of charged PLs has a substantial effect on the ZP. The liposomes produced with the conventional round bottom flask method showed the same ZPs. Even lower, negative values were measured for the batches GHP 2, suc-lac and xyl.

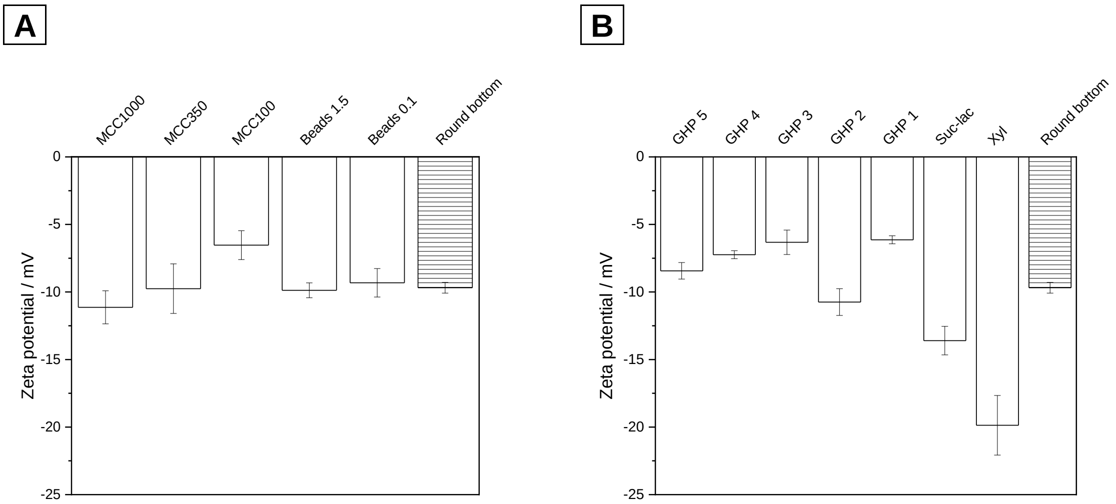

Figure 40: ZPs of untreated liposomal dispersions that were reconstituted out of (**A**) water-insoluble and (**B**) water-soluble carriers containing PLs (n = 3, 2*σ*).

For water-insoluble MCC batches a correlation between ZP and liposomal size (extruded and raw dispersion) can be observed. The smaller the MCC carriers the smaller the vesicle and the lower the ZP. No significant correlation was seen for the water-soluble carrier batches.

4.2.4 Stability study of liposomal formulations

PLs containing water-soluble carriers were investigated in order to analyze their storage stability up to 6 months of storage. All proliposomal formulations had the same lipid-solution composition but different water-soluble carriers for the materials used (*c.f.* **Table 18**). Samples were filled in glass vials, tightly closed with a screw cap and paraffin film in order to avoid evaporation and stored in conditioning cabinets at 40 °C. Liposomal properties as size, PDI and ZP were analyzed at different time points: immediately after preparation (t_1 = 0 weeks) as well as after t_2 = 8 weeks and t_3 = 24 weeks. Within this time frame, a constant quality of the reconstituted liposomes out of PLs during storage was achieved. This confirms the conformity in the preparation process and shows the successful transformation of proliposomal materials to liposomal vesicles. In general, PLs maintained their initial appearance.

Figure 41 presents the liposomal size after the rehydration of PLs. At the beginning of stability study (t_1 = 0 weeks), a broad size distribution of all samples was observed. Liposomal size for 0.4 µm extruded samples (**A**) was between 265 nm - 330 nm and a division into two size values was discernable. Here, liposomal size for carrier material bigger than ~1300 µm (GHP 2-5) resulted in a liposomal size above a value of 300 nm. Whereas the sucrose (GHP 1), xylitol and sucrose-lactose carrier smaller than 1300 µm led to smaller liposomes at t_1 = 0 weeks.

After 8 weeks (t_2) of storage, the liposomal size of the formulation extruded with a 0.4 µm membrane resulted in a decrease between 256-323 nm. The reduction in liposomal size continued for almost all samples and created a narrow liposomal size range between 263 - 307 nm after 6 months. However, two exceptions could be observed. Both batches, PLs with sucrose carriers (~ 1,200 µm; GHP 1) and sucrose-lactose carriers (1,250 µm; suc-lac), showed an increase in liposomal size which indicated fusion and aggregation of liposomes.

Aside, scheme **B** depicts the behavior for formulations extruded through a 0.1 µm polycarbonate membrane. In contrast there was a slight increase observable in liposomal size within a time frame up to 24 weeks (t_3) reaching a value of 154-160 nm for the sucrose carriers (800 – 3,300 µm; GHP 1-5), of 157 nm for the sucrose-lactose type (1,250 µm; suc-lac) and of 153 nm for the xylitol carrier (1,250 µm; xyl). Though strong influences depending on the pore size of the extrusion membrane (either 0.1 µm or 0.4 µm) could be noted, liposomal dispersions were still stable in size during storage in a conditioning cabinet at 40 °C for 6 months. The formulations revealed liposomal sizes < 160 nm and offer the possibility to be used as drug loading materials with a physical stability for half a year.

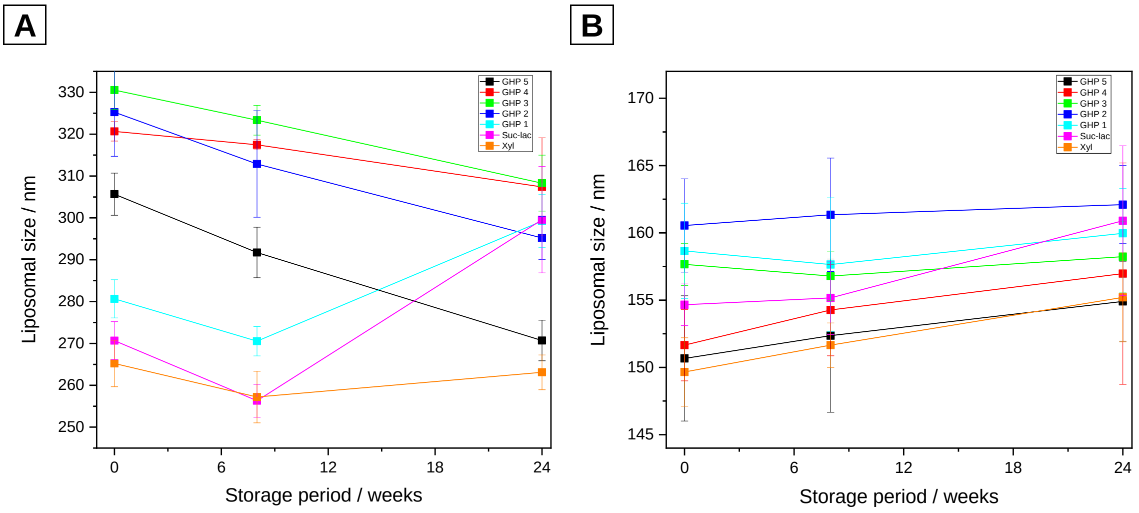

Figure 41: Liposomal size after extrusion through 0.4 µm (**A**) and 0.1 µm (**B**) polycarbonate membrane filters during a storage time of 24 weeks at 40 °C in conditioning cabinet. Please note different axis scales (n = 3, 2σ).

The size distributions of rehydrated PLs are depicted in **Figure 42**. No substantial changes in the PDI were measured after 8 weeks of storage. The PDI values remained for 0.4 µm extruded samples (**A**) below 0.3 at any point of the experiment. Also, with an additional extrusion step through a 0.1 µm filter (**B**), PDI values were < 0.1 which indicated a very narrow size distribution. However, they slightly increased after 24 weeks of storage but were still in the framework for an acceptable and stable proliposomal formulation. A big advantage is the missing tendency for liposomal fusion or aggregation as it can be observed for aqueous liposomal dispersions. All in all, the results of size distribution measurement were in good correlation with the measurements at $t_1 = 0$ weeks. They confirmed once more the high stability of the PLs for a period of 6 months giving comparable results upon extrusion for size and size distribution.

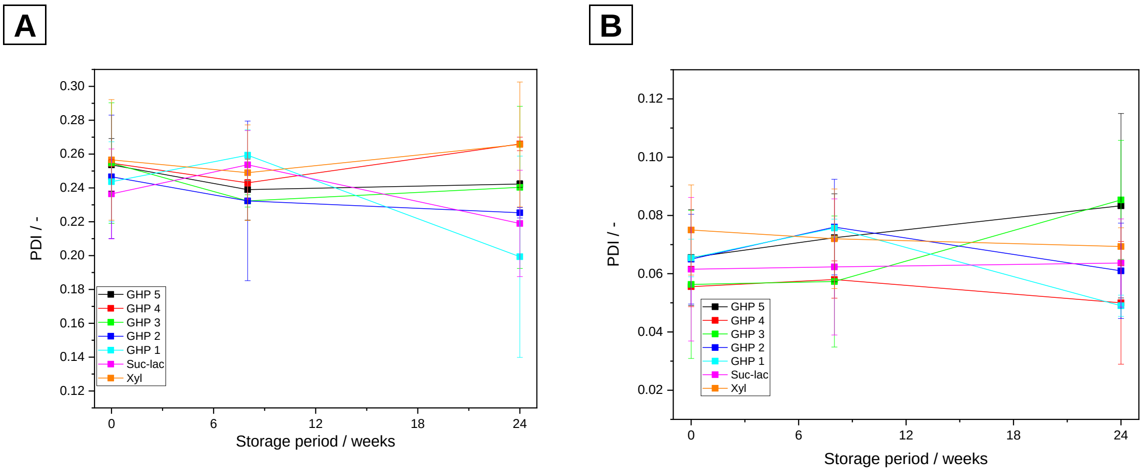

Figure 42: PDIs after extrusion through a 0.4 µm (**A**) and a 0.1 µm (**B**) polycarbonate membrane over a storage time of 24 weeks (40°C). Please note different axis scales (n = 3, 2σ).

Figure 43 displays the ZP of liposomal dispersions for a storage stability study of 6 months. The measured ZP for 0.4 µm extruded samples (**A**) was in the range of - 9 mV and - 23 mV. Graph **B** shows a potential of about - 5 mV and -17 mV at the beginning of the stability storage ($t_1 = 0$ weeks). Over the period of 24 weeks, the ZP of all samples increased and led to more negative values. No correlation between the stability of liposomes relating to size or distribution and the ZP could be drawn. Zeta potentials were constantly irrespective regarding their size or size distribution.

In summary, the storage of PLs consisting of water-soluble carriers had no influence on the size for the liposomes formed or size distribution. Considering ZP, the stability of the liposomal dispersion was enhanced. Xylitol (1,250 µm; xyl) and sucrose carrier (~ 2,900 µm; GHP 5) seemed to be the most stable formulations in terms of size of the liposomes formed upon rehydration regarding both, extrusion through a 0.4 µm filter and the subsequent extrusion step through a 0.1µm membrane. Moreover, the PDI of these carrier types remained stable and indicated a narrow size distribution, whereas ZP increased up to a value of ~ - 20 mV. The stability study supports the good stability of the PLs over a period of at least six months. These results might indicate a low drug leakage, giving a high concentration of encapsulated API at the site of action even after longer storage times

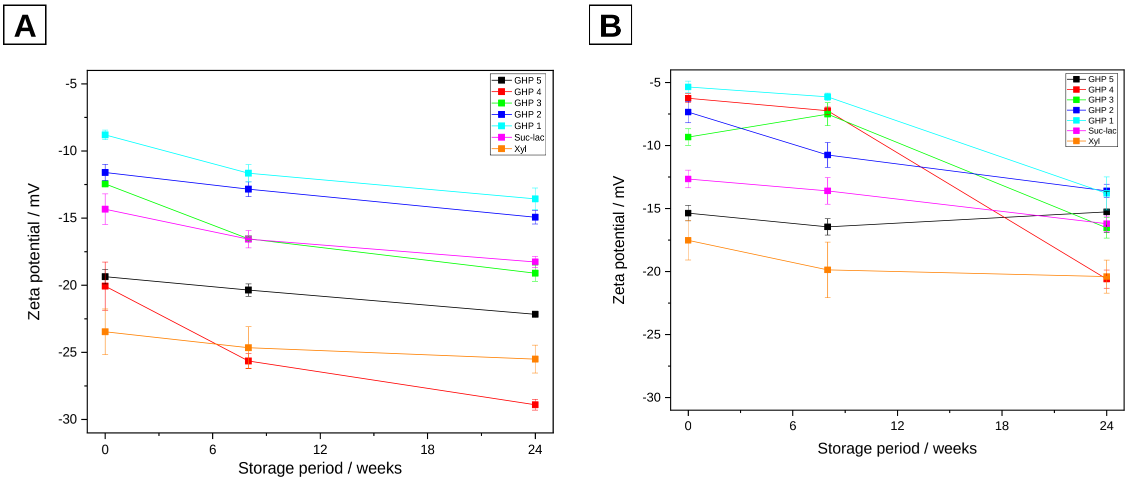

Figure 43: Liposomal ZPs after extrusion through a 0.4 µm (**A**) and 0.1 µm (**B**) polycarbonate membrane during a storage time frame of 24 weeks. (n = 3, 2σ).

4.2.5 Influence of carrier material, shape and carrier-to-lipid ratio

The standard coating formulation used was with a DSPC-to-cholesterol molar ratio of 4:1, lipid-to-sucrose carrier ratio of 1:10 (see also chapter **3.2.2.1 Coating method**) was varied regarding (i) carrier material and (ii) carrier-to-lipid ratio. The latter was modified from 10:1 in 5:1 (“5 to 1”). Furthermore, two tableting excipients, Granulac 200 (“Lac D80”) and spray dried lactose (“SD Lac”), were tested since both are well established adjuvants in tablet formulations and might serve as alternative carrier materials for the production of proliposomal granules. **Figure 44** shows SEM images of either Lac D80 (**A**, **B**) or SD Lac (**C**, **D**) in form of raw carrier materials and PLs. For both excipients, a waxy lipid cover was not detected as it was already observed for the standards of the spherical carriers. Moreover, the product had a coarse-grained look with a high similarity to the genuine granules before coating.

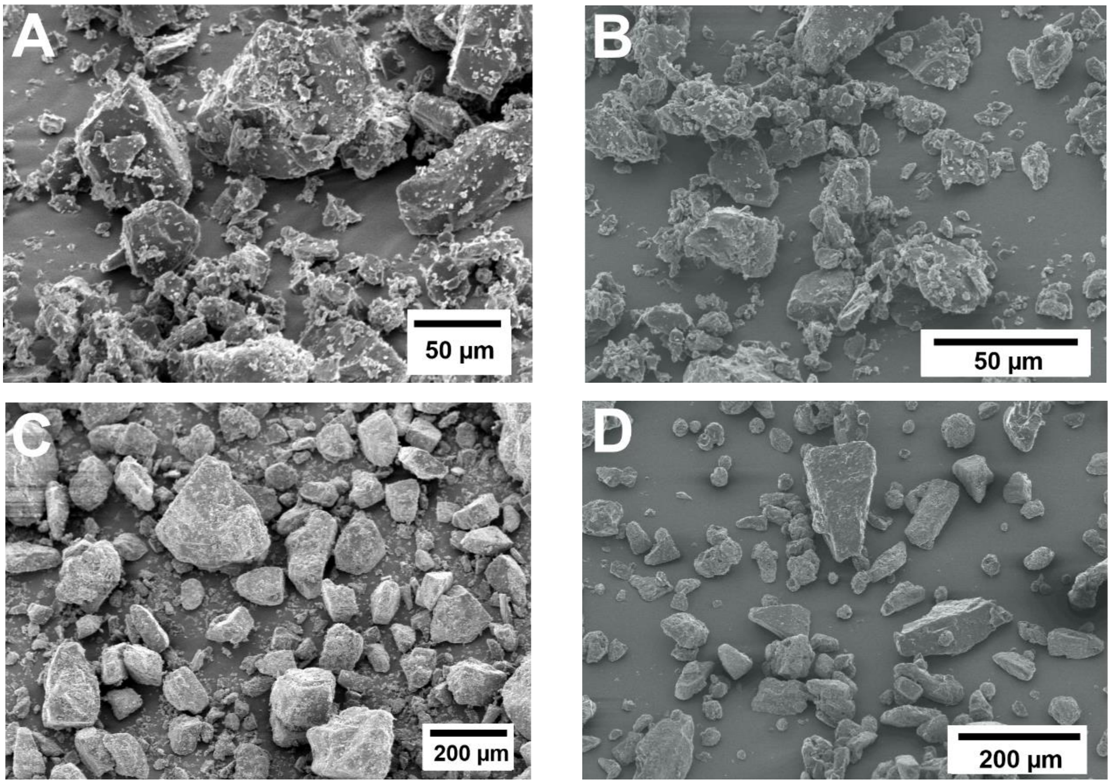

Figure 44: SEM images (500x magnification) of the excipient Lac D80 in different modifications: (**A**) before and (**B**) after coating as well as SD Lac in (**C**) untreated state and (**D**) with lipid cover.

Table 19: Liposomal size measurements of the different raw dispersions after ultrasonic sound treatment for one minute (n = 3; 2σ)

Sample	d_{10}	2σ	d_{50}	2σ	d_{90}	2σ
10:1*	3.21	0.11	9.34	0.15	33.96	0.46
5:1*	2.81	0.03	7.36	0.05	18.27	0.02
Lac D80	3.80	0.02	10.28	0.14	36.74	3.47
SD Lac	2.08	0.08	11.17	0.53	143.30	36.83

*sucrose carrier ~ 2,900 µm (GHP 5)

An overview of the results of the measurements of the liposomal size of the raw dispersions is given in **Table 19**. By varying the carrier-to-lipid ratio from 10:1 to 5:1, a smaller d_{50}-value (~ 7 µm) was measured in comparison to liposomes formed out of the standard proliposomal formulation with the same carrier type (**4.2.3**). In this case, the size range was between 9-12 µm. Thus, a variation in lipid-to-carrier ratio seems to be a promising approach when focus is put on the potential factors which have an effect on the size of the vesicles upon rehydration.

By changing the type of carrier with a lipid-to-carrier ratio of 10:1, a liposomal size within 10 - 11 µm was confirmed. Samples prepared out of SD Lac showed a relatively high d_{90}-value with about 143 µm which indicates an agglomeration of the vesicles.

In summary, carrier round-shaped were more suitable for smaller and more stable liposomes promoted by the uniform surface. Nevertheless, it was also possible to form liposomes using granular carriers.

4.2.6 Effect of lipid species on size and number of liposomes

Four different lipids were chosen as model lipids in order to check the influence of different lipid species on vesicular size and total number of liposomes per mm^3 of the crude dispersions. The lipids chosen comprise: (i) DSPC (as reference; uncharged; $T_m = 55$ °C), (ii) egg-PC ($T_m = -7$ °C), (iii) DOTAP-Cl (cationic; $T_m < 5$ °C) and (iv) HSPC ($T_m = 53$ °C). The ratio of lipid-to-cholesterol was set to 4:1, with a total of 17.1 $mg{*}ml^{-1}$ and 4.3 $mg{*}ml^{-1}$ of lipid and cholesterol, respectively. The carrier-to-lipid ratio was set to 10:1. Liposomes that were loaded with either fenofibrate or ibuprofen had a total API concentration of 10.71 $mg{*}ml^{-1}$. **Figure 45** shows polarization microscope images of the four different formulations with changing kind of lipid. All images prove the presence of liposomes by visualizing the prominent Maltese crosses when using a polarized light filter.

The standard lipid DSPC resulted in liposomes with d_{50}-values of 9 µm (**Figure 46 A**) the values measured for the lipids DOTAP and HSPC with d_{50}-values are 7 µm and 10 µm, respectively. These two lipids are in a range of size which is comparable to that of DSPC with the vesicles formed from the DOTAP samples show clearly larger standard deviations. In contrast, the formulation containing egg-PC resulted in a distinct smaller size of raw vesicles of only ~ 2 µm. Soema *et al.* performed a DoE study of liposomal lipid composition on the physicochemical characteristic lipid size. Next to DOTAP also egg-PC was investigated. Egg-PC was suitable for stable liposomal formulation due to not being influenced by most responses like liposomes' size or charge. Furthermore, liposomes containing DOTAP were bigger in size than formulations with less or without this component [201]. In contrast to this work, the round bottom flask method was used including an extrusion step which resulted in the formation of SUVs. Next to the raw lipid DOTAP also the lipids DOTAP, DOPE, egg-PC and DC-cholesterol were mixed in different ratios. Comparing d_{50}-values in our study with the total number of liposomes per mm^3, there was a good correlation between these two parameters (**B**): the smaller the size, the more vesicles were counted. The number of vesicles was calculated counting liposomes in 80 squares and grossing up for the whole sample (see chapter **3.2.3.4 Thoma cell counting chamber**). A total number of about 72,000 liposomes was estimated for egg-PC. This is considerably higher than with the standard lipid DSCP, where only 21,400 liposomes were calculated. Summing up the lipid components, there was the same amount of lipid available in each formulation. Hence, the smaller the size of the vesicles depending on the individual lipid components effect on the size the larger the total amount of liposomes which were formed. Compared to HSPC and DOTAP formulation the liposomal size was in a range of 6 - 10 µm which might result in a larger number of vesicles. Nevertheless, the total number of liposomes showed the lower level than for egg-PC and DSPC (10,000 - 15,000 vesicles). This fact might indicate the formation of agglomerates which is also shown on image **C** for the lipid DOTAP, **Figure 45**.

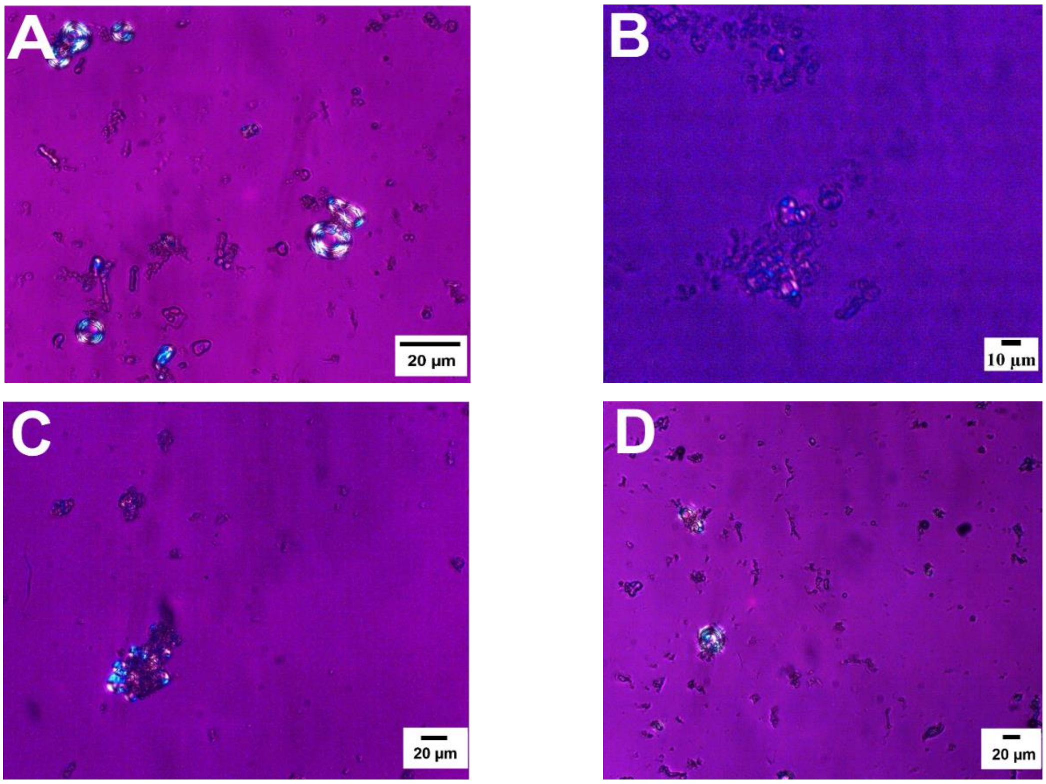

Figure 45: Polarization microscope images as proof of liposomal presence. Dispersions with four different types of lipids were characterized regarding the verification of liposome formation. The various lipids are as followed: (**A**) DSPC; (**B**) egg-PC; (**C**) DOTAP; (**D**) HSPC.

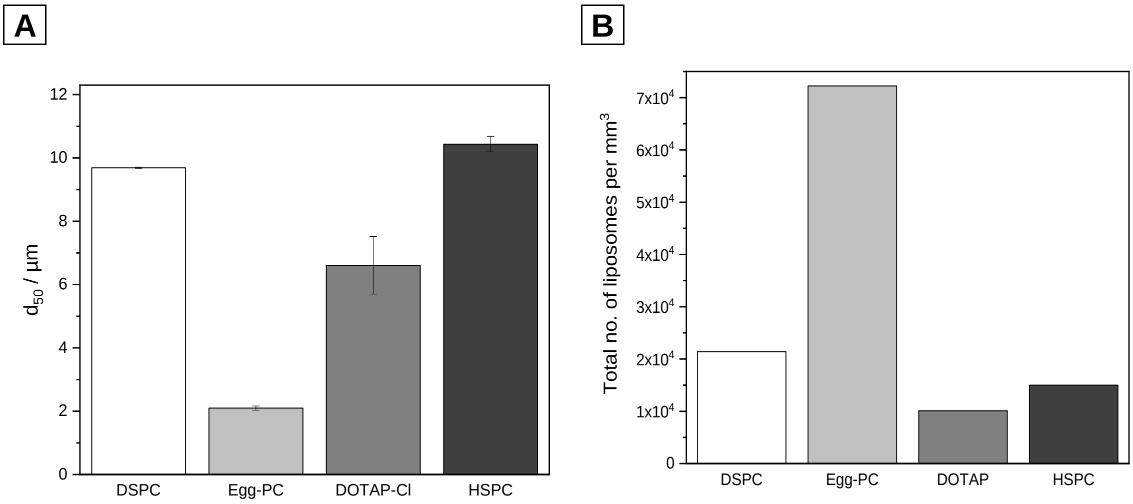

Figure 46: Overview of LD measurements with respect to (**A**) the four different types of lipids. The total number of liposomes per mm^3 is represented in graph (**B**).

Due to the high number of vesicles and the excellent liposomal sizes of the egg-PC formulation, the effect of incorporated API was investigated. Both APIs fenofibrate as well as ibuprofen were added to the formulation with egg-PC. With a liposomal size of 4 µm, the formulation with fenofibrate indicated integration in the membrane of the API due to its lipophilicity. Fenofibrate had a substantial effect on the size measured upon rehydration when compared with the blank. This might be a result of fenofibrate becoming an integral part of the membrane, thus increasing the amount of “wall” constituents in the formulation. This could have an impact on the liposomal size and lead to larger vesicles. In contrast no effect on size was observed for the ibuprofen containing solution. Since ibuprofen is likely to be dissolve in the aqueous compartment. This might result in a better EE for the API fenofibrate than for ibuprofen, which is presented and discussed in chapter **4.2.8**. The size of fenofibrate containing liposomes was again increased compared to liposomes with ibuprofen. Ibuprofen seemed not to be an integral part of the bilayer - as is fenofibrate - its effect on the size is expected to be reduced. As a result almost, no effect on the size of the liposomes was measured in the presence of ibuprofen.

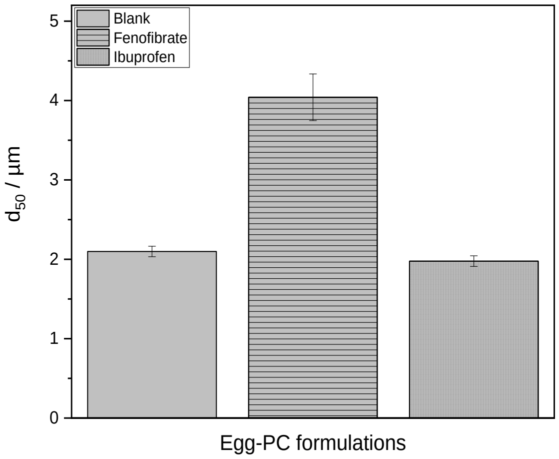

Figure 47: Overview of LD measurements with focus on drug loaded egg-PC formulations containing ibuprofen and fenofibrate.

4.2.7 Comparison of liposomal size with modified round bottom flask method

The conventional round bottom flask method was modified to allow for a better comparison with the coating method in terms of carrier surface. First, a water-soluble, sucrose-based carrier was added to the flask with an ethanolic lipid solution (batch “mod flask”) in order to offer a larger surface area for the lipids to dry on compared to the classical round-bottom flask method. The reconstitution medium was water. In another set-up, sucrose-based carrier material was dissolved in water with a concentration of 10 % (w/w) in order to evaluate potential effects of the reconstitution solution on the liposomes (batch “mod solution”).

Figure 48 depicts the crude vesicles visualized *via* polarized light microscopy. The liposomes were big in shape and showed a size range of ~ 40 µm which is slightly bigger compared to liposomes produced by coating method (~ 12 µm). The characteristic Maltese cross appearance for the verification of successful liposome formation was observed.

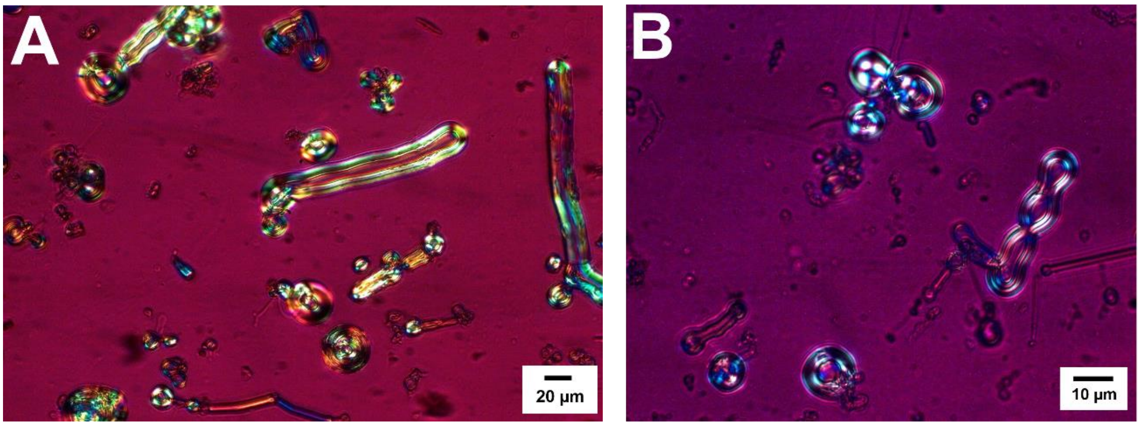

Figure 48: Comparison of the modified preparation methods: (**A**) sample with 6 g of water-soluble, sucrose-based carrier produced *via* round bottom flask method and (**B**) image of sample reconstituted with 10 % (w/w) sucrose carrier solution.

Size determination *via* optical analysis was confirmed by the LD measurements. Without ultrasonication treatment, the vesicles of the batch “mod flask” had d_{50}-values of 39 µm. They were comparable in size to the “mod solution” formulation with a d_{50}-value of about 42 µm. This is in contrast to the liposomes manufactured *via* the conventional round bottom flask method which gave much smaller liposomes with a d_{50} of 11 µm. An interpretation of these results hypothesizes the formation of agglomerates. Furthermore, the augmented water-soluble carrier was accumulated in the middle of the round bottom flask during rotation and inhibited the formation of a complete dried lipid film. Overall, a modification of the conventional preparation procedure showed no benefit in comparison to the established approach. After ultrasonication treatment of the samples, all batches were in a liposomal size range between 8 and 15 µm independent of the method chosen. For the PLs produced using the coating method there was the tendency to form aggregates direct after addition with aqueous medium that can be reduced by ultrasonication.

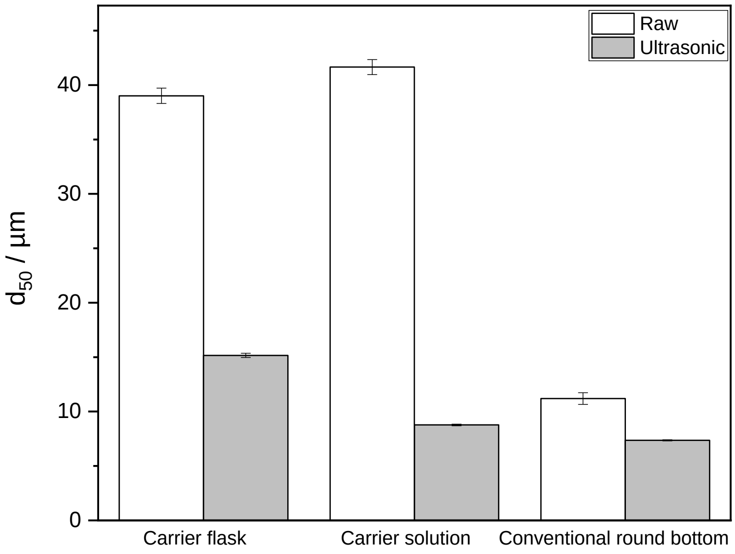

Figure 49 LD measurements of conventional round bottom flask method (reconstitution only with water) and modified versions. D_{50}-values were measured directly after reconstitution and ultrasonication treatment for one minute.

4.2.8 Tableting of proliposomal granules

By adding different tableting excipients to proliposomal granules, the production of tablets was investigated. The finished tablets were examined with respect to the formation of liposomes after contact with water. The vesicles formed out of granules and tablets were treated analogously as described in previous chapters and characterized before as well as after extrusion.

In this study, fenofibrate and ibuprofen were chosen as two possible representatives for poorly soluble drugs for proliposomal granules. The production process of PLs is described in chapter **3.2.2**. As carrier, Tablettose® 80 was chosen due to its excellent properties as filler. After the addition of different tableting excipients (see chapter **3.1.3 Excipients and reagents**), the tableting blend was compressed to form tablets on a single punch press (see chapter **3.2.9**). **Table 20** summarizes the composition of the individual batches prepared. Furthermore, photos of the compressed tablets with (1) ibuprofen, (2) fenofibrate or a (3) blank formulation without drug loading were taken in order to show the successful compression process (see **Figure 50**).

Table 20: Overview of produced batches (sample 1-3) with lipid and API concentrations, respectively.

Batch no.	Model substance	API concentration / mg*ml^{-1}	DSPC to cholesterol / mg*ml^{-1}	Lipid-to-carrier ratio	Amount of PLs in tableting blend / %
1	Blank	-	17.1 : 4.3	1:10	66.0*
2	Ibuprofen	16.1	17.1 : 4.3	1:10	66.0*
3	Fenofibrate	16.1	17.1 : 4.3	1:10	66.0*

* 25.0 % VIVAPUR® 301, 3.0 % VIVASOL®, 1.8 % Magnesium stearate, 3.6 % Talc, 0.6 % Aerosil® Type 200

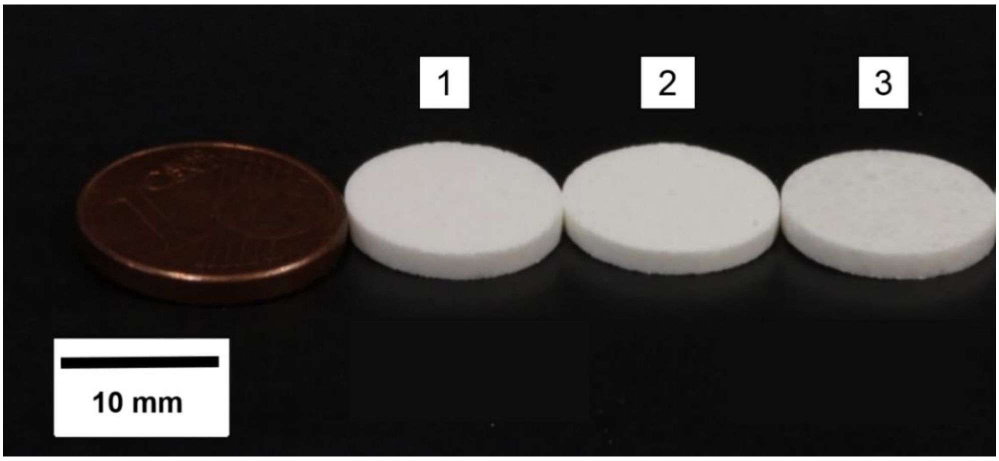

Figure 50: Picture of pressed proliposomal tablets with a diameter of 13 mm, an adjusted mass of 250 ±10 mg and a hardness > 30 N. The tablets include (1) ibuprofen; (2) fenofibrate and (3) a blank formulation without drug loading. A European cent coin is photographed as scale reference.

After compression, the tablets were rehydrated in 10 ml water in order to form MLVs out of the solid dosage form. Therefore, **Figure 51** shows the result after rehydration for both, proliposomal granules and tablets. Obviously, liposomes were formed in all samples examined. The liposomal dispersions from granules and tablets showed a similar appearance. They exhibited a spherical shape when observed under the microscope equipped and showed the characteristic Maltese crosses. The concentration of vesicles in both dosage forms was also comparable. However, some vesicles deviated from the described appearance. Liposomal size was about ~ 10 µm as evaluated using an object micrometer disk (24 mm diameter x 1.5 mm). Image **A** and **B** show liposomes of the blank formulations. Liposomal aggregates of the blank proliposomal granules were observed up to a size of several micrometers whereas in the blank formulation of the tablets no agglomerates were noted. By comparing the formulation containing fenofibrate (**C**; **D**) with those loaded with ibuprofen (**E**; **F**), a reduction in the number of vesicles was observed.

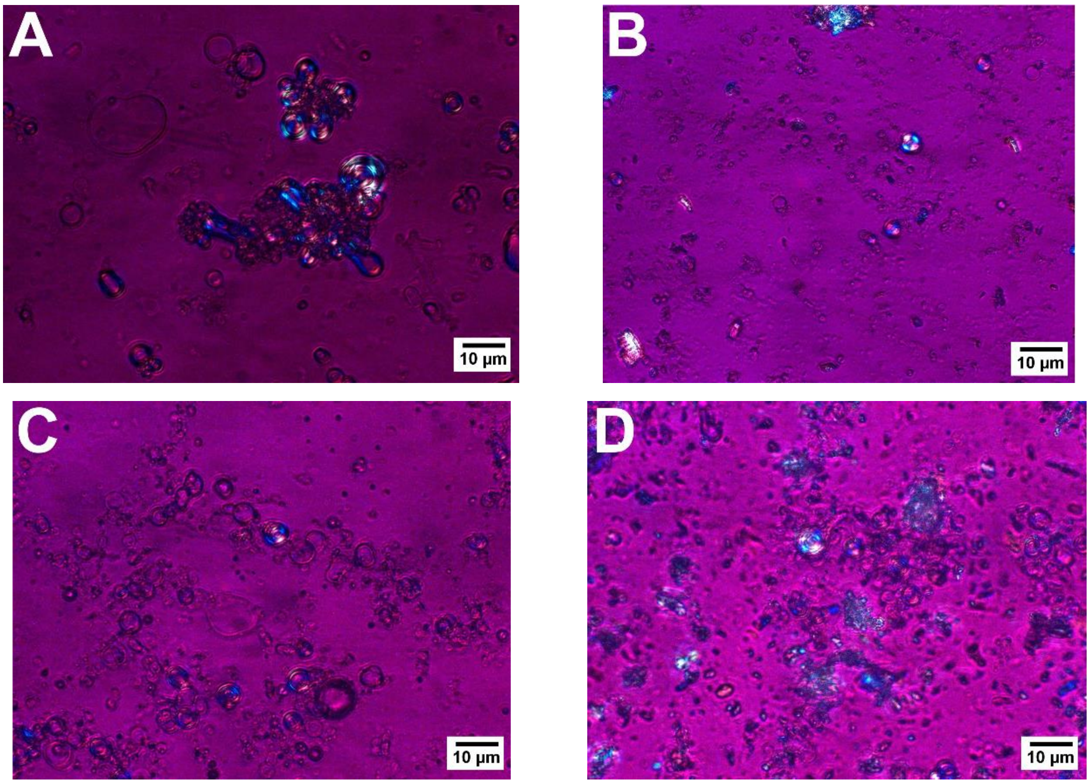

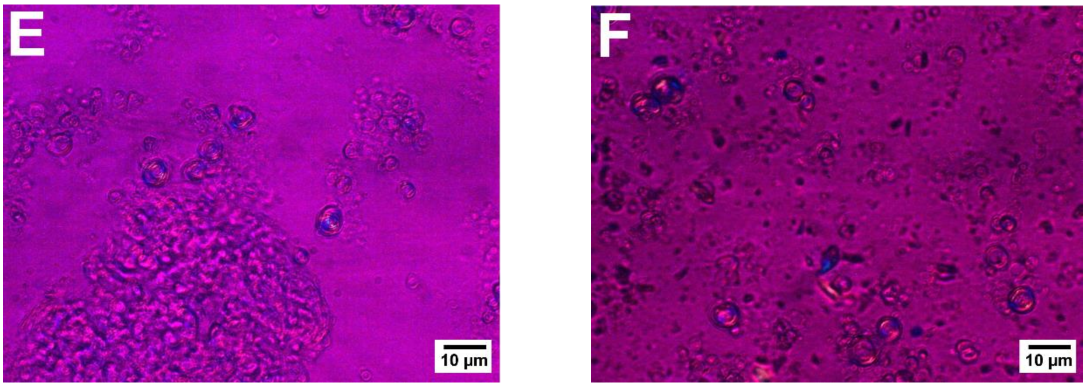

Figure 51: Photomicrographs of liposomal dispersion.
(**A**) Blank - reconstitution of PLs; (**B**) Blank - reconstitution of tablets; (**C**) Fenofibrate - reconstitution of PLs; (**D**) Fenofibrate - reconstitution of proliposomal tablets; (**E**) Ibuprofen - reconstitution of PLs; (**F**) Ibuprofen - reconstitution of proliposomal tablets.

Figure 52 summarizes the vesicle size directly after reconstitution *i.e.* the raw liposomal dispersion without any further extrusion step as determined by LD. The mean particle size (d_{50}-value) is in the range of 10 µm which is in good agreement with the results of optical examination with polarized light microscopy. Regarding liposomal size for the PLs, the blank batch showed larger vesicles (~ 15 µm) than the batches containing API. The use of the non-spherical carrier such as lactose D80 and spray dried lactose resulted also in bigger liposomes with a size value of also 10 - 11 µm (chapter **4.2.5 Influence of carrier material, shape and carrier-to-lipid ratio**). The tablets with fenofibrate formed slightly smaller liposomes compared to PLs granules, analogously to the blank batch. In contrast to that effect, the formulation containing ibuprofen showed the reverse effect with bigger liposomes formed out of tablets after rehydration. The API (ibuprofen or fenofibrate) had a significant effect on the size of vesicles formed. Furthermore, compression and tableting excipients had an influence on liposomal size.

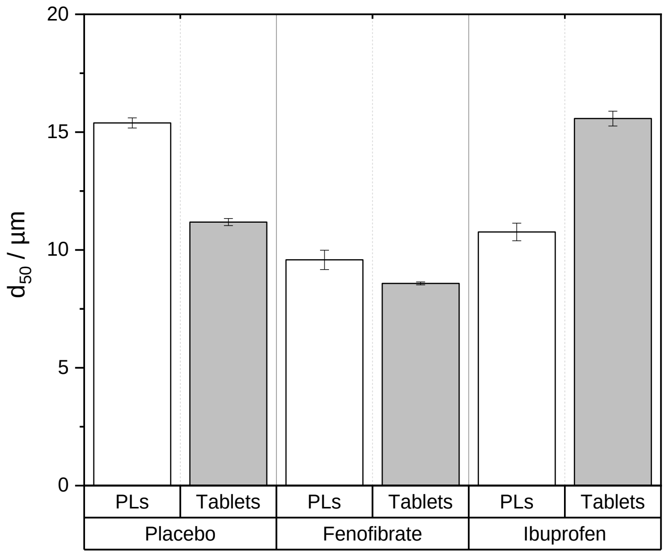

Figure 52: D_{50}-value of the volume-based size distribution of the three different batches blank, fenofibrate and ibuprofen (n = 3, 2*σ*).

All in all it was possible to manufacture tablets with the PLs. Depending on the API the tabletting procedure had an effect on MLVs' size. The proliposomal granules were compressible and the targets of tablet weight and hardness could be reached reproducibly. Since the PL powders might have a lubricating effect, the lubricant magnesium stearate added might not have been necessary. However, this was not investigated in this study.

In another experiment the liposomes formed *in situ* after hydration of PLs in granules or tablets were extruded in a subsequent step upon rehydration. **Figure 53** represents the liposomal size after extrusion of the proliposomal granules and tablets, respectively. The PL powder particles were separated by adjuvants and in consequence they might have no effect on the characterization. After this standardized step, the vesicle size resulted in a Z-ave of 150 nm. As described before, liposomes were larger than the pore diameters of the polycarbonate membrane filters (100 nm). This phenomenon can be explained by a given elasticity and “shapeability” of the vesicles [59]. The Z-ave values of the blank and the fenofibrate formulation were higher than there for liposomes derived from the tablets. This reflects the results of the LD measurements as shown in for the non-extruded liposomes. The compression of the placebo batch had little effect on the PDI (**Figure 53**) in contrast to the batches containing an API. This confirms the assumption that the tableting process and the adjuvants have a substantial effect on the characteristics of the liposomes formed, an observation that is preserved either after the extrusion step.

The EE was determined *via* several centrifugation steps with a further quantification by UV measurements. From a typical point of view of a tablet as classic solid dosage form, these steps represent minor importance. However, for a compressible formulation of proliposomal powders these proofs of principle studies are of interest. In literature, the compression of PLs with *in situ* formation of liposomes was investigated by Željka *et al.* [202]. They developed tablets of spray dried proliposomal powder containing metronidazole, lecithin and different tableting excipients. This delivery system could protect and encapsulate drugs and provided an increased stability for the compressed formulation. Another study reported on the development of delayed-release proliposomal tablets for oral protein drug delivery. Bovine serum albumin solid dosage forms could completely be reconstituted into liposomes with adequate resistance to the hostile environment in gastrointestinal tract [203].

Concerning the results for the batch containing the API ibuprofen, only 5.2 % (PLs) and 31.3 % (tablets) of the pain-relieving drug could be encapsulated. However, in the case of fenofibrate, the included amount of drug was approximately 100 %. The different molecular structure and lipophilic nature of the drug contribute to the very good EE that was reached. This result could be further explained by the different log P values of ibuprofen (log P = 3.72) [204] and fenofibrate (log P = 5.575) [205]. Fenofibrate is a highly lipophilic drug which could be easily incorporated in a hydrophobic region between the double layers of the phospholipids [206]. Tran *et al.* [207] described fenofibrate-loaded nanostructured lipid carriers with an EE of 93 %, increasing the amount encapsulated to 99 % upon the addition of a nonionic water-dispersible surfactant, Labrafil®. This compound had a solubilizing effect and increased the oral bioavailability of poorly water-soluble APIs like fenofibrate or lornoxicam [208]. Ibuprofen is presumably located in both inner of vesicles and the surrounding aqueous medium. Thus, the amount encapsulated is limited corresponding to the total volume encapsulated in relation to the overall volume.

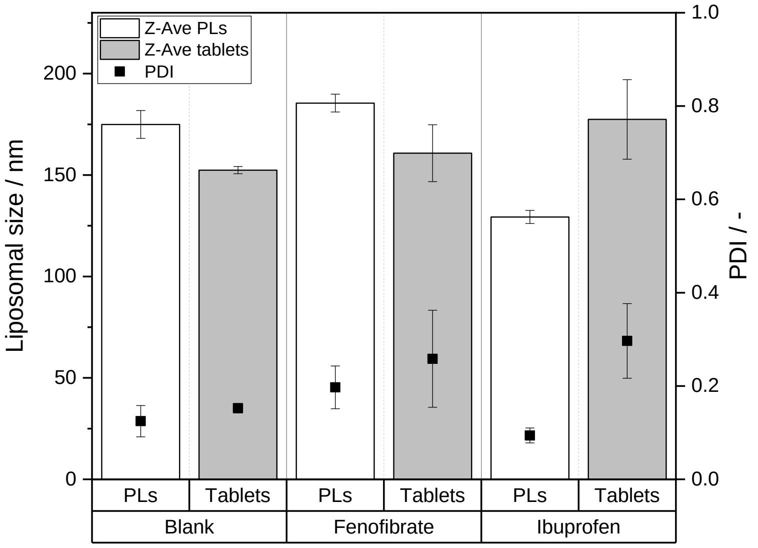

Figure 53: Liposomal sizes and PDI s of rehydrated liposomes out of PLs and tablet batches as determined *via* DLS.

An overview of the different EEs for fenofibrate and ibuprofen is listed in **Table 21**.Tablets show higher EE than PLs. This could be due to influence of pH-value. Furthermore, the bigger ibuprofen containing liposomes derived from tablets might lead to a higher EE than for PLs. Additionally, Anderson and Omri examined the effect of different lipid components on the *in vitro* stability and release kinetics of liposomes formulations. In their studies they carved out that DSPC which was also used for these experiments had the best EE [209].

Table 21: Overview of EE of both APIs, fenofibrate and ibuprofen.

Sample	**Encapsulation efficiency / %**	
	Proliposomes	*Tablets*
2 (Ibuprofen)	5.2	31.3
3 (Fenofibrate)	99.8	99.7

4.2.9 Release studies of proliposomal formulations

Calibration of HPLC-Method

Calibration of the method was performed using standard solutions of known fenofibrate concentrations within a range of 5 - 500 µg*ml^{-1}. The calibration curve as well as corresponding equation and regression are shown in **Figure 54**.

Both, the limit of quantification (LOQ) as well as limit of detection (LOD) were calculated according to DIN norm 32645 resulting in a LOQ of 23.158 µg*ml^{-1} and LOD of 6.624 µg*ml^{-1}.

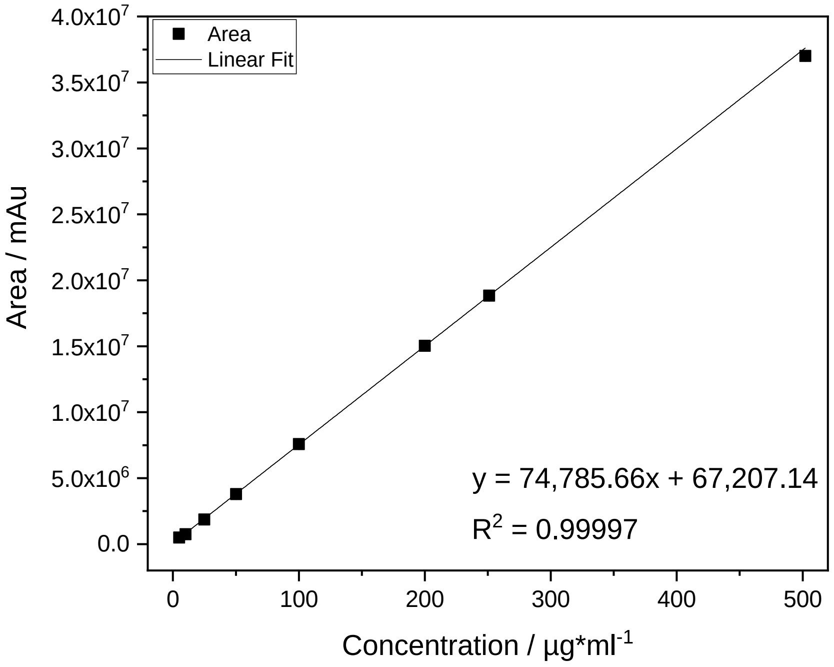

Figure 54: Calibration curve of different fenofibrate standards within a concentration of 5-500 µg*ml^{-1} obtained by HPLC.

Release profiles

The mean cumulative percentage of fenofibrate release from loaded PLs with various formulations in lipids (egg-PC *versus* DSPC) is shown in **Figure 55**. The total amount of API released from liposomes was determined by the addition of 10 % Triton X (w/V) prior the measurement with subsequent filtration step through 0.2 µm RC filter membranes. Triton X as detergent was used in order to destroy the liposomal vesicular structure. The MLVs were formed spontaneously and rapidly after the addition of the reconstitution media *i.e.* PBS buffer pH 7.4. The API fenofibrate was quantitatively existing and available from the MLVs. A remarkable high release of almost 100 % was reached after 180 min. After 24 h there was no further change in the concentration of fenofibrate, which confirmed a burst release within 3 h. The liberation profiles are depicted in **Figure 55** for 24 h (**A**) as well as a (**B**) detailed depiction of the first 3 h. The standard deviations were very small for all measurement points. Furthermore, no indication of the formation of a “grease ball” of fenofibrate was found, due to its lipophilic nature [210]. Therefore, it is assumed that all API was solubilized in the MLVs.

Cha *et al.* investigated the enhancement of the dissolution rate and bioavailability of fenofibrate by a melt-adsorption method using supercritical carbon dioxide [211]. In this study they also performed release testing of raw fenofibrate over a time period of 60 min. After one hour ~ 60 % were released. The proliposomal formulations in this study showed a clear improvement in comparison to these results, where more than 70 % were released within 60 min.

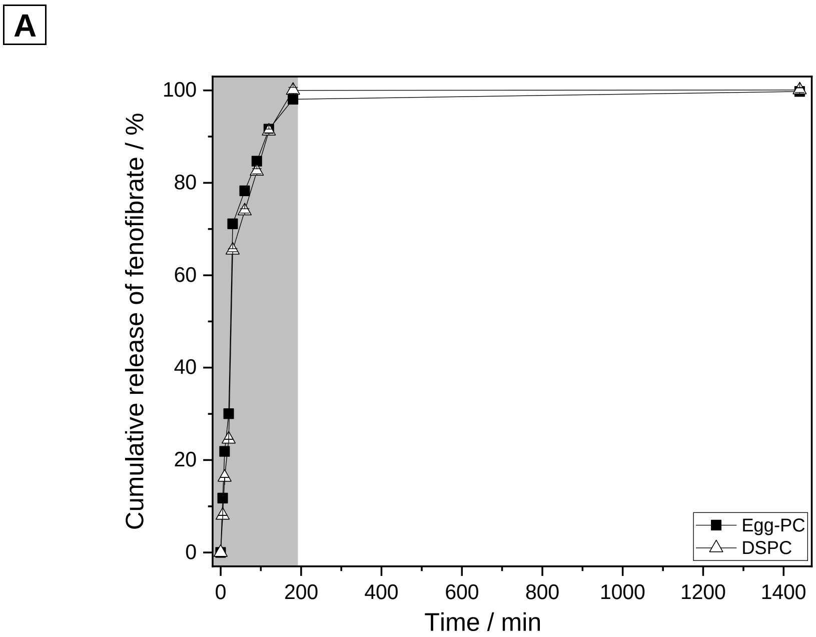

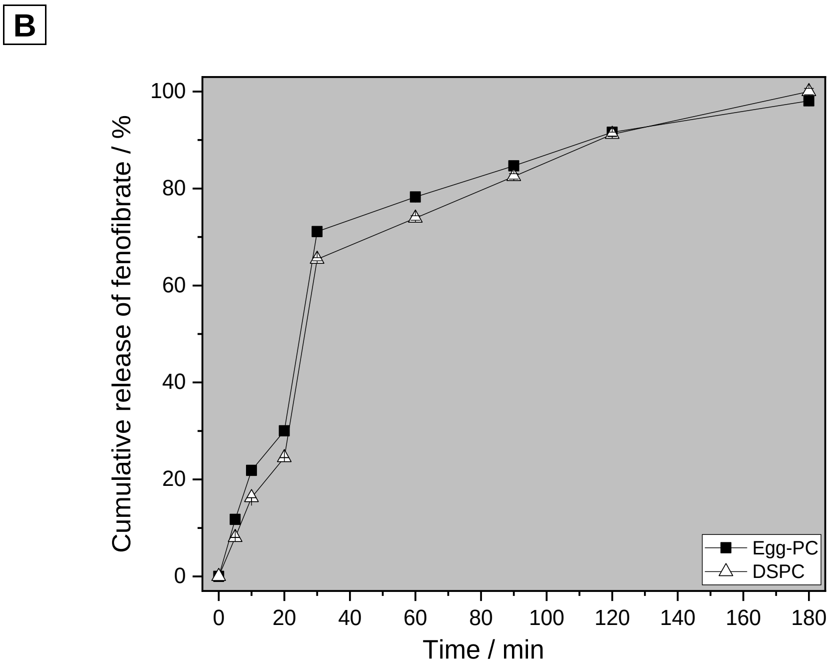

Figure 55: *In vitro* drug release of fenofibrate from proliposomal formulations with drug-to-lipid ratios of 1:1.07 in pH 7.4 phosphate buffer saline (Ph.Eur.). Each point represents the mean value ± SD of three different determinations. (**B**) zooms in the area grey marked in graph (**A**).

After 30 min of incubation time more than 60 % of the drug was released from the proliposomal formulation in the PBS buffer pH 7.4. This phenomenon could also be observed in a study of Gupta *et al.* [212]. They developed PLs loaded with the pain-killer aceclofenac for topical delivery and investigated the formulation's *in vitro* releasing profile. Drug liberation determined was between 1 and 24 h whereas a higher amount of API was released out of the sample after 5 - 6 h. Hereby, the drug release from a treated cellophane membrane was measured by dialysis which could explain the longer release time. In this thesis, the proliposomal formulation containing fenofibrate showed an immediate release as observed by Yanamandra *et al.* [213] for proliposomal tablets loaded with lovastatin. In another approach, Sunil *et al.* [214] characterized the *in vitro* drug release of metoclopramide *via* formation of MLVs. The vesicle size was ~ 2 µm whereby the type and concentration of the phospholipid and the hydrophilic polymer had shown different effects on the drug release (between 40 % and 100 %). The hydrophilic polymer included reduces the burst release and controls the drug release. A near zero order kinetic could be achieved. In this study, the API was encapsulated in proliposomal tablets.

4.2.10 Design of experiments approach

For the production of PL in a well-established coating device, which is suitable for scale up for larger batch sizes it is desirable to show the applicability of the coating technique when using a standard coater as it is commonplace in the pharmaceutical industry. First, a suitable formulation should be established using this coating equipment which was accomplished in a DoE approach. Due to preliminary experiments in lab scale which revealed a successful formation of liposomes after reconstitution, the lipid film coating method was used in this study. The main goal was the development of a suitable formulation that favors on this project the formation of vesicles with the following properties: (i) smallest liposomal size since larger liposomes can be achieved more easily as found in previous experiments, (ii) highest ZP for good stability of the liposomes after reconstitution and(iii) most effective EE to have as much as possible of the drug included in the desired liposomal carrier.

For each factor, an applicable range was defined based on previous investigations in order to set experimental limits. On the other hand, also qualitative factors were specified to choose adequate components for the up-scaled formulations. Therefore, a full-factorial screening design with three quantitative factors at two levels was planned. The subsequent quantitative factors were selected and further varied according to the design matrix (**Table 22**) generated by MODDE® Pro 12.0.1. Consequently, the quantitative factors were adjusted in the coating experiments between their low (-) and high (+) levels and analyzed regarding their type or presence of lipid or charge (+: DSPC, -: egg-PC; +: presence of negative component, -: no addition of negative lipid).

- Lipid concentration (Lip) (between 16.7 (-) and 26.7 mM (+))
- Type of lipid (Typ) (DSPC or egg-PC)
- Addition of the negative lipid (Neg) DMPG (yes or no)

The type of lipid and its concentration was chosen based on previous experiment. A small liposomal size should be reached which is more difficult to obtain as previous experiments have shown as well as an effective EE as marker for an efficient process. A negatively charged lipid should be added to get a high ZP for increased stability of the liposomal dispersion.

During all experiments, the following criteria were kept constant and not changed to reduce the amount of further influencing parameters: (i) percentage of cholesterol (20 % (w/w), (ii) ratio of lipid-to-carrier (1:100), (iii) carrier material (sucrose carrier; 2,500 - 3,300 µm; GHP 5) and (iv) drug substance (fenofibrate). Additionally, four center points (run No. 9, 10, 11, 12) were included for evaluation of reproducibility, resulting in a total number of 12 runs. The factor lipid concentration was set at the average values (= 21.7 mM).

Table 22: Design matrix as generated by MODDE® Pro 12.0.1 statistical software (- low level, + high level, o center point).

Run No.	Lipid concentration Lip	Type Typ	Negatively charged Neg
1	–	Egg-PC	yes
2	+	Egg-PC	yes
3	–	DSPC	yes
4	+	DSPC	yes
5	–	Egg-PC	no
6	+	Egg-PC	no
7	–	DSPC	no
8	+	DSPC	no
10	o	Egg-PC	yes
11	o	Egg-PC	yes
13	o	DSPC	yes
14	o	DSPC	yes

The responses of main focus were (i) liposomal size, (ii) ZP and (iii) EE. Additionally, the percentage of applied amount of the different carrier materials was monitored. A mathematical model was calculated by the MODDE® software and used for interpretation, optimization as well as prediction.

The overall fit plot (**Figure 56**) illustrates a summary of the basic model statistics with four characteristic parameters: (i) the model fit (R2) which explains significance, (ii) future prediction precision (Q2), (iii) model validity as test of diverse model problems and (iv) reproducibility as variation of replicates compared to overall variability. A sum of 1, which means 100 %, describes perfect correlation for each characteristic parameter.

For liposomal size and EE, the difference between R2 and Q2 (∆ = R2 - Q2) was calculated as 0.59 (liposomal size) and 0.72 (EE), respectively. Usually, both values should be close in size in order to predict a good modeling. Preferably, the difference should be less than 0.3. This could be reached for the ZP with a difference of 0.3. Model validity led to values higher than 0.25 indicating no statistically significant model problems as for example the presence of outliers, an incorrect model or a transformation. In case of responses, the model appeared to be of good fit for all parameters

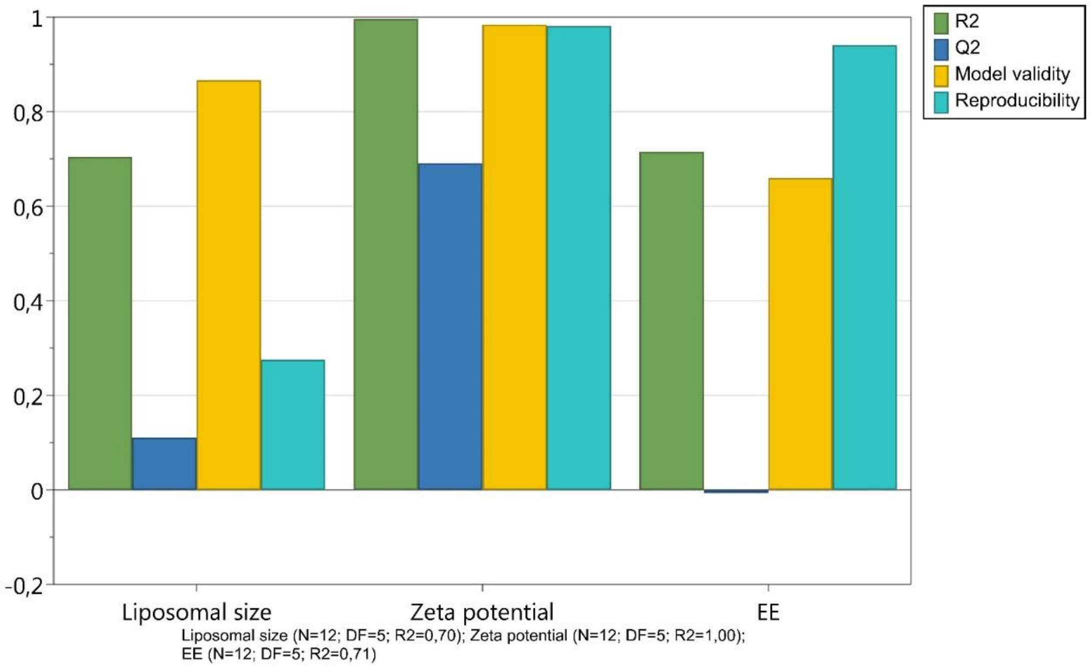

Figure 56: Summary of fit plot.

Liposomal size

Regarding liposomal size, a desired value of 8 µm was chosen as upper limit which was previously determined by the preliminary LD measurement of raw liposomal dispersions. The type of lipid has a major effect on liposomal size, as well as charge, which is negative in presence of DMPG (**Figure 57 A**). Both, scheme **C** and **D**, show the contour plots which illustrate the decrease in vesicular size for the formulation containing egg-PC in comparison to DSPC. Furthermore, a higher lipid concentration resulted in larger liposomes in the absence of the charged component. With the addition of the negatively/positively charged component DMPG, the target size of 8 µm could be reached with an egg-PC lipid concentration of 26.7 mM. Plot **B** displays the observed *versus* predicted response values. Outliers in the relationship are points far away from the 1:1 line.

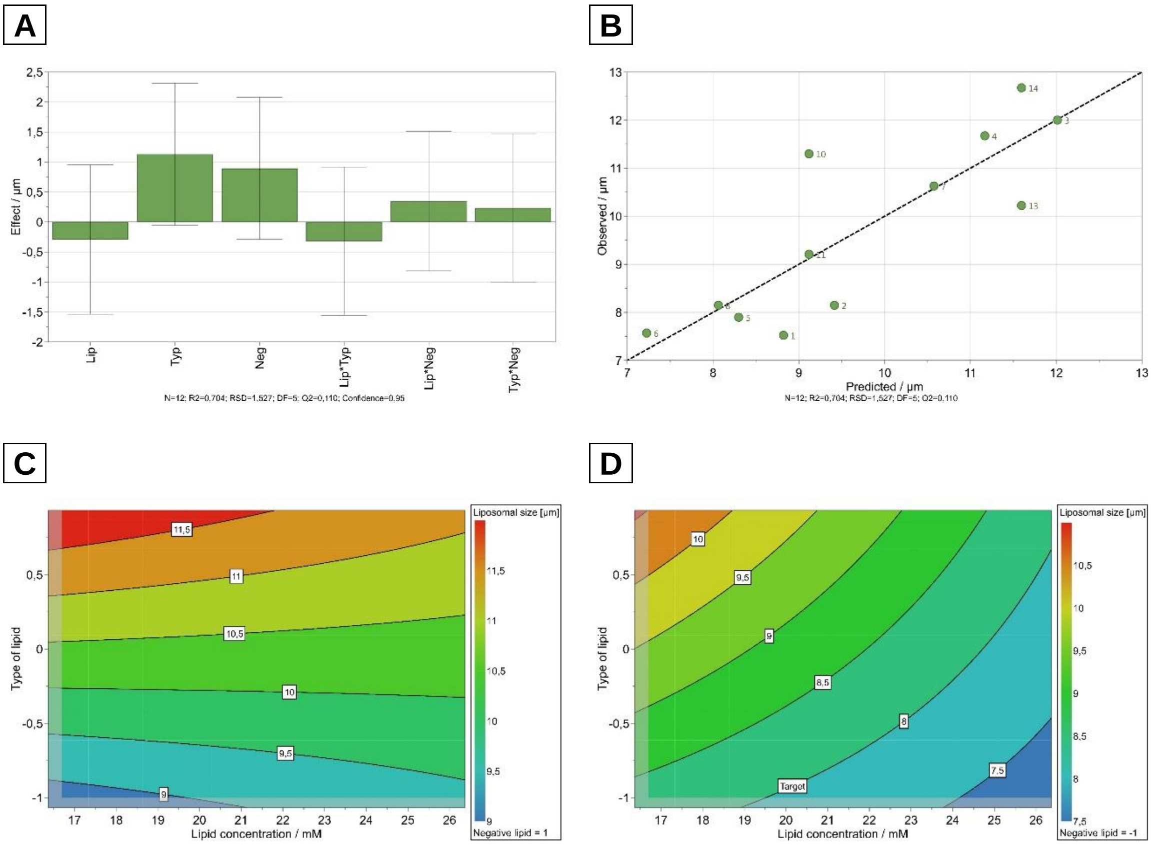

Figure 57: (**A**) Effect plot as well as (**B**) observed and predicted plots of liposomal size response. Scheme shows the response surface plot of liposomal size with addition of DMPG (**C**) and without a charged component (**D**). Lip: lipid concentration; Typ: type of lipid; Neg: addition of negative lipid; *: correlation of two factors, for instance Lip*Typ: correlation of lipid concentration and type of lipid.

Zeta potential

ZP of the liposomal dispersion was used as an indication for dispersion's stability. Formulations containing DMPG showed negative values between - 12 mV and - 7 mV (set target from previous experiment = - 10 mV). Though, fenofibrate was not charged, one possible explanation for the lipid-induced negative ZP values might be the fact that drug encapsulation causes significant changes in liposomal surface structure. This phenomenon was also observed by Vargha-Butler and Hurst [215]. It is known from literature that these negative values indicate sufficient stabilization [200] which was also shown in the 6 months stability study presented here (see chapter **4.2.4**). Furthermore, another trend can be recognized: the higher the lipid concentration, the more the lipid DMPG was comprised and the more positive the resulted ZP. Vesicles without charged components showed a weak ZP modulus. Expectedly, **Figure 58 A** verifies that the presence of DMPG had the biggest influence on ZP followed by the type of lipid. Here, DSPC generated higher values in comparison to egg-PC. Graph **B** illustrates observed responses *versus* predicted values. The points were close to a straight line which again confirms a very good model.

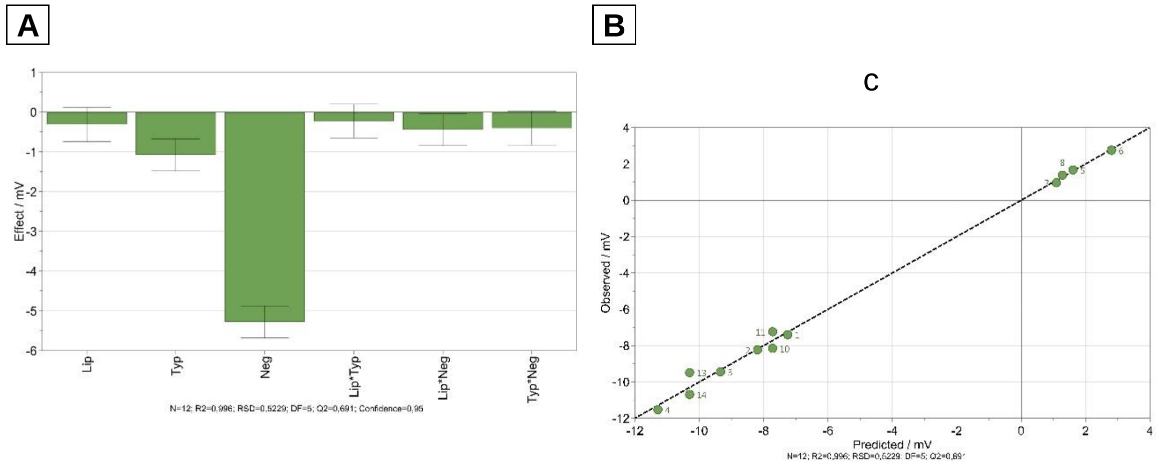

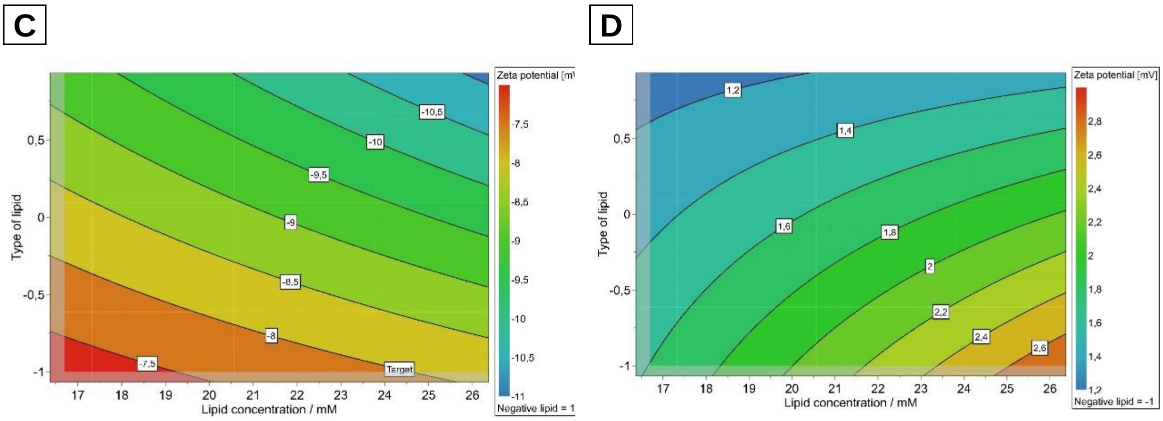

Figure 58: (**A**) Effect plot and (**B**) observed vs. predicted plot of ZP response. Scheme (**C**) shows the response surface plot of ZP with addition of DMPG and (**D**) without charged component.

Encapsulation efficiency

The EE was in all cases between 99 and 100 % which indicated a total entrapment of fenofibrate in the lipid bilayer. The target was set at 99 %. The temperature of the EE’s determination was at room temperature (T = ~ 23 °C) for all the performed experiments. In this study fenofibrate might be a component of the lipid bilayer due to the lipophilic properties and a logP value of 5.4. The biggest influence factor on EE was the presence of the negative lipid DMPG. This might be the result of the low T_m of DMPG (T_m = 23 °C) which creates a more irregular and looser structure of the lipid membrane so that the API would penetrate easily into the bilayer [216]. The liposomal membrane could become most permeable due to transient bilayer defects which are caused by the dramatic lateral area changes of lipid domains as they fluctuate between the gel and fluid states in dynamic equilibrium [217]. According to Torchilin and Weissig, the highest permeability of the bilayer is in their T_m [30]. Moreover, the higher the lipid concentration, the higher the EE in presence of the charged lipid and *vice versa*. All in all, the differences between the individual experiments were small, probably due to the general tendency of fenofibrate to be part of the liposomal membrane.

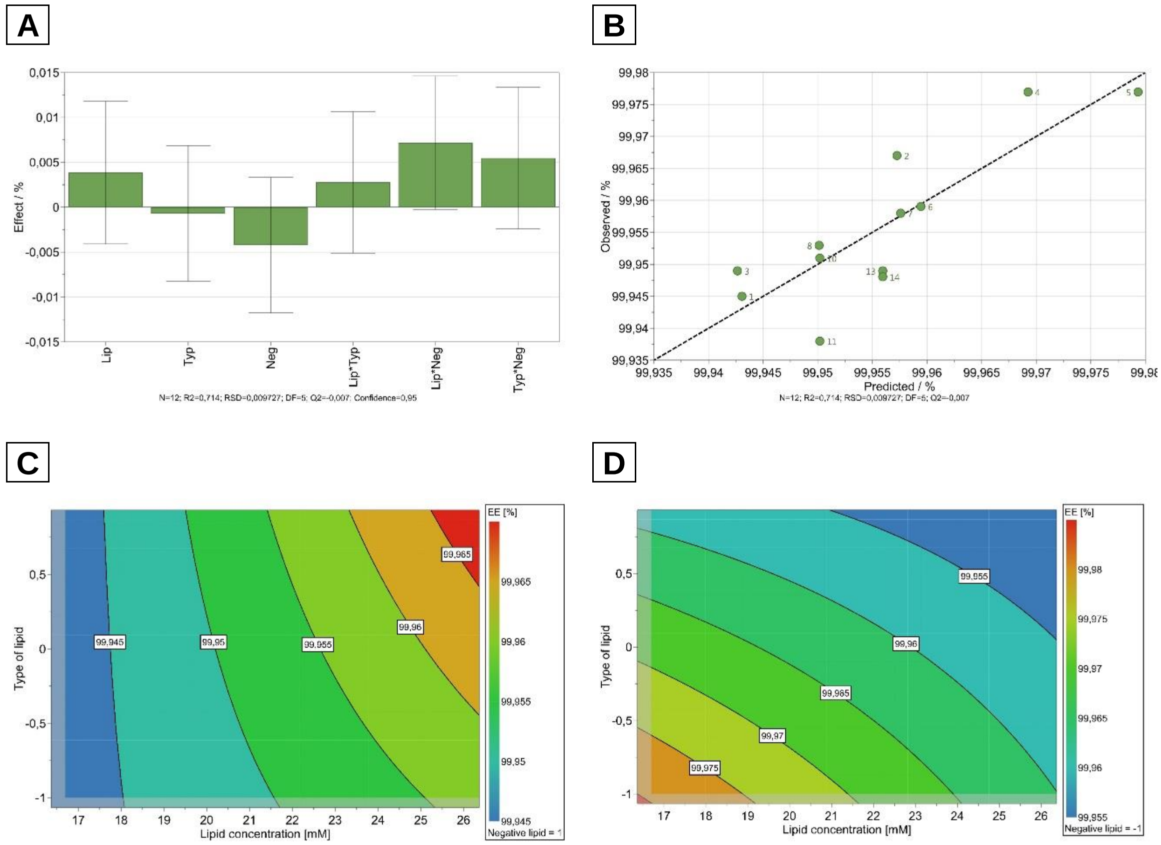

Figure 59: (**A**) Effect plot and (**B**) observed *vs.* predicted plot of EE response. Scheme (**C**) shows the response surface plot of EE with addition of DMPG and (**D**) without a charged component.

The best result of the DoE with the lowest log(D) was determined by the software MODDE$^{®}$ Pro. The log(D) value is selected automatically on the lowest probability of failure instead. Minimum for log(D) = - 10 (on target). A log(D) < 0 means that all results are within specification limits or very close. With a calculated value of log(D) = - 1.03, run no. 1 was selected as the most suitable to obtain PLs with the characteristics defined as target beforehand. The composition of this formulation including the corresponding results of the responses chosen is listed in **Table 23**.

Table 23: Compositions for the determined formulation in large scale production including the corresponding results for the three factors liposomal size, EE and ZP.

Formulation for large scale production		**Results of responses**	
Lipid concentration	-	Liposomal size / µm	8.80 ± 0.51
Type of lipid	Egg-PC	EE / %	99.95
Charged component DMPG	Yes	ZP / mV	- 7.38 ± 0.61

4.2.11 Scale-up of proliposomal preparation

After identification and evaluation of important parameters within the DoE experiment for the production of PLs was performed in a Glatt® coater to give proof of the possibility to transfer the process to a commonplace coating device. Three different batches were performed: (i) two placebo batches (blanks) with either egg-PC or DSPC as lipid component and (ii) the most suitable run of the DoE (see chapter **4.2.10**). **Table 24** summarizes the exact compositions of the prepared formulations. 100 g of carrier material were given in the drum, equilibrated at ~ 65 °C T_{inlet} (temperature chosen for lab scale experiments: 55 °C) and afterwards coated with ethanolic lipid solution. All coating runs could be smoothly performed within ~ 80 min at 5.5 $g*ml^{-1}$ feeding rate.

Table 24: Formulations of the two placebo batches containing either egg-PC or DSPC and the best batch for large scale production determined *via* DoE.

	Placebo batches		**API batch (DoE)**
Substances	*Initial weight / g*		
Sucrose carrier with a size of 2,500 to 3,300 µm (GHP 5)	100	100	100
DSPC	8	-	-
Egg-PC	-	8	8
DMPG	-	-	0.4
Cholesterol	2	2	2
Fenofibrate	-	-	7.5
Ethanol	368.46	368.46	368.46

After addition of PBS buffer pH 7.4 to the dry PL powder the presence of MLVs was tested with the polarization microscopy. Typical round shaped vesicles with Maltese crosses were clearly visible in all the samples. **Figure 60** shows the images of all three batches ((**A**) and (**C**) are placebo batches with egg-PC and DSPC, respectively and (**B**) is the chosen DoE batch). It is remarkable, that the amount of PLs in the liposomal dispersion was six times higher than for PLs produced in lab scale to obtain the same lipid concentration. This can be explained by the loss of ethanolic lipid solution in the coating drum during the preparation process (no overage of lipid solution was sprayed). Consequently, the total number of vesicles per mm^3 increased depending on the increasing proliposomal concentrations in the reconstitution media (**Figure 61**): (i) 0.12 $mg*ml^{-1}$, (ii) 0.36 $mg*ml^{-1}$ and (iii) 0.72 $mg*ml^{-1}$. The latter concentration correlates with the results of DSPC and egg-PC already described in chapter **4.2.6**. Here, the same amount of lipid was available in every formulation. A total number of ~ 70 000 and ~ 21 000 vesicles per mm^3 was calculated for egg-PC as well as DSPC, respectively. The smaller the size of the vesicles the bigger the total amount of liposomes which were formed.

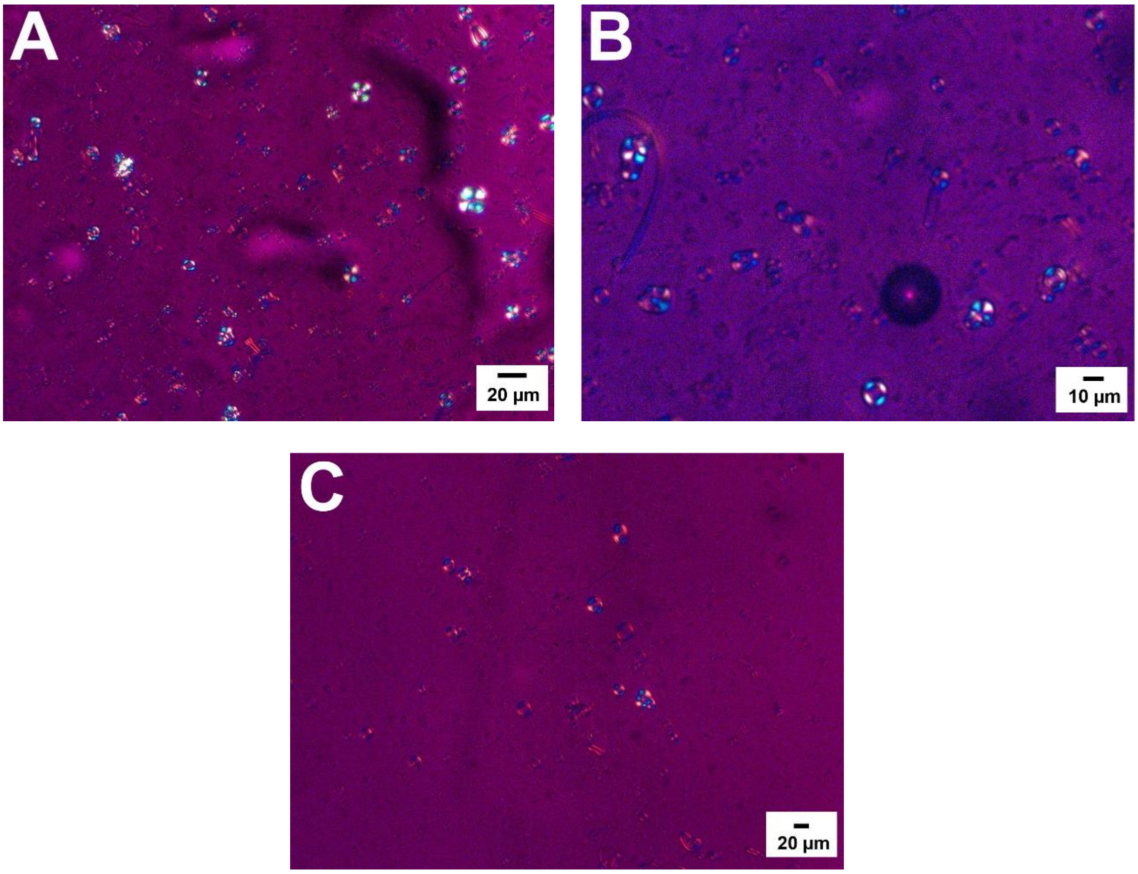

Figure 60: Photomicrographs for the verification of liposomal formation. The dispersions are depicted as follows:
(**A**) Placebo batch containing egg-PC; proliposomal reconstitution concentration 0.72 $g*ml^{-1}$, (**B**) DoE batch; proliposomal reconstitution concentration 0.72 $g*ml^{-1}$, (**C**) Placebo batch containing DSPC; proliposomal reconstitution concentration 0.36 $g*ml^{-1}$.

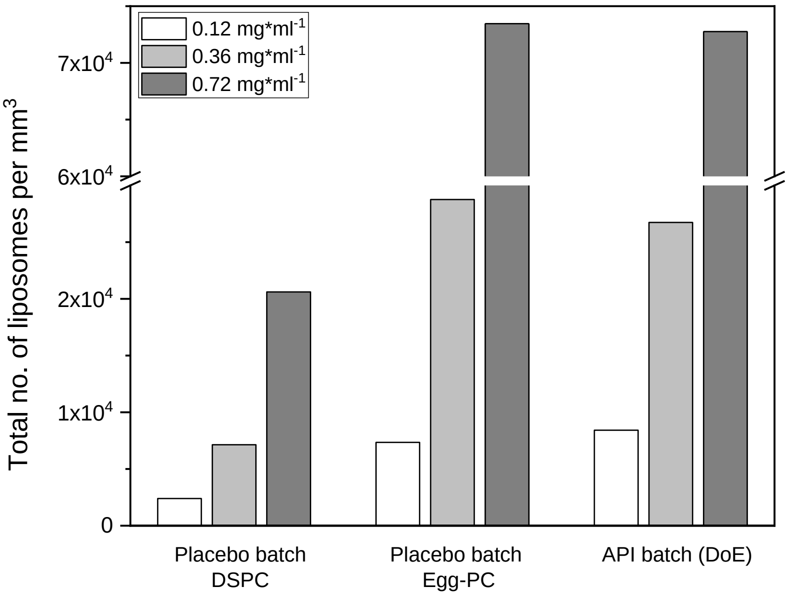

Figure 61: Total number of liposomes per mm^3 sorted by increased reconstitution concentration of PLs.

Figure 62 shows the volume-based size distribution of the three production batches as determined using LD. The results of vesicular sizes are comparable to those measured for lab scale production of PLs although the process control of the Glatt® coater differed from the discontinuous lab scale process (spraying and drying in turns). D_{50}-values of the placebo batch were in a size range from 6.3 - 7.7 µm. Liposomes including the negatively charged lipid DMPG as well as the API fenofibrate were slightly bigger and led to mean liposome siges in the range of 8.76 ± 0.32 µm. These results can be correlated with the LD measurement of the best selected run of the performed DoE (8.80 ± 0.51 µm). Moreover, also ZP values of - 7.38 ± 0.04 mV (- 7.26 ± 0.61 mV) and a calculated EE of 99.97 % (99.95 %) as confirmed by Zetasizer and UV measurements agree well with the named DoE run.

In summary, it was possible to transfer the lab scale production of PLs to bulk manufacturing procedures using a Glatt® coater. The results for liposomal size, ZP and EE were comparable to those of the DoE and proved the transfer from lab scale to a continuous larger scale setting to be successful.

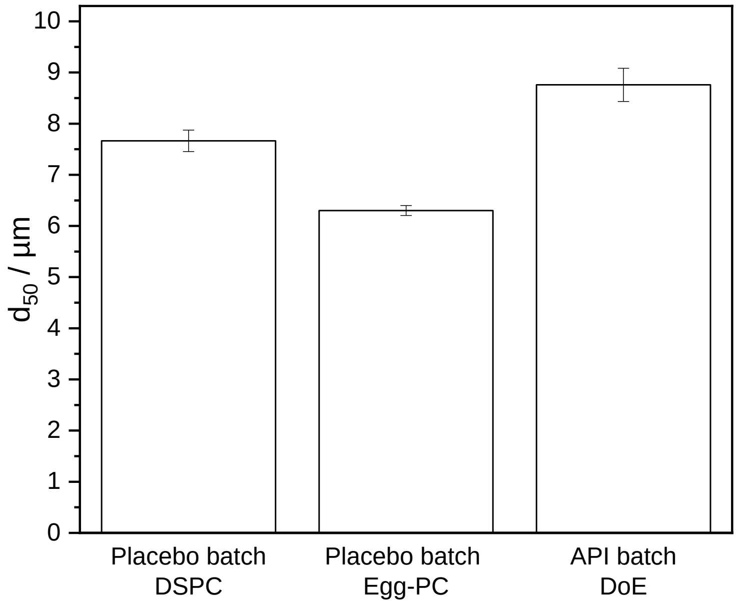

Figure 62: D_{50}-value of the volume based size distribution (n = 3, 2σ) of the three large scale production batches. Measurements were taken from the concentration of 0.72 mg*ml^{-1} due to comparable total number of counted liposomes per mm^3.

4.3 Production of proliposomes *via* spray drying

The third part of this work describes spray drying as one-step process and suitable production procedure for PLs. First, microparticulated mannitol was produced as carrier material Mannitol solutions with different concentrations were spray dried or spray-freeze dried. Differences in particle size distribution was further investigated. Proliposomal properties were determined using XRD, LD and SEM. Furthermore, liposomes formed out of proliposomal powders were counted using a Thoma counting chamber and compared with microscopic analysis (polarization microscope).

4.3.1 Production of microparticulated mannitol as carrier for proliposomal formulations

Microparticulated mannitol was produced *via* a spray drying process according to Rojanarat *et al.* [135]. A detailed description of the used process parameters can be found in chapter **3.2.2.2**. With mannitol as selected core carrier for the formulation of PLs, a possible candidate with a small size distribution was chosen. Therefore, lipids could easily form a thin and homogenous layer around the solid microparticles. To allow for free passing of the carrier material through a spraying nozzle, a d_{50}-value of about 4 µm was set as goal for particle size. Sorbitol can be advantageous when using it as carrier for microporous matrix of carrier particles [131, 218] since it gives free flowing proliposomal powders after SD. For the mannitol solutions two different concentrations (1 % (w/w) and 10 % (w/w) solid) were used. The following parameters of the spray dried microparticulated mannitol were investigated: (i) yield (defined as percental weight fraction of powder that could be recovered from the collecting vessel attached to the bottom of the cyclone) and (ii) d_{50}-value. One carrier batch was produced *via* spray freeze drying (1 % (w/w)) and analyzed analogously as described before.

Figure 63 shows the reached yield of the spray dried PLs. It is remarkable that the yield increased with higher T_{inlet} up to 130 °C. Increased value of T_{inlet} consequently resulted in higher T_{outlet} (60 °C / 75 °C / 90 °C). Thus, a lower T_{outlet} indirectly reflected a reduced rate of enthalpy throughput [219]. Moreover, the highest powder yield required the highest drying temperature of microparticulated mannitol without causing stickiness. Regarding particle size of microparticulated mannitol (**Figure 64**), low T_{inlet} favoured the formation of smaller crystals whereas high temperatures resulted in bigger particles. Furthermore, an increase in flow rate of up to 3 ml*min^{-1} resulted in smaller d_{50}-values. This effect was noticed by increasing the liquid feed rate that led to smaller droplets of the prepared sprayed solution.

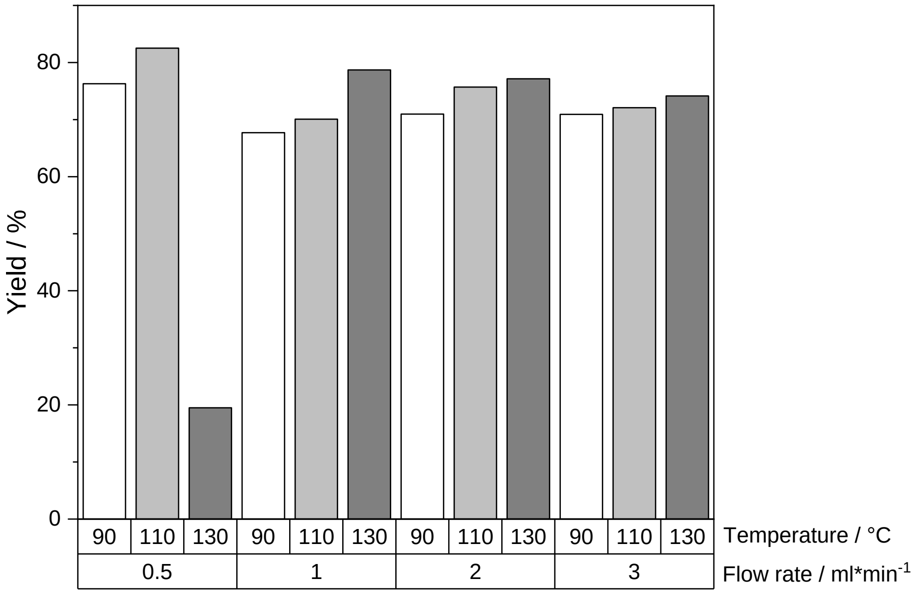

Figure 63: Effect of T_{inlet} (90 / 110 / 130 °C) and pump speed (0.5 / 1 / 2 / 3 ml*min^{-1}) on powder yield of spray dried mannitol.

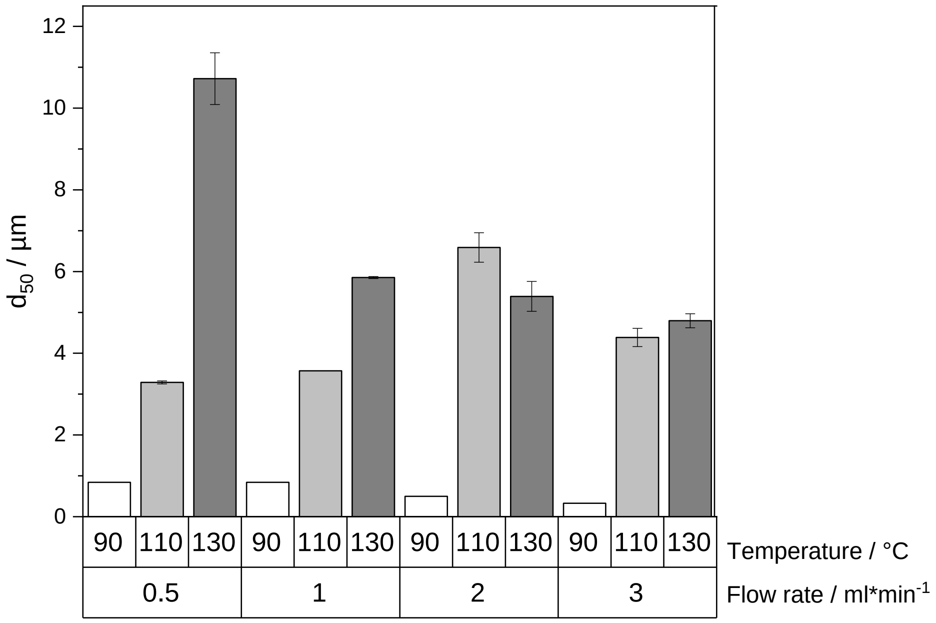

Figure 64: D_{50}-values of microparticulated mannitol with three different T_{inlet} (90 / 110 / 130 °C) and four different pump speeds (0.5 / 1 / 2 / 3 ml*min^{-1}).

The molecular structure of the spray dried and spray-freeze dried powder was investigated. The former showed typical crystalline WAXD measurement for all samples [220], whereas spray-freeze-dried carriers were predominantly amorphous with typical halo pattern (**Figure 65**) and only small crystalline peaks, indicating some small crystalline fraction. A SFD-based carrier as chosen as alternative due to the more porous surface which might influence liposome formation after rehydration. SEM pictures of microparticulated mannitol were taken (**Figure 66**) and the appearance of the produced carrier material was similar to spray dried mannitol at equal T_{outlet} of ~ 65 °C as described in studies of Littringer *et al.* [221]

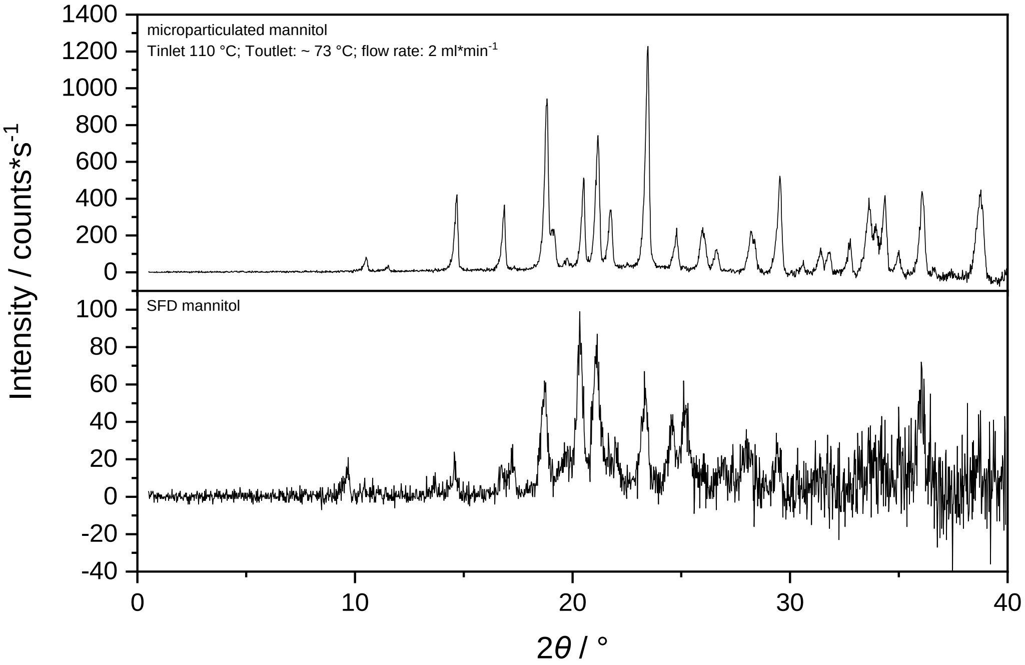

Figure 65: WAXD of crystalline microparticulated mannitol *via* spray drying and amorph carrier *via* SFD.

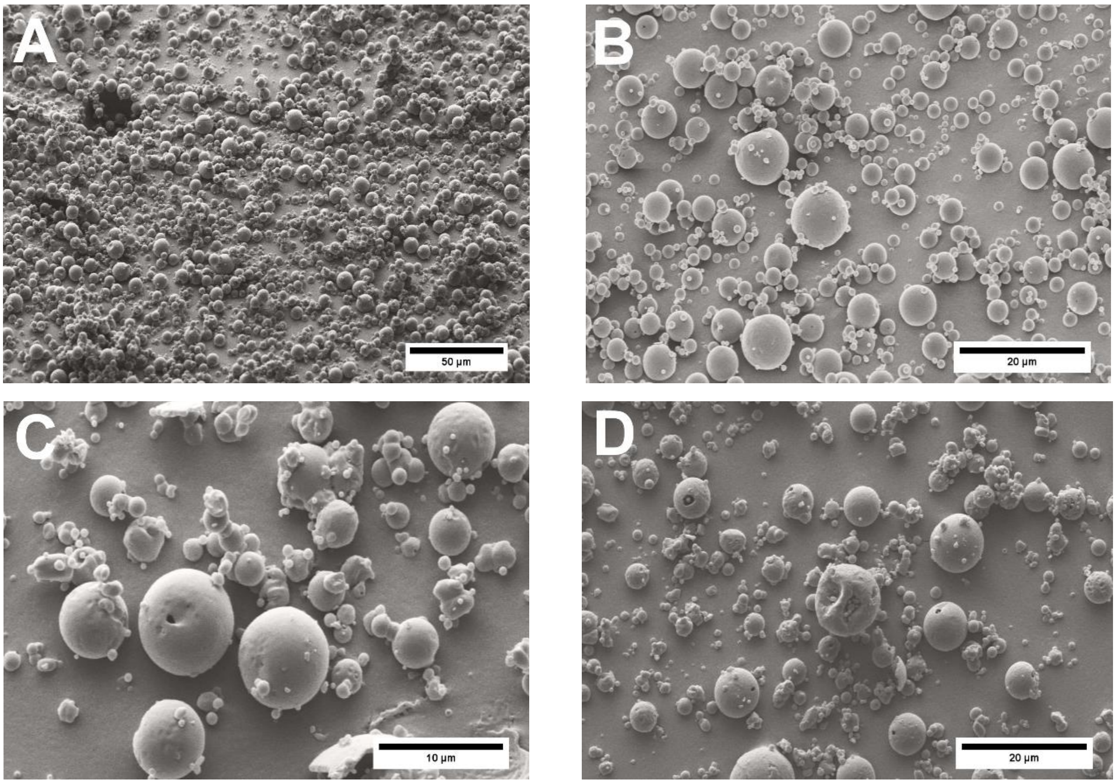
A
50 µm
B
20 µm
C
10 µm
D
20 µm

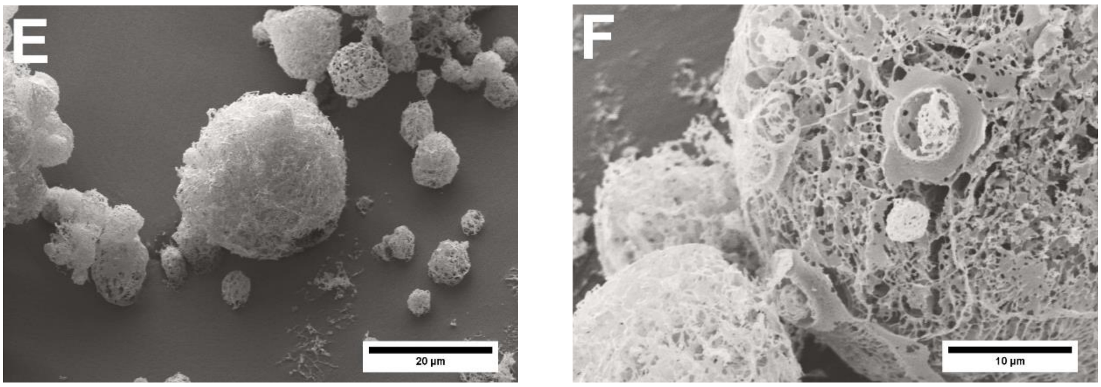

Figure 66: SEM micrographs of microparticulated mannitol:
(**A**) T_{inlet} 110 °C; T_{outlet}: ~ 73 °C; flow rate: 3 ml*min^{-1}; 300x magnification, (**B**) T_{inlet} 110 °C; T_{outlet}: ~ 66 °C; flow rate: 2 ml*min^{-1}; 2000x magnification, (**C**) T_{inlet} 130 °C; T_{outlet}: ~ 88 °C; flow rate: 2 ml*min^{-1}; 3000x magnification, (**D**) T_{inlet} 130 °C; T_{outlet}: ~ 88 °C; flow rate: 2 ml*min^{-1}; 1000x magnification, (**E**) Spray-freeze dried sample; 1000x magnification, (**F**) Spray-freeze dried sample; 2000x magnification.

4.3.2 Characterization of proliposomes and liposomes

A successful preparation of different carrier materials *via* spray drying with a small particle size distribution and crystalline as well as amorphous character were chosen for proliposomal production again by spray drying. For the following experiments, T_{inlet} was set to 130 °C with a flow rate of 3 ml*min^{-1} resulting in a T_{outlet} of about 70 °C. In order to investigate the influence of different carrier size and ratio on the drug loading capacity of PLs with fenofibrate, four different types of combinations were tested. **Table 25** gives an overview of the different types of carrier used for proliposomal production.

Table 25: Overview of the different types of carrier materials including percental amount of mannitol in the formulations, d_{50}-values and phase compositions.

Sample no.	Percentage of carrier material (microparticulated mannitol or SFD mannitol) in formulation / %	d_{50} / µm ± 2σ	Structure
1	1	1.01 ± 0.00	crystalline
2	10	5.02 ± 0.37	crystalline
3*	1	13.10 ± 0.03	“amorphous”
4	1	7.00 ± 0.36	crystalline

*SFD product

SEM photomicrographs of spray dried formulations are depicted in **Figure 67**. Picture **A** represents a rough surface of freshly prepared PLs out of DSPC whereas image **B** shows smoother spherical particles of egg-PC PLs. One possible explanation might be the T_m of the two lipids (T_m (DSPC) = ~ 55 °C; T_m (egg-PC) = - 7 °C). In a study of Patil-Gadhe and Pokharakar [222], the same type of PLs are treated with the antibiotic rifapentine in order to generate a formulation for an inhalative application. It seemed that the PLs of the spray dried product containing egg-PC stuck together and were similar to the waxy appearance of egg-PC coated PLs as described in chapter **4.2.1**.

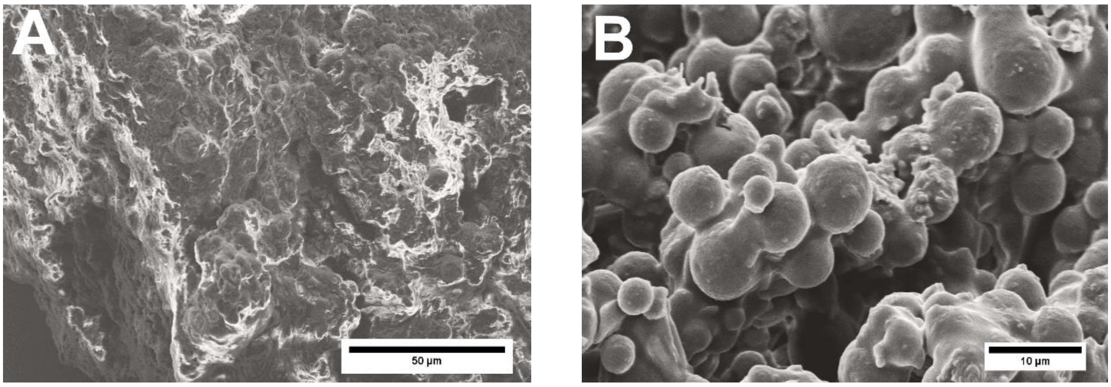

Figure 67: SEM micrographs of fenofibrate PLs containing the lipids (**A**) DSPC or (**B**) egg-PC with the carrier sample no. 2 for both batches, (**A**) and (**B**).

The reconstitution of PLs with demineralized water resulted in a successful formation of liposomes. The presence of vesicles was proved by polarization microscopy. Characteristic Maltese crosses were visible. The number of liposomes formed was substantially lower in comparison to batches prepared *via* the coating method after rehydration of equal amounts of “phospholipids” (**Figure 68**). **Table** 26 shows a comparison of counted liposomes with the Thoma counting cell chamber. The yield of spray dried product for all batches was in a range between 7 % and 28 % (see **Table 27**). This low yield could be explained by substantial powder residues found in the cyclone and on several connecting pieces of the machine. Additionally, the chosen T_{inlet} value of 110 °C was above the T_m of the two lipids and was thus influencing the spray drying process making the powder stickier and more prone to impaction on the glass walls of the spray dryer.

Table 26: Comparison of total number of liposomes per mm^3 using Thoma counting chamber of proliposomal formulations produced *via* coating method and spray drying, respectively.

Type of lipid	PLs *via* coating method	PLs *via* spray drying
egg-PC	72,250	33,745
DSPC	21,400	11,250

Table 27: Overview of the yield referring to the type of carrier and percentage amount in the formulation.

Batch no.	Type of carrier (% amount (w/w))	Yield / %
	egg-PC	
1	Microparticulated mannitol (1 %)	9
2	Microparticulated mannitol (10 %)	25
3	SFD mannitol (1 %)	19
4	Microparticulated mannitol (1 %)	10
	DSPC	
1	Microparticulated mannitol (1 %)	14
2	Microparticulated mannitol (10 %)	17
3	SFD mannitol (1 %)	28
4	Microparticulated mannitol (1 %)	7

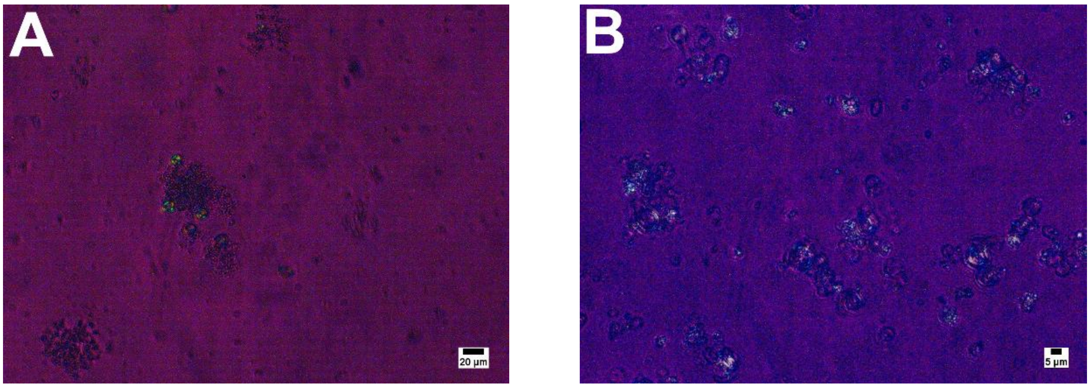

Figure 68: Photomicrographs for the verification of a successful formation of liposomes out of PLs. Liposomal dispersions containing (**A**) DSPC or (**B**) egg-PC were produced with following process parameters: T_{inlet} 110 °C; T_{outlet}: ~ 71 °C; flow rate: 3 ml*min^{-1}; carrier**:** 1 % microparticulated mannitol.

Figure 69 shows the d_{50}-values of spray dried PLs and reconstituted PLs as well as the d_{50}-values of the carrier used. The lipid concentration was the same for all formulations. For the lipid egg-PC (**A**) the liposomal vesicles were constantly larger than the PLs they were reconstituted from. For sample 1 and 4, the same carrier material (1 % microparticulated mannitol) but with different d_{50}-value (~ 1 µm and ~ 7 µm) was used which resulted in similar liposomal sizes of ~ 7 µm. The amorphous character of sample 3 (SFD mannitol as carrier material) led to smaller vesicles with a size of ~ 3 µm. The highly porous SFD particles offer a much larger surface area for adsorption of the lipids. Thus, it might be possible that the SFD particles were “soggy” with proliposomal ethanolic lipid solution which led to smaller liposomal sizes. Sample number 2 seemed to be the most preferable formulation with 10 % (w/w) instead of 1 % (w/w) microparticulated mannitol since the carrier size of ~ 4 µm is preferred due to nozzle compatibility. Additionally, next to the liposomes also the PLs were small with a d_{50}-value of ~ 1 µm.

In contrast to egg-PC, the other chosen lipid DSCP (**B**) showed a different outcome with regard to the PLs. The formed PLs showed increased d_{50}-values of up to 10 - 50 µm. Sample 1 and 4 show high sizes of the proliposomes with values > 20 µm, whereas sample 2 showed a mean size of about 7 µm. The liposomes formed out of these PLs were also bigger in size than those of sample 3 (SFD mannitol, d_{50}: 4 µm) and sample 2 (10 % microparticulated mannitol, d_{50}: 5 µm). One possibility for the broader particle size distribution could be explained by the stickier tendency of the prepared PLs and the consequently favoured formation of agglomerates.

Regarding values of liposomal size (constant lipid concentrations for each formulation), both lipids led to similar d_{50}-values. This fact rises the assumption, that the size of the formed vesicles is affected by the structure and particle size and surface area of the carrier material and not by the spray dried PLs. In conclusion sample 2 was used for further analysis matching with the set targets of particle size as well as small liposomal size.

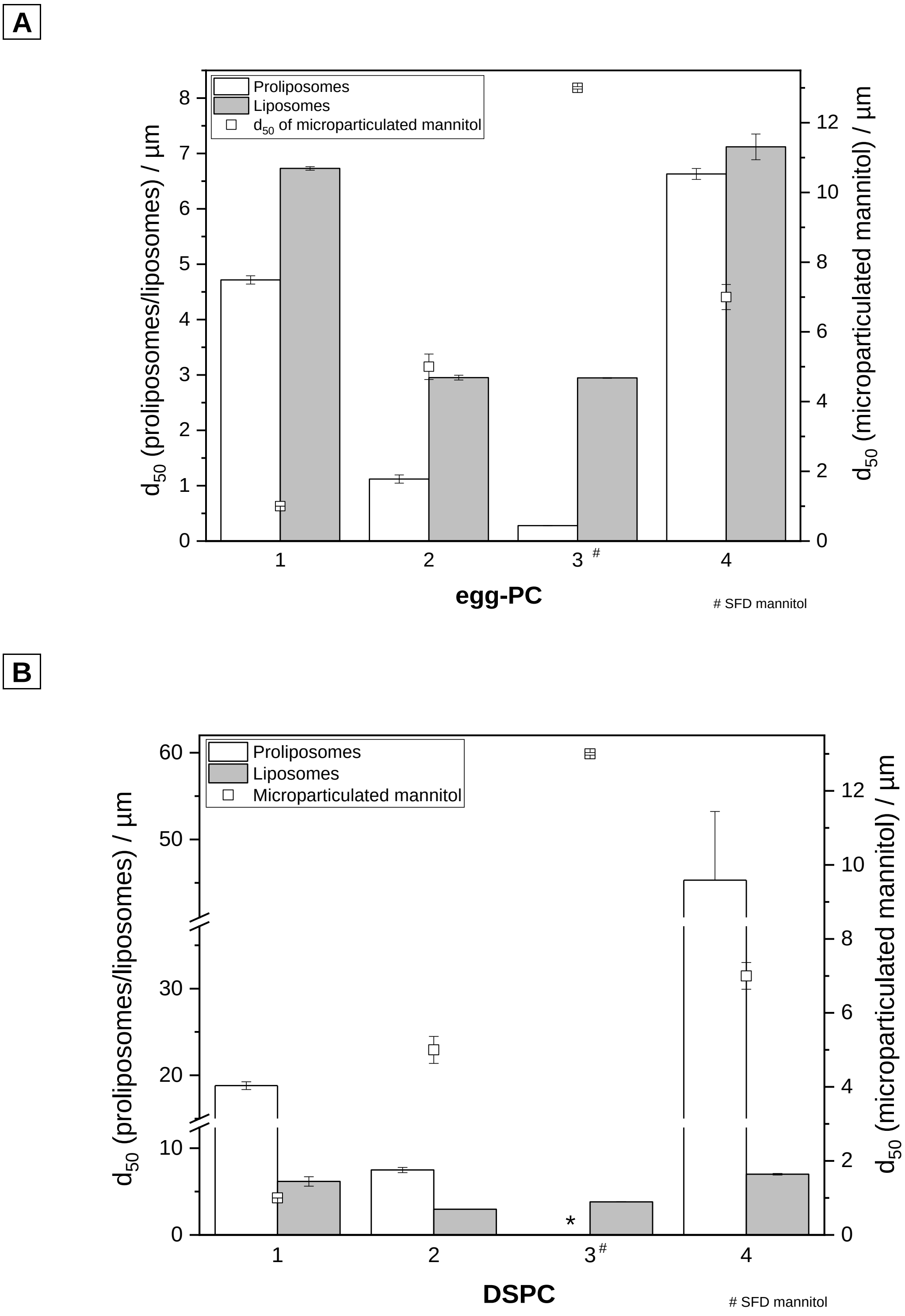

Figure 69: D$_{50}$-values (measured using LD) of spray dried PLs and reconstituted PLS out of (**A**) egg-PC and (**B**) DSPC. Furthermore, d$_{50}$-values of microparticulated mannitol as carrier material is additionally depicted in the graph. T$_{inlet}$ 110 °C; T$_{outlet}$: ~ 71 °C; flow rate: 3 ml*min^{-1}; carrier:
1: 1 % microparticulated mannitol
2: 10 % microparticulated mannitol
3: 1 % spray-freeze-dried mannitol
4: 1 % microparticulated mannitol
Please note different axis scales; *no data available.

4.4 Summary of the spray drying experiment and coating method applied

Summing up, a clear section is dedicated to the direct comparison of the two preparation methods, spray drying versus coating, with focus on different aspects like yield, liposomal size or large-scale production. Furthermore, an outlook for further directions of future perspectives is discussed.

Table 28 gives an overview of different parameters varied in production of PLs. By comparison of the coating method and spray drying process, the following aspects were relevant for the experiments carried out in this work. The different points of view and additional aspects are discussed in the following section.

Table 28: Overview of different production parameters and characteristic results for both production methods, spray drying and coating. To be determined (tbd) means that further experiments have to be performed.

Parameter	Coating method	Spray drying
Yield	~ 75 %	~ 17 %
Preliminary stage	Not necessary	Production of carrier materials
API	Fenofibrate / Ibuprofen	Fenofibrate
Liposomal size / with extrusion step	~ 8-10 µm / 150 nm	~ 3-7 µm / tbd
Zeta potential	~ - 12 mV	tbd
EE	Fenofibrate: > 99 % Ibuprofen: 5-31 %	tbd
Total number of liposomes per mm^3	Egg-PC: 72 250 DSPC: 21 400	Egg-PC: 33 745 DSPC: 11 250
Release studies	Release of nearly 100 % of the loaded drug within 180 min	tbd

- Yield:

  Considering the yield of both processes, the coating method had the edge over the spray drying process. In small lab scale as well as with Glatt® coater, nearly 70 % of lipid or API were recovered from the carrier material. Only ~ 20 % of PLs referred to all solid components could be reached *via* spray drying process due to losses *e.g*. in the cyclone.
- Preliminary stage:

  In order to facilitate the production of PLs *via* spray drying, it was necessary that an appropriate carrier material needs to be prepared. In this work, mannitol was spray dried and thus a microparticulated type of the carrier was created. No pre-treatment of carrier was necessary for the coating method which is a time saving benefit of this preparation procedure when no commercial carrier material with suitable particle size is available.
- API:

  As representative candidates for poorly soluble drugs, fenofibrate and ibuprofen were encapsulated in the liposomal formulations. It was possible to produce PLs by spray drying containing fenofibrate. Ibuprofen was not suitable for the spray drying process due to the fact that no dry powder could be collected in the collecting container. All product adhered on the wall of the cyclone and it seemed that a melt of the drug was formed. Even with a T_{inlet} reduced to 40 °C and aspirator performance of 100 %, a successful production was not possible. Alternative poorly soluble drugs that could be tested in another proof-of-principle study with the same formulation conditions could be carbamazepine or naproxen.
- Liposomal size:

  For the coating method, the liposomal size of the raw dispersion was within the range of 8 and 10 µm. After extrusion, the liposomal size lay at approximately 150 nm. Regarding the spray drying process, the size of the vesicles (without extrusion step) reached values of 3 µm (10% microparticulated mannitol and 1 % SFD mannitol as carrier) and 7 µm (1 % microparticulated mannitol as carrier material).

- Zeta potential:

  The averaged absolute value of ZP was between - 12 mV which indicated regions of limited flocculation. For spray drying process, further experiments are needed.
- Encapsulation efficiency:

  Considering EE, the coating method showed more than > 99 % drug release for fenofibrate. In contrast, ibuprofen was encapsulated at a level of only ~ 30 %.
- Total number of liposomes per mm^3:

  Overall, the coating method was more suitable for the production of batches with higher total numbers of liposomes per mm^3 formed upon rehydration. Egg-PC formed three times higher amounts of liposomal vesicles than with DSPC. Comparing the coating process and the spray drying method two times higher number of vesicles were counted for the samples of the coating method.
- Large-scale production:

  For the coating method, it was possible to transfer the small-scale lab process to a larger scale production machine like the Glatt® coater due to the good flowability of the round shaped product. There are several other possibilities that might be tested as alternative spray driers for the bench top Büchi machine, for example the rotary atomizer Niro Mobile Minor (GEA, Copenhagen, Denmark), which pushes the limit for particle size of the carrier materials Overall, both procedures are presumably scalable.
- Release studies:

  Nearly 100 % of fenofibrate PLs was released within 180 min. Sucrose was used as carrier material. Water insoluble carriers might give a different behavior, thus MCC350 could be examined. A proliposomal release temperature of 37 °C was suitable.
- Stability study:

  Stability testing was only performed for liposomes produced *via* the coating method and stored in the climatic chamber at 40 °C. The formulations revealed liposomal sizes < 160 nm with PDI values < 0.1, ZP increased up to a value of ~ -20 mV and could be used as drug loading materials with a stability for half a year.

(Further storage conditions should be tested for a long-term study for example 24 weeks, at various temperatures like - 80 °C or 4 °C and different humidity).

In summary both PLs production procedures were suitable to produce PLs with an advantage of the coating method regarding the outcome of the product. Additionally, no production step in advance is necessary in comparison to the spray drying process. The size of the MLVs was rather high for both methods with a value of several µm. Dissolution studies were investigated for the PLs produced by the coating method with a release of nearly 100 % of fenofibrate after ~ 180 min. The coating method process parameters were established in small scale and then successfully transferred to the Glatt® Coater. Next to release studies, final spray drying products could be also investigated regarding (i) moisture content determined by Karl-Fischer titration, (ii) the behaviour of phase transition temperatures characterized *via* differential scanning calorimetry (DSC), physical structure changes that are detectable by XRD or the influence of extrusion after reconstitution. Furthermore, biological *in vitro* experiments with for example Caco-2 cell lines could be investigated in order to estimate the permeability of PLs across the different liposomal layers [223, 224].

5 CONCLUSION / ZUSAMMENFASSUNG

Conclusion

Liposomes have been of great pharmaceutical interest for many years due to their potential as colloidal systems that are used for incorporation of hydrophilic active substances into the aqueous core as well as intermediate layers. However, hydrophobic compounds can be embedded between the lipid layers that have a protective function against enzymatic degradation in the body. The main disadvantage of such vehicles is their limitation regarding shelf life and large-scale production of liposomal dispersions. To overcome these drawbacks, the development of proliposomes (PLs) is one possible approach because they are are characterized by their solid state as dry, free-flowing granular products, which form multilamellar vesicles (MLVs) after the addition of water or after having contact with biological fluids *in vivo.* Furthermore, they can show good oral bioavailability, prolonged shelf life time and easier handling of scale up.

Overall, this thesis deals with the development of proliposomal formulations and corresponding liposomes which are formed *in situ* with subsequent analysis regarding size, zeta potential (ZP) and encapsulation efficiency (EE) for two poorly water-soluble water drugs.

Hereby, the development of manufacturing methods for PLs was focused on an in-depth analysis and characterization of *in situ* formed liposomes. Initially, a coating process for small batch sizes was created and afterwards transferred to larger scale production using a Glatt® Coater. In addition, the production of PLs by spray drying was also investigated. The aim of the project was the formation of PLs with established coating or spray drying processes that resulted in good reconstitutability and EE. Furthermore, PLs were suitable precursors for direct compression producing tablets. Fenofibrate and ibuprofen were selected as model drugs representing poorly water-soluble compounds according to Biopharmaceutics Classification System (BCS) class II.

First, liposomes were produced using the conventional round bottom flask method as a reference for the manufacture of liposomes. By varying the treatment procedure (filtration, addition of ultrasonic sound or vortexing) of the liposomal dispersion after reconstitution, the limits of the method regarding on vesicles' size, polydispersity index (PDI) were investigated as well. The observation time was set to 48 h. It was shown that the mean liposome size of the placebo batch was ~ 320 nm. A slight decrease in nanoparticular size was observed after 48 h (~ 300 nm). The smallest vesicles were achieved by the combination of all three treatment methods (filtration, ultrasonic sound and vortexing). The smallest effect on the vesicle size was shown for the batch treated by vortexing. However, even smaller vesicles (~ 250 nm) were formed with encapsulation of the active pharmaceutical ingredient (API) ibuprofen. Here, the liposomal size as well as the PDI were both stable during the investigation period. All batches showed smaller vesicles than the untreated reference dispersion. The ZP exhibited a tendency towards negative values over 48 h for both batches irrespective of drug loading. Highest ZP values were achieved after ultrasonic sound application, both, for placebo as well as API batches. Furthermore, the stability of liposomal dispersions was investigated for 48 h by varying the pH-value. A shift to more basic conditions with pH-levels of ~ 11 had the highest impact factor on a uniform liposomal size. Moreover, also the ZP was stabilized in the range of - 30 mV by increasing the pH-level. The reconstitution medium (water or 10% (w/V) lactose solution) did not have any influence on the liposomal size or ZP.

In the second part, a lab scale coating method was developed as a tool for small scale investigations on various parameters affecting the manufacture of PLs and liposomes formed thereof. After defining promising process parameters, the process was successfully transferred to a larger scale using a Glatt® Coater and a promising formulation was prepared. Using scanning electron microscopy (SEM) and macroscopic investigations, the surface of different carrier materials (water-soluble and water-insoluble) was examined. The applied layers were clearly recognizable and the various lipid types could be differentiated. With polarization microcopy and cryo-/transmission electron microscopy (TEM), the formation, presence and differentiation of liposomes and PLs after reconstitution were successfully investigated. Spherical vesicles were visible by absorption of complementary polarized light with Maltese crosses as a typical characteristic feature. The images showed unilamellar vesicles (ULVs) after extrusion, whose size also corresponded to the dynamic light scattering (DLS) measurements. Furthermore, a comparison of the two different preparation methods (conventional round bottom flask on the one hand and liposomes formed out of PLs after addition of aqueous phase on the other hand) was performed. Different kind of carriers (water-soluble, water-insoluble) were examined. No significant differences in size of raw liposomal dispersions were measured. After extrusion through a 0.4 µm polycarbonate membrane, smaller carriers resulted in the formation of smaller liposomes. In summary, the developed manufacturing methods of PLs showed no disadvantages in comparison to the conventional method. Furthermore, the classical round bottom flask method was modified and varied with an adaption to the production of PLs. A storage stability study was performed for six months choosing a temperature of 40 °C in a drying cabinet. The prevailing conditions revealed no negative influence on liposomal size or size distribution for proliposomal formulations consisting of water-soluble carriers. The stability of the liposomal dispersion was improved regarding ZP. Xylitol and sucrose seemed to be the most stable formulations with respect to a uniform liposomal size. In addition, the PDI of the two formulations was stable during six months with a narrow size distribution. ZP increased up to ~ - 20 mV. During proliposomal formulation development, changes in powder carrier materials and lipid-to-carrier ratio were performed. The latter variation seems to be a promising approach with focus on the preparation of smaller vesicles. In addition to giving proof of the existence of PLs using polarization microscopy, the total number of vesicles per mm^3 for different types of lipids was determined using a Thoma counting chamber. With higher total numbers, liposomal size decreased. 1,2-Dioctadecanoyl-*sn*-glycero-3-phosphocholine (18:0; DSPC) and egg-phosphatidylcholine (egg-PC) were identified as promising lipids for a design of experiments (DoE) approach. Based on these results, a larger-scale production of PLs was established with the Glatt® Coater. The combination of the lipids egg-PC, 1,2-ditetradecanoyl-*sn*-glycero-3-phospho-(1'-*rac*-glycerol) (14:0; DMPG) and cholesterol was chosen as most suitable formulation regarding the favored properties of size, ZP and EE. With respect to the phase transition temperature of the lipid components that is below 37 °C, this condition was chosen as release temperature for HPLC experiments.

Furthermore, a proliposomal granulate using Tablettose® as carrier and fenofibrate or ibuprofen as API was produced, which enabled a successful further compression to tablets as solid dosage form. Even after reconstitution of the tablets, liposomes were formed spontaneously. An EE of almost 100 % was determined for the poorly soluble drug fenofibrate. Due to its lipophilicity, the API might integrate in the membrane and increase the vesicle size. Moreover, release studies with the same active ingredient were carried out in order to determine the released drug amount. Proliposomal formulations based on the sucrose carrier (2,500 - 3,300 µm; GHP 5) showed an initial burst release within three hours. There was no tendency for a "grease ball" formation of fenofibrate and consequently the whole API amount was homogenously solubilized in the vesicles.

In the last part, a manufacturing method for PLs *via* spray drying was developed. First, a suitable carrier material had to be produced, which should have a narrow particle size distribution to guarantee no choking of the nozzle. The lipids formed a layer around the suspended carrier particles. The influence of the inlet air temperature (T_{inlet}) and flow rate was investigated with a temperature of 110 °C and a flow rate of 3 ml*min^{-1}. The average yield was at 75 %, with d_{50}-value of ~ 4 µm. In addition to three microparticulated mannitol samples for the production of PLs, one sample was also prepared by spray freeze drying with a d_{50}-value of ~ 12.5 µm. Four batches of spray dried PLs were investigated. After reconstitution with water, liposomes were formed spontaneously, and their presence was approved by polarization microscopy. However, it should be mentioned that the total number of liposomes per mm^3 was two times the number of liposomes formed *via* coating method. The vesicle size (d_{50}-value between 3 and 7 µm) was dependent on the size of microparticulated mannitol and not on the size of PLs. 10 % (w/V) of spray dried mannitol provided the most preferred result with narrow size distribution, a slightly negative potential and a homogenous reconstitutability. Furthermore, the porous character of spray-freeze dried mannitol led to small vesicles. Finally, both manufacturing methods were directly compared regarding their characterization and approaches for possible future directions were shown.

With respect to the development of different proliposomal formulations with poorly water-soluble drugs, two production methods were successfully established by spray drying and coating. All formulations were storage-stable and formed spontaneously liposomes after reconstitution in aqueous medium. These vesicles have been investigated *i.a*. by cryo-TEM and revealed homogenously distributed, round shaped ULVs. Furthermore, the liposomes have been characterized with respect to size, EE, ZP and release behaviour. By means of a DoE, the coating method was successfully transferred from the laboratory to a larger production scale. In addition, proliposomal granules were pressed into tablets, which represents a promising approach for increasing the bioavailability of sparingly soluble substances.

Zusammenfassung

Liposomen sind seit vielen Jahren von großem pharmazeutischem Interesse. Es ist möglich hydrophile Wirkstoffe in den wässrigen Kern sowie in wässrige Zwischenschichten von Liposomen einzulagern. Hydrophobe Wirkstoffe werden jedoch in der Lipid-Doppelmembran eingebaut, die eine Art Schutzfunktion auf die eingeschlossenen Wirkstoffe ausübt und den enzymatischen Abbau im Körper behindert. Ein Nachteil liposomaler Dispersionen ist ihre begrenzte Haltbarkeit, sowie die begrenzte Herstellung im größeren Maßstab. Eine Abhilfe gegenüber genannten Einschränkungen, stellt die Entwicklung von Proliposomen (PL) dar, die sich durch ihre feste Ausgangsform auszeichnen. Sie sind definiert als granulatartige, frei-fließende Produkte, die *in situ* multilamellare Vesikel (MLVs) nach der Zugabe von Wasser oder biologischen Flüssigkeiten bilden. Weiterhin weißen sie eine gute orale Bioverfügbarkeit, verlängerte Haltbarkeit und leichtere Herstellungsmöglichkeiten im größeren Maßstab auf.

Im Fokus dieser Arbeit stand die Entwicklung verschiedener proliposomaler Formulierungen sowie die anschließende Charakterisierung der sich *in situ* bildenden Liposomen hinsichtlich liposomaler Größe, Zetapotential (ZP) und Einschlusseffizienz (EE) zweier schwer wasserlöslicher Wirkstoffe analysiert wurden.

Hierbei stand die Entwicklung von proliposomalen Herstellungsmethoden und der sich daraus bildenden Liposomen im Fokus. Zunächst wurde ein Coating-Verfahren im Kleinmaßstab entwickelt, das im Anschluss auf einen Glatt® Coater im größeren Labormaßstab transferiert wurde. Daneben fand auch die Herstellung von Liposomenzubereitungen mittels Sprühtrocknung Anwendung. Ziel der Arbeit war es, PL mit den beiden etablierten Verfahren zu produzieren, die eine gute Rekonstituierbarkeit und EE aufweisen und unter anderem auch zur direkten Tablettierung mit einer Exzenterpresse geeignet sein sollten. Als Modellarzneistoffe für schwer wasserlösliche Substanzen nach dem Biopharmazeutischen Klassifizierungssystem (BCS) Klasse II, fiel die Wahl auf den Lipidsenker Fenofibrat sowie das Analgetikum Ibuprofen.

Zunächst wurden Liposomen mittels konventioneller Rundkolbenmethode, welche als Referenz fungieren sollte, hergestellt. Dabei sollte die liposomale Größe, der

Polydispersitätsindex (PDI) sowie das ZP nach unterschiedlicher Vorbehandlung (Filtration, Zugabe von Ultraschall oder Vortexen) der liposomalen Dispersion untersucht werden, um die Grenzen des Verfahrens auszutesten. Das Ganze wurde über einen Zeitraum von 48 h ab Zeitpunkt der Herstellung beobachtet. Es konnte gezeigt werden, dass die mittlere Liposomengröße in der Placebo-Charge bei einem Wert von ~ 320 nm lag, die über nach zwei Tagen auf ~ 300 nm gesunken ist. Die kleinsten Vesikel wurden durch die Kombination aller drei Behandlungsmethoden, Vortexen, Ultraschall sowie Filtration, erreicht. Geringsten Einfluss hatte lediglich vorheriges Vortexen. Bei den Chargen, die den verkapselten Wirkstoff Ibuprofen enthielten, bildeten sich kleinere Vesikel (~ 250 nm). Die Größe sowie der PDI waren in diesem Fall über zwei Tage stabil. Hierbei konnte kein eindeutiger Trend durch eine Nachbehandlung der liposomalen Dispersion erkannt werden. Bei der Placebo-Charge war jedoch ein leichter Abfall in der Größenmessung zu erkennen. Das ZP veränderte sich bei beiden Versuchsästen über einen Zeitraum von 48 h hin zu negativeren Werten. Der höchste Betrag des Zetapotentials wurde nach dem Zusatz von Ultraschall sowohl bei Placebo- als auch bei Wirkstoff-Chargen erreicht. Desweiteren wurde die Stabilität von Liposomendispersionen über 48 h durch Variation des pH-Wertes untersucht. Es hat sich gezeigt, dass eine Verschiebung zu basischerem pH-Wert (~ 11) den größten Effekt auf eine einheitliche Liposomengröße hat. Dies spiegelte sich auch in einem stabilisierenden ZP mit einem Wert von - 30 mV wieder. Die verschiedenen Rekonstitutionsmedien (Wasser oder 10%-iger (m/V) Lactoselösung) hatten keinen Einfluss auf die Liposomengröße und das Zetapotential.

Im zweiten Teil der Arbeit gelang es eine Coating-Methode im Labormaßstab zu entwickeln, die im Anschluss nach der Definition versprechenden Prozessparameter erfolgreich mit einer vielversprechenden Formulierung auf den Produktionsmaßstab im Glatt® Coater transferiert wurde. Mittels Rasterelektronenmikroskopie (REM) und makroskopischen Analysen wurden die Oberflächen der verschiedenen Trägermaterialien vor und nach dem Coating untersucht. Die aufgetragenen Schichten waren deutlich erkennbar. Ebenso konnten die unterschiedlichen Lipidarten differenziert werden. Der Beweis für die Bildung und Anwesenheit von aus Proliposomen gebildeten Liposomen wurde mit

Hilfe von Polarisationsmikroskopie und (Cryo-) Transmissionselektronenmikroskopie (TEM) erfolgreich erbracht. Durch die Absorption von komplementär polarisiertem Licht durch den Polfilter wurden sphärische Vesikel mit Malteserkreuzen, als typisch charakteristisches Merkmal, sichtbar. Die TEM-Aufnahmen gaben ebenfalls Hinweise auf die Bildung von Liposomen. Deutlicher Beweis, dass es sich nach Rekonstitution um Liposomen handelte, stellte die Cryo-TEM dar. Die Aufnahmen zeigten nach Extrusion eindeutige unilamellare Vesikel (ULVs), deren Größe auch mit den dynamischen Lichtstreuungs-Messungen (DLS) übereinstimmten. Ebenfalls wurde die Charakterisierung von Liposomen basierend auf der konventionellen Rundkolbenmethode und der Rekonstitution von Proliposomen verglichen. Unterschiedliche Arten von Trägern (wasserlöslich, wasserunlöslich) kamen zum Einsatz. Die unbehandelte Liposomendispersion wies keinen wesentlichen Unterschied hinsichtlich der Größe der Vesikel auf. Nach Extrusion durch die 0,4 µm Membran zeigte sich, dass sich bei kleinerer Trägergröße auch kleinere Liposomen bildeten. Es stellte sich heraus, dass die entwickelte Herstellungsmethode gegenüber der konventionellen keine Nachteile mit sich brachte. Zusätzlich wurde die klassische Rundkolbenmethode modifiziert und verändert, um diese mehr an den Prozess der PL-Herstellung anzugleichen. Eine Stabilitätsstudie zur Lagerung von Proliposomen wurde für sechs Monate bei 40 °C im Klimaschrank durchgeführt. Durch die vorherrschenden Bedingungen zeigte sich kein negativer Einfluss auf die liposomale Größe und deren Verteilung für proliposomale Formulierungen bestehend aus wasserlöslichen Trägern. Unter Berücksichtigung des ZPs wurde die Stabilität der liposomalen Dispersion verbessert. Xylitol und Saccharose schienen die bestgeeignetsten Träger für stabile Formulierungen in Bezug auf eine vereinheitlichte Liposomengröße zu sein. Darüber hinaus war der PDI der beiden Formulierungen stabil und zeigte eine enge Größenverteilung. Das Zetapotential stieg auf einen Wert von ~ - 20 mV. Im Zuge der Formulierungsentwicklung wurden alternative pulverartige Trägermaterialien und unterschiedliche Lipid-Träger-Verhältnisse getestet. Letzteres stellte einen vielversprechenden Ansatz für die Herstellung kleiner Liposomen dar. Neben der Existenz von Proliposomen mit Hilfe von Polarisationsmikroskopie wurde auch die totale Anzahl an Vesikeln pro mm^3 für unterschiedliche Lipide unter Verwendung einer Thoma-Zählkammer bestimmt. Je größer die Anzahl der gezählten Teilchen, umso kleiner die sich bildenden Liposomen. Unter Berücksichtigung der Anzahl wurden Dioctadecanoyl-*sn*-glycero-3-phosphocholin (18:0; DSPC) und Ei-Phosphatidylcholin (Ei-PC) als vielversprechende Lipide für ein Design of Experiment (DoE) ermittelt. Auf diesen Ergebnissen basierend, wurde eine Herstellung von PL im größeren Maßstab mit dem Glatt® Coater etabliert. Dabei stellte die Kombination der Lipide Ei-PC, 1,2-ditetradecanoyl-*sn*-glycero-3-phospho-(1'-*rac*-glycerol) (14:0; DMPG) und Cholesterol eine geeignete Fromulierung hinsichtlich der gewünschten Targets von Vesikelgröße, ZP und EE dar. Da die Phasenübergangstemperaturen der Lipide unterhalb von 23 °C liegen, konnte für spätere HPLC Versuche 37 °C als Freisetzungstemperatur gewählt werden. Weiterhin wurde ein proliposomales Granulat mit Tablettose® als Träger sowie den Wirkstoffen Ibuprofen und Fenofibrat hergestellt, dass eine erfolgreiche Weiterverarbeitung zu Tabletten ermöglichte. Auch nach Rekonstitution der Tabletten bildeten sich spontan Liposome. Für den Wirkstoff Fenofibrat wurde eine EE von nahezu 100 % ermittelt, was darauf schließen lässt, dass sich der Wirkstoff möglicherweise aufgrund seiner Lipophilie in die Lipidmembran eingelagert hat. Dies könnte auch in eine Vergrößerung der Liposomengröße resultieren. Desweiteren wurden Freisetzungsstudien mit Fenofibrat durchgeführt. Als Trägermaterial wurden Saccharose Träger (2 500 - 3 300 µm; GHP 5) verwendet. Die PL zeigten eine Initialfreisetzung mit Freigabe des Wirkstoffes innerhalb von drei Stunden. Es zeigte sich, dass der gesamte Wirkstoff in den MLVs solubilisiert war und keine Aggregation der Fenofibratmoleküle bei Kontakt mit Wasser stattfand.

Im letzten Teil wurde eine Herstellungsmethode von Proliposomen mit Hilfe von Sprühtrocknung entwickelt. Zuerst wurde ein geeignetes Trägermaterial hergestellt, dass eine enge Korngrößenverteilung haben sollte, um das sich die Lipide schichten sollten. Der Einfluss von Zulufttemperatur (T_{inlet}) und Flussrate wurde untersucht, wobei sich eine Temperatur von 110 °C sowie eine Flussrate von 3 $ml*min^{-1}$ etablierte. Die Ausbeute lag im Schnitt bei 75 % und einem d_{50}-Wert von ~ 4 µm. Neben drei mikropartikulären Mannitolproben zur Herstellung von Proliposomen, wurde ebenfalls eine Probe mittels Sprühgefriertrocknungsverfahren hergestellt, die bei einem d_{50}-Wert von ~ 12,5 µm lag. Es wurden vier Chargen an sprühgetrockneten Proliposomen hergestellt. Nach Rekonstitution mit bidestilliertem Wasser bildeten sich Liposomen, die mittels Polarisationsmikrokopie nachgewiesen wurden. Allerdings soll erwähnt werden, dass die totale Anzahl an Liposomen pro mm^3 bei der Coating-Methode doppelt so hoch war. Desweiteren war erkennbar, dass die Vesikelgröße (d_{50}-Werte zwischen 3 und 7 µm) von der Größe des sprühgetrockneten Trägermaterials abhängig war und nicht von der Größe der Proliposomen. Der poröse Charakter der sprühgefriergetrockneten Probe führte zu kleinen Liposomen. 10 % (m/m) Anteil an sprühgetrocknetem Mannitol lieferte das beste Ergebnis. Abschließend wurden beide Herstellungsmethoden im direkten Vergleich gegenübergestellt und Ansätze für mögliche Folgeversuche aufgezeigt.

Im Hinblick auf die Entwicklung verschiedener proliposomaler Formulierungen mit schwer wasserlöslichen Wirkstoffen wurden in der vorliegenden Arbeit zwei Herstellungsvarianten entwickelt: das Coating Verfahren und der Sprühtrocknungsprozess. Es ist gelungen lagerstabile Proliposomen herzustellen, die nach Zusatz von wässrigem Medium spontan Liposomen bildeten. Diese wurden unter anderem erfolgreich mittels Cryo-TEM hinsichtlich einer einheitlichen Größenverteilung und runden ULVs nachgewiesen. Desweiteren wurden die Liposomen hinsichtlich Größer, EE, ZP und Freisetzungsverhalten untersucht. Mittels eines DoE ist es gelungen, die Coating-Methode vom Labormaßstab in einen größeren Produktionsmaßstab erfolgreich zu transferieren. Daneben wurden granulatartige Proliposomen zu Tabletten verpresst, was einen vielversprechenden Ansatz zur Erhöhung der Bioverfügbarkeit schwerlöslicher Stoffe darstellt.

6 APPENDIX

Characterization of the carrier material MCC 350

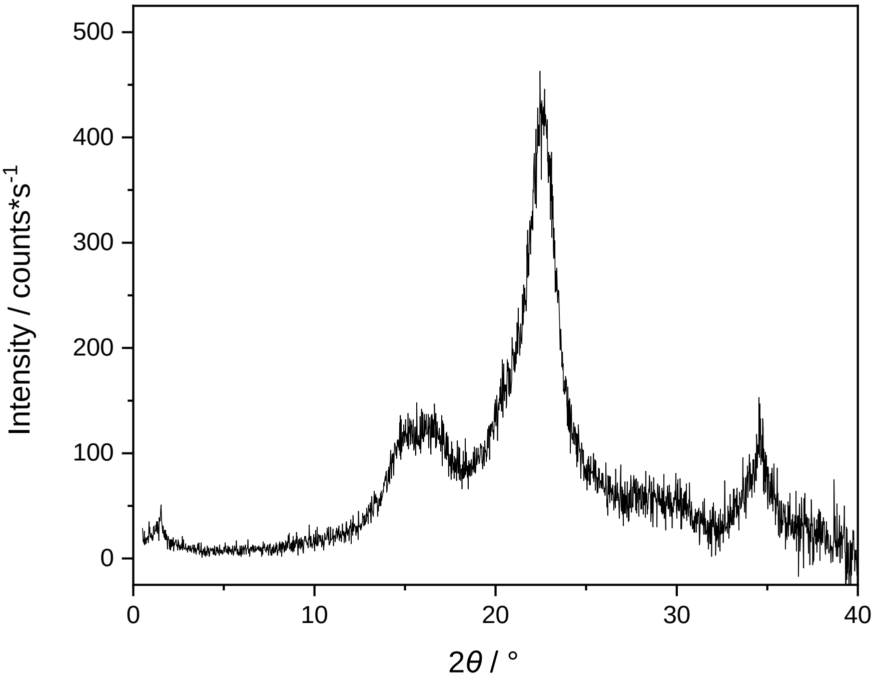

Figure 70: WAXD of MCC 350.

DoE results of all performed experiments

Table 29: Results of liposomal size, EE and ZP of DoE approach.

Run no.	Liposomal size / µm	EE / %	ZP / mV
1	8.74 ± 0.79	99.96	- 7.38 ± 0.61
2	8.06 ± 0.63	99.97	- 8.24 ± 0.50
3	12.00 ± 0.07	99.95	- 9.43 ± 0.87
4	11.30 ± 0.13	99.98	- 11.53 ± 1.53
5	7.89 ± 0.17	99.98	1.69 ± 1.36

Run no.	Liposomal size / µm	EE / %	ZP / mV
6	7.57 ± 0.86	99.96	2.77 ± 0.58
7	10.63 ± 0.07	99.95	0.96 ± 0.22
8	8.15 ± 0.27	99.97	1.38 ± 0.10
10	11.30 ± 0.27	99.95	- 8.16 ± 1.07
11	9.21 ± 0.48	99.94	- 7.23 ± 2.19
13	10.24 ± 0.06	99.95	- 9.50 ± 0.91
14	12.68 ± 0.23	99.95	- 10.70 ± 1.51

7 REFERENCES

1. Bangham, A.D. and R.W. Horne, *Negative Staining of Phospholipids and their Structural Modification by Surface-active Agents as observed in the Electron Microscope.* J. Mol. Biol., 1964. **8**: p. 660-680.
2. Deamer, D.W., *From "Banghasomes" to liposomes: A memoir of Alec Bangham, 1921–2010.* The FASEB Journal, 2010. **24**(5): p. 1308-1310.
3. Torchilin, V.P., *Recent advances with liposomes as pharmaceutical carriers.* Nat. Rev. Drug. Discov., 2005. **4**(2): p. 145-160.
4. Bulbake, U., et al., *Liposomal Formulations in Clinical Use: An Updated Review.* pharmaceutics, 2017. **9**(12).
5. Tiphine, M., V. Letscher-Bru, and R. Herbrecht, *Amphotericin B and its new formulations: pharmacologic characteristics, clinical efficacy, and tolerability.* Transpl. Infect. Dis., 1999. **1**(4): p. 273-283.
6. Phillips, W.T., *Delivery of gamma-imaging agents by liposomes.* Adv. Drug. Deliv. Rev., 1999. **37**(1-3): p. 13-32.
7. Simoes, S., et al., *Cationic liposomes for gene delivery.* Expert Opin. Drug. Deliv., 2005. **2**(2): p. 237-254.
8. Meybeck, A., *Past, Present and Future of Liposome Cosmetics*. Liposome Dermatics: Griesbach Conference, ed. O. Braun-Falco, H.C. Korting, and H.I. Maibach. 1992, Berlin, Heidelberg: Springer Berlin Heidelberg. 341-345.
9. Sharma, A. and U.S. Sharma, *Liposome in drug delivery: progress and limitations.* Int. J. Pharm., 1997. **154**.
10. Immordino, M.L., F. Dosio, and L. Cattel, *Stealth liposomes: review of the basic science, rationale, and clinical applications, existing and potential.* Int. J. Nanomedicine, 2006. **1**(3): p. 297-315.
11. Tripathi, G., K. Chaurasiya, and P. Katare, *Liposomal current status, evaluation and recent advances.* 2013. **5**: p. 4-14.
12. Ickenstein, L.M., et al., *Effects of phospholipid hydrolysis on the aggregate structure in DPPC/DSPE-PEG2000 liposome preparations after gel to liquid crystalline phase transition.* Biochim. Biophys. Acta., 2006. **1758**(2): p. 171-180.
13. Payne, N.I., et al., *Proliposomes: A Novel Solution to an Old Problem.* J. Pharm. Sci., 1986. **75**(4): p. 325-329.
14. Janga, K.Y., et al., *Bioavailability enhancement of zaleplon via proliposomes: Role of surface charge.* Eur. J. Pharm. Biopharm., 2012. **80**(2): p. 347-357.
15. Xu, H., et al., *Optimized preparation of vinpocetine proliposomes by a novel method and in vivo evaluation of its pharmacokinetics in New Zealand rabbits.* J. Control. Release, 2009. **140**(1): p. 61-68.
16. Bansal, S., et al., *A Comparative Review on Vesicular Drug Delivery System and Stability Issues.* Int. J. Res. Pharm. Chem., 2012. **2**(3): p. 704-713.

17. Wang, Q., et al., *A novel formulation of [6]-gingerol: Proliposomes with enhanced oral bioavailability and antitumor effect.* Int. J. Pharm., 2018. **535**(1): p. 308-315.
18. Kumara, B.C., et al., *Proliposome a novel approach to carrier drug delivery system.* Int. J. Biopharm., 2015. **6**(2): p. 98-106.
19. EMA, *Caelyx - Doxorubicin Hydrochlorid*. 2010, European Medicines Agency Science Medicines Health.
20. Gubernator, J., *Active methods of drug loading into liposomes: recent strategies for stable drug entrapment and increased in vivo activity.* Expert Opin. Drug Deliv., 2011. **8**(5): p. 565-580.
21. Laouini, A., et al., *Preparation, Characterization and Applications of Liposomes: State of the Art.* J. Colloid Sci. Biotechnol. , 2012. **1**: p. 147-168.
22. Straubinger, R.M., et al., *Endocytosis of liposomes and intracellular fate of encapsulated molecules: encounter with a low pH compartment after internalization in coated vesicles.* Cell, 1983. **32**(4): p. 1069-1079.
23. Karanth, H. and R.S. Murthy, *pH-sensitive liposomes--principle and application in cancer therapy.* J. Pharm. Pharmacol., 2007. **59**(4): p. 469-483.
24. Paszko, E. and M.O. Senge, *Immunoliposomes.* Curr. Med. Chem., 2012. **19**(31): p. 5239-5277.
25. Oku, N. and Y. Namba, *Long-circulating liposomes.* Crit. Rev. Ther. Drug Carrier Syst., 1994. **11**(4): p. 231-270.
26. Sercombe, L., et al., *Advances and Challenges of Liposome Assisted Drug Delivery.* Front. Pharmacol., 2015. **6**.
27. Charron, D.M., J. Chen, and G. Zheng, *Theranostic lipid nanoparticles for cancer medicine.* Cancer Treat. Res., 2015. **166**: p. 103-127.
28. Cole, J.T. and N.B. Holland, *Multifunctional nanoparticles for use in theranostic applications.* Drug Deliv. Transl. Res., 2015. **5**(3): p. 295-309.
29. Bangham, A.D., M.M. Standish, and J.C. Watkins, *Diffusion of univalent ions across the lamellae of swollen phospholipids.* J. Mol. Biol., 1965. **13**(1): p. 238-252.
30. Torchilin, V. and V. Weissig, *Liposomes: a pracital approach*. 2003: Oxford University Press.
31. Szoka, F., Jr. and D. Papahadjopoulos, *Procedure for preparation of liposomes with large internal aqueous space and high capture by reverse-phase evaporation.* Proc. Natl. Acad. Sci. USA, 1978. **75**(9): p. 4194-4198.
32. Akbarzadeh, A., et al., *Liposome: classification, preparation, and applications.* Nanoscale Res. Lett., 2013. **8**(1).
33. Riaz, M., *Liposomes preparation methods.* Pak. J. Pharm. Sci., 1996. **9**(1): p. 65-77.
34. Batzri, S. and E.D. Korn, *Single bilayer liposomes prepared without sonication.* Biochim. Biophys. Acta, 1973. **298**(4): p. 1015-1019.
35. Pons, M., M. Foradada, and J. Estelrich, *Liposomes obtained by the ethanol injection method.* Int. J. Pharm., 1993. **95**(1): p. 51-56.
36. Deamer, D. and A.D. Bangham, *Large volume liposomes by an ether vaporization method.* Biochim. Biophys. Acta, 1976. **443**(3): p. 629-634.
37. Schieren, H., et al., *Comparison of large unilamellar vesicles prepared by a petroleum ether vaporization method with multilamellar vesicles: ESR, diffusion and entrapment analyses.* Biochim. Biophys. Acta, 1978. **542**(1): p. 137-153.

38. Milsmann, M.H., R.A. Schwendener, and H.G. Weder, *The preparation of large single bilayer liposomes by a fast and controlled dialysis.* Biochim. Biophys. Acta, 1978. **512**(1): p. 147-155.
39. Zumbuehl, O. and H.G. Weder, *Liposomes of controllable size in the range of 40 to 180 nm by defined dialysis of lipid/detergent mixed micelles.* Biochim. Biophys. Acta, 1981. **640**(1): p. 252-262.
40. Schurtenberger, P., et al., *Preparation of monodisperse vesicles with variable size by dilution of mixed micellar solutions of bile salt and phosphatidylcholine.* Biochim. Biophys. Acta, 1984. **775**(1): p. 111-114.
41. Brunner, J., P. Skrabal, and H. Hauser, *Single bilayer vesicles prepared without sonication. Physico-chemical properties.* Biochim. Biophys. Acta, 1976. **455**(2): p. 322-331.
42. Holloway, P.W., *A simple procedure for removal of Triton X-100 from protein samples.* Anal. Biochem., 1973. **53**(1): p. 304-308.
43. Kirby, C. and G. Gregoriadis, *Dehydration-Rehydration Vesicles: A Simple Method for High Yield Drug Entrapment in Liposomes.* Nat. Biotechnol., 1984. **2**: p. 979-984.
44. Maulucci, G., et al., *Particle size distribution in DMPC vesicles solutions undergoing different sonication times.* Biophys. J., 2005. **88**(5): p. 3545-3550.
45. Cornell, B.A., et al., *The lower limit to the size of small sonicated phospholipid vesicles.* Biochim. Biophys. Acta, 1982. **690**(1): p. 15-19.
46. Huang, C.-H., *Phosphatidylcholine vesicles. Formation and physical characteristics.* Biochemistry, 1969. **8**(1): p. 344-352.
47. Hamilton, R.L., Jr., et al., *Unilamellar liposomes made with the French pressure cell: a simple preparative and semiquantitative technique.* J. Lipid Res., 1980. **21**(8): p. 981-992.
48. Woodbury, D.J., et al., *Reducing liposome size with ultrasound: bimodal size distributions.* J. Liposome Res., 2006. **16**(1): p. 57-80.
49. Driessen, A.J., et al., *Mechanistic studies of lantibiotic-induced permeabilization of phospholipid vesicles.* Biochemistry, 1995. **34**(5): p. 1606-1614.
50. Hunter, D.G. and B.J. Frisken, *Effect of extrusion pressure and lipid properties on the size and polydispersity of lipid vesicles.* Biophys. J., 1998. **74**(6): p. 2996-3002.
51. MacDonald, R.C., et al., *Small-volume extrusion apparatus for preparation of large, unilamellar vesicles.* Biochim. Biophys. Acta, 1991. **1061**(2): p. 297-303.
52. Mayer, L.D., M.J. Hope, and P.R. Cullis, *Vesicles of variable sizes produced by a rapid extrusion procedure.* Biochim. Biophys. Acta, 1986. **858**(1): p. 161-168.
53. Unger, E.C., et al., *Liposomal Gd-DTPA: effect of encapsulation on enhancement of hepatoma model by MRI.* Magn. Reson. Imaging, 1989. **7**(4): p. 417-423.
54. Cuccovia, I.M., et al., *Characterization of dioctadecyldimethylammonium chloride vesicles prepared by membrane extrusion and dichloromethane injection.* J. Mol. Liq. , 1997. **72**(1): p. 323-336.
55. Lapinski, M.M., et al., *Comparison of Liposomes Formed by Sonication and Extrusion: Rotational and Translational Diffusion of an Embedded Chromophore.* Langmuir, 2007. **23**(23): p. 11677-11683.

56. Feitosa, E., P.C. Barreleiro, and G. Olofsson, *Phase transition in dioctadecyldimethylammonium bromide and chloride vesicles prepared by different methods.* Chem. Phys. Lipids, 2000. **105**(2): p. 201-213.
57. Olson, F., et al., *Preparation of liposomes of defined size distribution by extrusion through polycarbonate membranes.* Biochim. Biophys. Acta, 1979. **557**(1): p. 9-23.
58. Ong, S.G., et al., *Evaluation of Extrusion Technique for Nanosizing Liposomes.* Pharmaceutics, 2016. **8**(4).
59. Berger, N., et al., *Filter extrusion of liposomes using different devices: comparison of liposome size, encapsulation efficiency, and process characteristics.* Int. J. Pharm., 2001. **223**(1-2): p. 55-68.
60. Brandl, M., et al., *Liposome Preparation by a New High Pressure Homogenizer Gaulin Micron Lab 40.* Drug Dev. Ind. Pharm., 1990. **16**(14): p. 2167-2191.
61. Braun-Falco O., K.H.C., Maibach H.I., *Liposome Dermatics*, ed. Springer-Verlag. 1992, Berlin.
62. Mayhew, E., et al., *Characterization of liposomes prepared using a microemulsifier.* Biochim. Biophys. Acta, 1984. **775**(2): p. 169-174.
63. Bachmann, D., M. Brandl, and G. Gregoriadis, *Preparation of liposomes using a Mini-Lab 8.30 H high-pressure homogenizer.* Int. J. Pharm., 1993. **91**(1): p. 69-74.
64. Barnadas-Rodríguez, R. and M. Sabés, *Factors involved in the production of liposomes with a high-pressure homogenizer.* Int. J. Pharm., 2001. **213**(1): p. 175-186.
65. Microfluidics^{TM}. *https://www.microfluidicscorp.com/*. 2018.
66. McAuliffe, L.N., et al., *Manufacture and Incorporation of Liposome-Entrapped Ethylenediaminetetraacetic Acid into Model Miniature Gouda-Type Cheese and Subsequent Effect on Starter Viability, pH, and Moisture Content.* J. Food Sci., 2016: p. 2708-2717.
67. Lelkes, P.I., *Liposome technolgy*. Vol. 1. 1984: CRC Press, Boca Raton.
68. Bachmann, D., *Liposomen zur intravenösen Applikation: Einstufige Herstellung, Charakterisierung und in vivo-Verhalten kleiner unilamellarer Phospohlipidvesikel*, in *Department of Pharmaceutical Technology and Biopharmacy*. 1994, University of Freiburg.
69. Montero, M.T., A. Martí, and J. Hernàndez-Borrell, *The active trapping of doxorubicin in liposomes by pH gradient: photon correlation spectroscopy and fluorimetric study.* Int. J. Pharm., 1993. **96**(1): p. 157-165.
70. Lasic, D.D., et al., *Sterically stabilized liposomes: a hypothesis on the molecular origin of the extended circulation times.* Biochim Biophys Acta, 1991. **1070**(1): p. 187-192.
71. Brandl, M., *Liposomes as drug carriers: a technological approach.* Biotechnol. Annu. Rev., 2001. **7**: p. 59-85.
72. Vemuri, S. and C.T. Rhodes, *Development and characterization of a liposome preparation by a pH-gradient method.* J. Pharm. Pharmacol., 1994. **46**(10): p. 778-783.
73. Dos Santos, N., et al., *pH gradient loading of anthracyclines into cholesterol-free liposomes: enhancing drug loading rates through use of ethanol.* Biochim. Biophys. Acta, 2004. **1661**(1): p. 47-60.

74. Haran, G., et al., *Transmembrane ammonium sulfate gradients in liposomes produce efficient and stable entrapment of amphipathic weak bases.* Biochim. Biophys. Acta, 1993. **1151**(2): p. 201-215.
75. Zucker, D., et al., *Liposome drugs' loading efficiency: a working model based on loading conditions and drug's physicochemical properties.* J. Control. Release, 2009. **139**(1): p. 73-80.
76. Clerc, S. and Y. Barenholz, *Loading of amphipathic weak acids into liposomes in response to transmembrane calcium acetate gradients.* Biochim. Biophys. Acta, 1995. **1240**(2): p. 257-265.
77. Cullis, P.R., et al., *Generating and loading of liposomal systems for drug-delivery applications.* Adv. Drug Delivery Rev., 1989. **3**(3): p. 267-282.
78. Bally, M.B., et al., *Uptake of safranine and other lipophilic cations into model membrane systems in response to a membrane potential.* Biochim. Biophys. Acta, 1985. **812**(1): p. 66-76.
79. Pick, U., *Liposomes with a large trapping capacity prepared by freezing and thawing of sonicated phospholipid mixtures.* Arch. Biochem. Biophys., 1981. **212**(1): p. 186-194.
80. Yang, R., et al., *Role of phospholipids and copolymers in enhancing stability and controlling degradation of intravenous lipid emulsions.* Colloids Surf. A, 2013. **436**: p. 434-442.
81. Haynes, D.H., *Phospholipid-coated microcrystals: injectable formulations of water-insoluble drugs*, in *Google Patents*. 1992: United States.
82. Cullis, P.R. and B. De Kruijff, *Lipid polymorphism and the functional roles of lipids in biological membranes.* Biochim. Biophys. Acta, 1979. **559**(4): p. 399-420.
83. Li, J., et al., *A review on phospholipids and their main applications in drug delivery systems.* ´Asian J. Pharm., 2015. **10**(2): p. 81-98.
84. Washington, C., *Stability of lipid emulsions for drug delivery.* Adv. Drug Delivery Rev., 1996. **20**(2): p. 131-145.
85. McElhaney, R.N., *The biological significance of alterations in the fatty acid composition of microbial membrane lipids in response to changes in environmental temperature* in *Extreme Environments*. 1976, Academic Press. p. 255-281.
86. Eze, M.O., *Phase Transitions in Phospholipid Bilayers: Lateral Phase Separations Play Vital Roles in Biomembranes.* Biochem. Educ., 1991. **19**(4): p. 204-208.
87. Chen, J., et al., *Influence of lipid composition on the phase transition temperature of liposomes composed of both DPPC and HSPC.* Drug. Dev. Ind. Pharm., 2013. **39**(2): p. 197-204.
88. Redondo-Morata, L., M.I. Giannotti, and F. Sanz, *Influence of cholesterol on the phase transition of lipid bilayers: a temperature-controlled force spectroscopy study.* Langmuir, 2012. **28**(35): p. 12851-12860.
89. Briuglia, M.L., et al., *Influence of cholesterol on liposome stability and on in vitro drug release.* Drug. Deliv. Transl. Res., 2015. **5**(3): p. 231-242.
90. Virden, J.W. and J.C. Berg, *Sodium chloride-induced aggregation of dipalmitoylphoshpatidylglycerol small unilamellar vesicles with varying amounts of incorporated cholesterol.* Langmuir, 1992. **8**(6): p. 1532-1537.
91. Mohammed, A.R., et al., *Liposome formulation of poorly water soluble drugs: optimisation of drug loading and ESEM analysis of stability.* Int. J. Pharm., 2004. **285**(1–2): p. 23-34.

92. New, R.R.C., *Liposomes: a pracitcal approach*, ed. N.Y. Oxford University Press. 1989.
93. Liu, D.-Z., et al., *Microcalorimetric and shear studies on the effects of cholesterol on the physical stability of lipid vesicles.* Colloids Surf. A, 2000. **172**(1): p. 57-67.
94. Needham, D. and R.S. Nunn, *Elastic deformation and failure of lipid bilayer membranes containing cholesterol.* Biophys. J., 1990. **58**(4): p. 997-1009.
95. Kirby, C., J. Clarke, and G. Gregoriadis, *Effect of the cholesterol content of small unilamellar liposomes on their stability in vivo and in vitro.* Biochem. J., 1980. **186**(2): p. 591-598.
96. Bartlett, G.R., *Phosphorus assay in column chromatography.* J. Biol. Chem., 1959. **234**(3): p. 466-468.
97. Worth, H.G. and D.J. Wright, *Colorimetric determination of phospholipids by use of molybdophosphate, and its application to amniotic fluid.* Clin. Chem., 1977. **23**(11): p. 1995-1200.
98. Stewart, J.C., *Colorimetric determination of phospholipids with ammonium ferrothiocyanate.* Anal. Biochem., 1980. **104**(1): p. 10-14.
99. Takayama, M., et al., *A new enzymatic method for determination of serum choline-containing phospholipids.* Clin. Chim. Acta, 1977. **79**(1): p. 93-98.
100. Edwards, K.A. and A.J. Baeumner, *Analysis of liposomes.* Talanta, 2006. **68**(5): p. 1432-1441.
101. Allain, C.C., et al., *Enzymatic determination of total serum cholesterol.* Clin. Chem., 1974. **20**(4): p. 470-475.
102. Jääskeläinen, I. and A. Urtti, *Liquid chromatography determination of liposome components using a light-scattering evaporative detector.* J. Pharm. Biomed. Anal., 1994. **12**(8): p. 977-982.
103. Grit, M., D.J.A. Crommelin, and J. Lang, *Determination of phosphatidylcholine, phosphatidylglycerol and their lyso forms from liposome dispersions by high-performance liquid chromatography using high-sensitivity refractive index detection.* J. Chrom. A, 1991. **585**(2): p. 239-246.
104. Oswald, M., et al., *HPLC analysis as a tool for assessing targeted liposome composition.* Int. J. Pharm., 2016. **497**(1-2): p. 293-300.
105. Frederik, P.M. and D.H. Hubert, *Cryoelectron microscopy of liposomes.* Meth. Enzymol., 2005. **391**: p. 431-448.
106. Grabielle-Madelmont, C., S. Lesieur, and M. Ollivon, *Characterization of loaded liposomes by size exclusion chromatography.* J. Biochem. Biophys. Methods, 2003. **56**(1-3): p. 189-217.
107. Moon, M.H. and J.C. Giddings, *Size distribution of liposomes by flow field-flow fractionation.* J. Pharm. Biomed. Anal., 1993. **11**(10): p. 911-920.
108. Ruozi, B., et al., *Atomic force microscopy and photon correlation spectroscopy: two techniques for rapid characterization of liposomes.* Eur. J. Pharm. Sci., 2005. **25**(1): p. 81-89.
109. Malvern, *Dynamic Light Scattering: An Introduction in 30 Minutes.* Malvern Instruments Ltd., 2014.
110. Malvern, *Zeta potential - An introduction in 30 Minutes.* Malvern Instruments Ltd., 2014.
111. Fry, D.W., J.C. White, and I.D. Goldman, *Rapid separation of low molecular weight solutes from liposomes without dilution.* Anal. Biochem., 1978. **90**(2): p. 809-815.

112. Kulkarni, B.S., R.S. Dipali, and V.G. Betageri, *Protamine-induced Aggregation of Unilamellar Liposomes.* Pharmaceutical Sciences, 1995. **1**(8): p. 359-362.
113. Gunter, K.K., et al., *A method of resuspending small vesicles separated from suspension by protamine aggregation and centrifugation.* Anal. Biochem., 1982. **120**(1): p. 113-124.
114. Fan, Y. and Q. Zhang, *Development of liposomal formulations: From concept to clinical investigations.* Asian Journal of Pharmaceutical Sciences, 2013. **8**(2): p. 81-87.
115. Bulbake, U., et al., *Liposomal Formulations in Clinical Use: An Updated Review.* Pharmaceutics, 2017. **9**(2): p. 1-33.
116. Drummond, D.C., et al., *Development of a highly active nanoliposomal irinotecan using a novel intraliposomal stabilization strategy.* Cancer Res., 2006. **66**(6): p. 3271-3277.
117. Wang-Gillam, A., et al., *Nanoliposomal irinotecan with fluorouracil and folinic acid in metastatic pancreatic cancer after previous gemcitabine-based therapy (NAPOLI-1): a global, randomised, open-label, phase 3 trial.* Lancet, 2016. **387**(10018): p. 545-557.
118. Janoff, A.S., et al., *Unusual lipid structures selectively reduce the toxicity of amphotericin B.* Proc. Natl. Acad. Sci. USA, 1988. **85**(16): p. 6122-6126.
119. Lister, J., *Amphotericin B Lipid Complex (Abelcet) in the treatment of invasive mycoses: the North American experience.* Eur. J. Haematol. Suppl., 1996. **57**: p. 18-23.
120. Olsen, S.J., et al., *Tissue distribution of amphotericin B lipid complex in laboratory animals.* J. Pharm. Pharmacol., 1991. **43**(12): p. 831-835.
121. Working, P.K. and A.D. Dayan, *Pharmacological-toxicological expert report. CAELYX. (Stealth liposomal doxorubicin HCl).* Hum. Exp. Toxicol., 1996. **15**(9): p. 751-785.
122. Gabizon, A., et al., *Prolonged circulation time and enhanced accumulation in malignant exudates of doxorubicin encapsulated in polyethylene-glycol coated liposomes.* Cancer Res., 1994. **54**(4): p. 987-992.
123. Batist, G., *Cardiac safety of liposomal anthracyclines.* Cardiovasc. Toxicol., 2007. **7**(2): p. 72-74.
124. Wicki, A., et al., *Nanomedicine in cancer therapy: challenges, opportunities, and clinical applications.* J. Control. Release, 2015. **200**: p. 138-157.
125. Ahmad, A., Y.F. Wang, and I. Ahmad, *Separation of liposome-entrapped mitoxantrone from nonliposomal mitoxantrone in plasma: pharmacokinetics in mice.* Meth. Enzymol., 2005. **391**: p. 176-185.
126. Mitra, A.K., C.H. Lee, and K. Cheng, *Advanced Drug Delivery*. 2013: John Wiley & Sons, Inc. Hoboken, New Jersey.
127. Eichhorn, M.E., et al., *Vascular targeting by EndoTAG-1 enhances therapeutic efficacy of conventional chemotherapy in lung and pancreatic cancer.* Int. J. Cancer, 2010. **126**(5): p. 1235-1245.
128. Lohr, J.M., et al., *Cationic liposomal paclitaxel plus gemcitabine or gemcitabine alone in patients with advanced pancreatic cancer: a randomized controlled phase II trial.* Ann. Oncol., 2012. **23**(5): p. 1214-1222.
129. Boulikas, T., *Clinical overview on Lipoplatin: a successful liposomal formulation of cisplatin.* Expert Opin. Investig. Drugs, 2009. **18**(8): p. 1197-1218.

130. Stathopoulos, G.P., et al., *Liposomal cisplatin combined with gemcitabine in pretreated advanced pancreatic cancer patients: a phase I-II study.* Oncol. Rep., 2006. **15**(5): p. 1201-1204.
131. Song, K.H., S.J. Chung, and C.K. Shim, *Preparation and evaluation of proliposomes containing salmon calcitonin.* J. Control. Release, 2002. **84**(1-2): p. 27-37.
132. Shaji, J. and V. Bhatia, *Proliposomes: a brief overview of novel delivery system.* Int. J. Pharm. Bio. Sci., 2013. **4**(1): p. 150-160.
133. Grave, A. and N. Pöllinger, *GLATT fluid bed technology for the coating of powders, pellets and micropellets*. 2011, Glatt Pharmaceutical Services, Binzen.
134. Masters, K., *Spray Drying in Practice*. 2002: SprayDryConsult International ApS Denmark.
135. Rojanarat, W., et al., *Isoniazid proliposome powders for inhalation-preparation, characterization and cell culture studies.* Int. J. Mol. Sci., 2011. **12**(7): p. 4414-4434.
136. Rojanarat, W., et al., *Inhaled pyrazinamide proliposome for targeting alveolar macrophages.* Drug Deliv., 2012. **19**(7): p. 334-345.
137. Lo, Y.-l., J.-c. Tsai, and J.-h. Kuo, *Liposomes and disaccharides as carriers in spray-dried powder formulations of superoxide dismutase.* J. Control. Release, 2004. **94**(2): p. 259-272.
138. Colonna, C., et al., *Non-viral dried powders for respiratory gene delivery prepared by cationic and chitosan loaded liposomes.* Int. J. Pharm., 2008. **364**(1): p. 108-118.
139. Hiremath, P.S., K.S. Soppimath, and G.V. Betageri, *Proliposomes of exemestane for improved oral delivery: formulation and in vitro evaluation using PAMPA, Caco-2 and rat intestine.* Int. J. Pharm., 2009. **380**(1-2): p. 96-104.
140. Nekkanti, V., N. Venkatesan, and G.V. Betageri, *Proliposomes for oral delivery: progress and challenges.* Curr. Pharm. Biotechnol., 2015. **16**(4): p. 303-312.
141. Brunner, G., *Supercritical fluids: technology and application to food processing.* J. Food Eng., 2005. **67**(1): p. 21-33.
142. Badens, E., C. Magnan, and G. Charbit, *Microparticles of soy lecithin formed by supercritical processes.* Biotechnol. Bioeng., 2001. **72**(2): p. 194-204.
143. Bridson, R.H., et al., *The preparation of liposomes using compressed carbon dioxide: strategies, important considerations and comparison with conventional techniques.* J. Pharm. Pharmacol., 2006. **58**(6): p. 775-785.
144. Magnan, C., et al., *Soy lecithin micronization by precipitation with a compressed fluid antisolvent — influence of process parameters.* J. Supercrit. Fluids, 2000. **19**(1): p. 69-77.
145. Xia, F., et al., *Preparation of lutein proliposomes by supercritical anti-solvent technique.* Food Hydrocoll., 2012. **26**(2): p. 456-463.
146. Mattea, F., Á. Martín, and M.J. Cocero, *Carotenoid processing with supercritical fluids.* J. Food. Eng., 2009. **93**(3): p. 255-265.
147. Fei, X., et al., *Preparation, characterization, and biodistribution of breviscapine proliposomes in heart.* J. Drug Target., 2009. **17**(5): p. 408-414.
148. Katare, O.P., S.P. Vyas, and V.K. Dixit, *Proliposomes of indomethacin for oral administration.* J. Microencapsul., 1991. **8**(1): p. 1-7.

149. Xiao, Y.Y., et al., *Preparation of silymarin proliposomes and its pharmacokinetics in rats.* Yao Xue Xue Bao, 2005. **40**(8): p. 758-763.
150. Vanic, Z., et al., *Tablets of pre-liposomes govern in situ formation of liposomes: concept and potential of the novel drug delivery system.* Eur. J. Pharm. Biopharm., 2014. **88**(2): p. 443-454.
151. Hwang, B.-Y., et al., *In vitro skin permeation of nicotine from proliposomes.* J. Control. Release, 1997. **49**(2): p. 177-184.
152. Gupta, V., A.K. Barupal, and S. Ramteke, *Formulation Development and in vitro Characterization of Proliposomes for Topical Delivery of Aceclofenac.* Indian J. Pharm. Sci., 2008. **70**(6): p. 768-775.
153. Gowda, D., et al., *Proliposomes: A novel approach to carrier drug delivery system*. Vol. 8. 2016. 348-354.
154. Mohammed, A.R., et al., *Lyophilisation and sterilisation of liposomal vaccines to produce stable and sterile products.* Methods, 2006. **40**(1): p. 30-38.
155. Katare, O.P., S.P. Vyas, and V.K. Dixit, *Preparation and performance evaluation of plain proliposomal systems for cytoprotection.* J. Microencapsul., 1991. **8**(3): p. 295-300.
156. Kumar, R., R.B. Gupta, and G.V. Betageri, *Formulation, characterization, and in vitro release of glyburide from proliposomal beads.* Drug Deliv., 2001. **8**(1): p. 25-27.
157. Bobbala, S.K. and P.R. Veerareddy, *Formulation, evaluation, and pharmacokinetics of isradipine proliposomes for oral delivery.* J. Liposome Res., 2012. **22**(4): p. 285-294.
158. Potluri, P. and G.V. Betageri, *Mixed-micellar proliposomal systems for enhanced oral delivery of progesterone.* Drug Deliv., 2006. **13**(3): p. 227-232.
159. Velpula, A., et al., *Proliposome powders for enhanced intestinal absorption and bioavailability of raloxifene hydrochloride: effect of surface charge.* Drug Dev. Ind. Pharm., 2013. **39**(12): p. 1895-1906.
160. Song, K.H., S.J. Chung, and C.K. Shim, *Enhanced intestinal absorption of salmon calcitonin (sCT) from proliposomes containing bile salts.* J. Control. Release, 2005. **106**(3): p. 298-308.
161. Lee, H.J., et al., *Pharmacokinetics and tissue distribution of adriamycin and adriamycinol after intravenous administration of adriamycin-loaded neutral proliposomes to rats.* Int. J. Pharm., 1995. **121**(1): p. 1-10.
162. Payne, N.I., et al., *In-vivo studies of amphotericin B liposomes derived from proliposomes: effect of formulation on toxicity and tissue disposition of the drug in mice.* J. Pharm. Pharmacol., 1987. **39**(1): p. 24-28.
163. Katare, O.P., S.P. Vyas, and V.K. Dixit, *Effervescent granule based proliposomes of ibuprofen.* J. Microencapsul., 1990. **7**(4): p. 455-462.
164. Park, J.M., et al., *The pharmacokinetics of methotrexate after intravenous administration of methotrexate-loaded proliposomes to rats.* Biopharm. Drug Dispos., 1994. **15**(5): p. 391-407.
165. Tsume, Y., et al., *The Biopharmaceutics Classification System: subclasses for in vivo predictive dissolution (IPD) methodology and IVIVC.* Eur. J. Pharm. Sci., 2014. **57**: p. 152-163.
166. Fachinformation, *Fenofibrat 200 Heumann.* Rote Liste Service GmbH, Januar 2018.

167. Staels, B., et al., *Mechanism of action of fibrates on lipid and lipoprotein metabolism.* Circulation, 1998. **98**(19): p. 2088-2093.
168. Bushra, R. and N. Aslam, *An Overview of Clinical Pharmacology of Ibuprofen.* Oman Med. J. , 2010. **25**(3): p. 155-161.
169. Abraham, P., K. Indirani, and K. Desigamani, *Nitro-arginine methyl ester, a non-selective inhibitor of nitric oxide synthase reduces ibuprofen-induced gastric mucosal injury in the rat.* Dig. Dis. Sci., 2005. **50**(9): p. 1632-1640.
170. Bradbury, F., *How important is the role of the physician in the correct use of a drug? An observational cohort study in general practice.* Int. J. Clin. Pract. Suppl., 2004(144): p. 27-32.
171. Wahbi, A.A., et al., *Spectrophotometric methods for the determination of Ibuprofen in tablets.* Pak. J. Pharm. Sci., 2005. **18**(4): p. 1-6.
172. Chavez, M.L. and C.J. DeKorte, *Valdecoxib: a review.* Clin Ther, 2003. **25**(3): p. 817-51.
173. Rödel, M., et al., *Bioceramics as drug delivery systems*. 2018. p. 153-194.
174. Rao, P. and E.E. Knaus, *Evolution of nonsteroidal anti-inflammatory drugs (NSAIDs): cyclooxygenase (COX) inhibition and beyond.* J. Pharm. Pharm. Sci., 2008. **11**(2): p. 81-110.
175. Ph.Eur., *Europäisches Arzneibuch (Pharmacopeia Europea)*. Vol. 9 inkl. 1. Nachtrag (Ph.Eur. 9.1). Grundwerk 2017: Deutscher Apotheker Verlag, Stuttgart.
176. Meng, X., et al., *Stabilizing dispersions of hydrophobic drug molecules using cellulose ethers during anti-solvent synthesis of micro-particulates.* Colloids Surf. B, 2009. **70**(1): p. 7-14.
177. Milhem, O.M., et al., *Polyamidoamine Starburst® dendrimers as solubility enhancers.* Int. J. Pharm., 2000. **197**(1): p. 239-241.
178. Blaschek, W., et al., *HagerROM Hagers HAndbuch der Drogen und Arzneistoffe*. 2002: Springer London.
179. Huesgen, A.G., *Determination of Log P for Compunds of Different Polarity Using the Agilent 1200 Infinity Series HDR-DAD Impurity Analyzer System*. 2014, Agilent Technologies, Inc. Waldbronn, Germany.
180. Pownall, H.J., et al., *Kinetics of lipid--protein interactions: interaction of apolipoprotein A-I from human plasma high density lipoproteins with phosphatidylcholines.* Biochemistry, 1978. **17**(7): p. 1183-1188.
181. Regelin, A.E., et al., *Biophysical and lipofection studies of DOTAP analogs.* Biochim. Biophys. Acta, 2000. **1464**(1): p. 151-164.
182. Lamy-Freund, M.T. and K.A. Riske, *The peculiar thermo-structural behavior of the anionic lipid DMPG.* Chem. Phys. Lipids, 2003. **122**(1-2): p. 19-32.
183. Lichtenberg, D. and Y. Barenholz, *Liposomes: preparation, characterization, and preservation.* Methods Biochem. Anal., 1988. **33**: p. 337-462.
184. Chapman, D., R.M. Williams, and B.D. Ladbrooke, *Physical studies of phospholipids. VI. Thermotropic and lyotropic mesomorphism of some 1,2-diacyl-phosphatidylcholines (lecithins).* Chem. Phys. Lipids, 1967. **1**(5): p. 445-475.
185. Jukanti, R., et al., *Enhanced bioavailability of exemestane via proliposomes based transdermal delivery.* J. Pharm. Sci., 2011. **100**(8): p. 3208-3222.
186. Glassware, M.L., *Zählkammer.* 2010.
187. Fatouros, D.G. and S.G. Antimisiaris, *Effect of Amphiphilic Drugs on the Stability and Zeta-Potential of Their Liposome Formulations: A Study with*

Prednisolone, Diazepam, and Griseofulvin. J. Colloid Interface Sci., 2002. **251**(2): p. 271-277.

188. Jones, M.N., *The surface properties of phospholipid liposome systems and their characterisation.* Adv. Colloid Interface Sci., 1995. **54**: p. 93-128.
189. Zhang, J.A. and J. Pawelchak, *Effect of pH, ionic strength and oxygen burden on the chemical stability of EPC/cholesterol liposomes under accelerated conditions. Part 1: Lipid hydrolysis.* Eur. J. Pharm. Biopharm., 2000. **50**(3): p. 357-364.
190. Sułkowski, W.W., et al., *The influence of temperature, cholesterol content and pH on liposome stability.* J. Mol. Struct., 2005. **744-747**: p. 737-747.
191. Garidel, P., et al., *The mixing behavior of pseudobinary phosphatidylcholine-phosphatidylglycerol mixtures as a function of pH and chain length.* Eur. Biophys. J., 1997. **26**: p. 447-459.
192. Blazek–Welsh, A.I. and D.G. Rhodes, *SEM Imaging Predicts Quality of Niosomes from Maltodextrin-Based Proniosomes.* Pharm. Res., 2001. **18**(5): p. 656-661.
193. Bibi, S., et al., *Microscopy imaging of liposomes: From coverslips to environmental SEM.* Int. J. Pharm., 2011. **417**(1): p. 138-150.
194. Roy, B., et al., *Influence of Lipid Composition, pH, and Temperature on Physicochemical Properties of Liposomes with Curcumin as Model Drug.* J. Oleo Sci., 2016. **65**(5): p. 399-411.
195. Almgren, M., K. Edwards, and J. Gustafsson, *Cryotransmission electron microscopy of thin vitrified samples.* Curr. Opin. Colloid Interface Sci., 1996. **1**(2): p. 270-278.
196. Talmon, Y., *Transmission Electron Microscopy of Complex Fluids: The State of the Art.* Berichte der Bunsengesellschaft für physikalische Chemie, 1996. **100**(3): p. 364-372.
197. Almgren, M., K. Edwards, and G. Karlsson, *Cryo transmission electron microscopy of liposomes and related structures.* Colloids Surf. A, 2000. **174**(1): p. 3-21.
198. Regev, O., C. Kang, and A. Khan, *Cryo-TEM and NMR studies of solution microstructures of double-tailed surfactant systems: didodecyldimethylammonium hydroxide, acetate, and sulfate.* J. Phys. Chem, 1994. **98**(26): p. 6619-6625.
199. Heurtault, B., et al., *Physico-chemical stability of colloidal lipid particles.* Biomaterials, 2003. **24**(23): p. 4283-4300.
200. Ney, P., *Zeta-Potentiale und Flotierbarkeit von Mineralien*. 1973, Springer.
201. Soema, P.C., et al., *Predicting the influence of liposomal lipid composition on liposome size, zeta potential and liposome-induced dendritic cell maturation using a design of experiments approach.* Eur. J. Pharm. Biopharm., 2015. **94**: p. 427-435.
202. Vanić, Ž., et al., *Tablets of pre-liposomes govern in situ formation of liposomes: Concept and potential of the novel drug delivery system.* Eur. J. Pharm. Biopharm., 2014. **88**(2): p. 443-454.
203. Tantisripreecha, C., et al., *Development of delayed-release proliposomes tablets for oral protein drug delivery.* Drug. Dev. Ind. Pharm., 2012. **38**(6): p. 718-727.
204. Nii, T. and F. Ishii, *Encapsulation efficiency of water-soluble and insoluble drugs in liposomes prepared by the microencapsulation vesicle method.* Int. J. Pharm., 2005. **298**(1): p. 198-205.

205. Niu, X., et al., *Mesoporous carbon as a novel drug carrier of fenofibrate for enhancement of the dissolution and oral bioavailability.* Int. J. Pharm., 2013. **452**(1-2): p. 382-389.
206. Kulkarni, S.B., G.V. Betageri, and M. Singh, *Factors affecting microencapsulation of drugs in liposomes.* J. Microencapsul., 1995. **12**(3): p. 229-246.
207. Tran, T.H., et al., *Preparation and characterization of fenofibrate-loaded nanostructured lipid carriers for oral bioavailability enhancement.* AAPS PharmSciTech., 2014. **15**(6): p. 1509-1515.
208. Li, F., et al., *Preparation and pharmacokinetics evaluation of oral self-emulsifying system for poorly water-soluble drug Lornoxicam.* Drug. Deliv., 2015. **22**(4): p. 487-498.
209. Anderson, M. and A. Omri, *The effect of different lipid components on the in vitro stability and release kinetics of liposome formulations.* Drug. Deliv., 2004. **11**(1): p. 33-39.
210. Savla, R., et al., *Review and analysis of FDA approved drugs using lipid-based formulations.* Drug. Dev. Ind. Pharm., 2017. **43**(11): p. 1743-1758.
211. Cha, K.H., et al., *Enhancement of the dissolution rate and bioavailability of fenofibrate by a melt-adsorption method using supercritical carbon dioxide.* Int. J. Nanomedicine, 2012. **7**: p. 5565-5575.
212. Gupta, D., A. K Barupal, and S. Ramteke, *Formulation Development and in vitro Characterization of Proliposomes for Topical Delivery of Aceclofenac.* Indian J. Pharm. Sci., 2008. **70**: p. 768-775.
213. Yanamandra, S., et al., *Proliposomes as a drug delivery system to decrease the hepatic first-pass metabolism: Case study using a model drug.* Eur. J. Pharm. Sci., 2014. **64**: p. 26-36.
214. Agnihotri, S.A., K.S. Soppimath, and G.V. Betageri, *Controlled release application of multilamellar vesicles: a novel drug delivery approach.* Drug Deliv., 2010. **17**(2): p. 92-101.
215. Vargha-Butler, E. and E. Hurst, *Study of liposomal drug delivery systems 1. Surface characterization of steroid loaded MLV liposomes.* Colloids Surf. B, 1995. **3**(5): p. 287-295.
216. Shariat, S., et al., *Optimization of a Method to Prepare Liposomes Containing HER2/Neu- Derived Peptide as a Vaccine Delivery System for Breast Cancer.* Iran. J. Pharm. Res., 2014. **13**(Suppl): p. 15-25.
217. Mouritsen, O.G., *Theoretical models of phospholipid phase transitions.* Chem. Phys. Lipids, 1991. **57**(2): p. 179-194.
218. Ahn, B.-N., S.-K. Kim, and C.-K. Shim, *Proliposomes as an intranasal dosage form for the sustained delivery of propranolol.* J. Control. Release, 1995. **34**(3): p. 203-210.
219. Maury, M., et al., *Effects of process variables on the powder yield of spray-dried trehalose on a laboratory spray-dryer.* Eur. J. Pharm. Biopharm., 2005. **59**(3): p. 565-573.
220. Mönckedieck, M., et al., *Spray drying of mannitol carrier particles with defined morphology and flow characteristics for dry powder inhalation.* Drying Technol., 2017. **35**(15): p. 1843-1857.
221. Littringer, E.M., et al., *The morphology of spray dried mannitol particles — The vital importance of droplet size.* Powder Technol., 2013. **239**: p. 162-174.

222. Patil-Gadhe, A. and V. Pokharkar, *Single step spray drying method to develop proliposomes for inhalation: A systematic study based on quality by design approach.* Pulm. Pharmacol. Ther., 2014. **27**(2): p. 197-207.
223. Yingsukwattana, K., et al., *Enhanced permeability across Caco-2 cell monolayers by specific mannosylating ligand of buserelin acetate proliposomes.* J. Liposome Res., 2016. **26**(1): p. 69-79.
224. Zidan, A.S., et al., *Formulation and transport properties of tenofovir loaded liposomes through Caco-2 cell model.* J. Liposome Res., 2013. **23**(4): p. 318-326.

8 CURRICULUM VITAE

Personal Data

Name	Christina Rödel

Professional and academic Training

10/14 - 11/18	Friedrich-Alexander-Universität Erlangen-Nürnberg Ph.D. studies in Pharmaceutics under the supervision of Dr. Stefan Seyferth and Prof. Dr. Geoffrey Lee
07/14	Licensed pharmacist 3rd state examination (Approbation)
11/13 - 04/14	Apotheke im Donau-Einkaufszentrum, Regensburg Pharmacist in internship at a community pharmacy
05/13 - 10/13	Boehringer Ingelheim, Biberach a. d. Riß Pharmacist in internship at the division “Formulation Development Solids”
10/08 - 04/13	University of Regensburg Undergraduate student in pharmacy 1st and 2nd state examination
09/99 - 06/08	Richard-Wagner-Gymnasium Bayreuth Abitur

Further information

12/14 - 12/18	Pharmacist at Richard-Wagner-Apotheke, Bayreuth
10/14 - 02/18	Specialist in Pharmaceutics (“Fachapothekerin für Pharmazeutische Technologie”)

9 ACKNOWLEDGEMENTS / DANKSAGUNG

An dieser Stelle möchte ich ein herzliches Dankeschön an alle Personen richten, die durch ihre Unterstützung zum Gelingen der vorliegenden Dissertation beigetragen haben.

Zuallererst möchte ich mich bei Prof. Dr. Geoffrey Lee bedanken, der mir die Arbeit an seinem Lehrstuhl ermöglicht hat und als mein Doktorvater und Gutachter fungierte. Ebenfalls ein herzliches Dankeschön, dass Sie die Teilnahme an Kongressen sowie Weiter- und Fortbildungen jederzeit unterstützt haben.

Ein besonderer Dank gilt meinem Betreuer Dr. Stefan Seyferth. Lieber Stefan, ich konnte bei Fragen aller Art immer und jederzeit zu dir kommen. Du hattest ein offenes Ohr und hast mich bei Fragestellungen in meiner Arbeit tatkräftig unterstützt. Dennoch hatte ich auch Freiraum, um eigene Strategien und Ideen auszuprobieren. Neben fachlichen Diskussionen haben wir aber auch über unsere Urlaube oder Geschichten deiner Jungs geplaudert. Nicht zu vergessen deine Annahme computerbezogener Probleme.

Herrn PD Dr. Henning Gieseler danke ich für die Begutachtung meiner Dissertation.

Dem Lehrstuhl für Feststoff- und Grenzflächenverfahrenstechnik von Herrn Prof. Dr. Peukert danke ich für die Möglichkeit, die Zetasizer-Messungen durchführen zu können.

Weiterhin geht ein großer Dank an Herrn Robert Brandscheid und Herrn Prof. Dr. Erdmann Spiecker vom Institute of Micro- and Nanostructure Research für die Anfertigung der Cryo-TEM-Aufnahmen.

Besonderer Dank gilt auch den Festangestellten unseres Lehrstuhls: Luise Schedl für die Aufnahme von mehr als 800 REM-Bildern, die netten AFL-Kurstage und die unzähligen Geschichten aus vergangenen Lehrstuhlzeiten; unserem Werkstattmeister Josef Hubert, der mit seiner Begeisterung und seinem Erfindergeist jedes Hindernis in der Versuchsdurchführung mit Geschick

überwunden hat, aber mich auch beim Basteln des Doktorhutes für Sandra sehr unterstützt hat; Christiane Blaha für das Ordern von Chemikalien oder Laborgeräten; Petra Neubarth für Support bei organisatorischen Dingen, Dienstreiseanträgen oder Abrechnungen.

Herzlicher Dank auch an meine Wahlpflichtfachstudentinnen und -studenten, besonders an Elisabeth Kupfer, die mich bei der Erstellung meiner Projektarbeit im Rahmen der Weiterbildung zum Fachapotheker für Pharmazeutische Technologie tatkräftig unterstützt hat.

Ebenfalls möchte ich mich bei Zahra Abbas und Katja Prax vom Lehrstuhl für Molekulare und klinische Pharmazie für das freundschaftliche Klima bedanken.

Den Kolleginnen und Kollegen der Station Solida ein Dankeschön für die angenehmen und abwechslungsreichen Praktikumstage. Hier sind zu nennen: Dr. Jens Holtappels, Dr. Claudia Kunz, Lukas Pietsch, Dr. Julia Staudenecker, Alexander Ullrich und Tim Wenzel.

Ebenfalls möchte ich mich für die schöne Zeit am Lehrstuhl bei Dr. Alexandra Braun, Dr. Alexander Grebner, Dr. Sandra Großberger, Zixin Huang, Natalie Keil, Julia Kosan, Dr. Anders Kunst, Felix Prihoda sowie Melinda Rupp bedanken.

Ein herzliches und besonders großes Dankeschön geht an meine lieben „Frollegen“, ohne die die Zeit am Lehrstuhl und das Drumherum nicht halb so wunderbar, amüsant und unvergesslich gewesen wären: Thomas Bach, Veronika Braig, Anna-Lena Funk, Bastian Haering sowie Pia Hiltl.

Lieber Thomas, ich danke dir für deine Worte und deinen Witz, die mir immer ein Lachen ins Gesicht gezaubert haben. Dein Junggesellenabschied war sagenhaft. Ein Dank gilt dir auch für deinen HPLC-Support. Alles Gute für dich und deine kleine Familie.

Liebe Pia, deine herzliche und humorvolle Art hat uns sehr schnell zu Freundinnen werden lassen. Danke für den tollen Trip nach Weil am Rhein, bei dem wir drei Länder in wenigen Minuten bereist und viel über Scale-Up gelernt haben. Bleib so toll, wie du bist, auf dass wir noch lange in Kontakt bleiben und viel Erfolg weiterhin für dich und deine Nanopartikel.

Liebe Anna-Lena, ich habe dich schon als Studentin in meinem ersten Semester betreut und nun waren wir noch Kolleginnen und Freundinnen. Neben dem gemeinsamen Musizieren haben wir auch Vieles zusammen erlebt. Auf dass

unsere Freundschaft lange anhält! Für deine Arbeit wünsche ich dir alles erdenklich Gute.
Lieber Basti, wir haben viele Kongresse in Glasgow, Bonn, Stockholm (Fika, fika!) und Meran erlebt. Sie werden mir immer in schöner Erinnerung bleiben. Des Öfteren habe ich auch dein Fahrrad-Know-How für meinen Porsche benötigt, der dank dir auf unserer waghalsigen Fahrradtour zum Walberla oder Sprints zu Carlo mit hundert Sachen lief. Einmalig war auch unser legendäres Doktoranden Pub-Quiz. Danke auch, dass du mich in der letzten Phase an der Uni zum „Schaffe, Schaffe Häusle baue“ motiviert hast und ein treuer Begleiter im unteren Stockwerk warst. Weiterhin hast du netterweise einen Teil meiner Arbeit Korrektur gelesen – vielen Dank. Ich hoffe, dass wir noch ganz lange befreundet bleiben. Viel Erfolg beim Endspurt für deine Dissertation.
Last but not least danke ich dir, liebe Vroni, dass wir wunderbare Jahre voller Ups and Downs im Labor verbracht haben, wobei die Ups zum Glück überwogen haben. Ich konnte mich bei fachlichen Fragestellungen immer auf deine Hilfe und deinen Rat verlassen. Gemeinsame Besuche von Weiterbildungsseminaren oder die Teilnahme an Kongressen in Schottland, Schweden und Spanien standen ebenfalls auf dem Programm - nicht zu vergessen gemeinsame schöne Erlebnisse. Für deine neue Stelle wünsche ich dir denkbar viel Erfolg und nur das Beste.

Weiter möchte ich auch außerhalb des universitären Umfeldes Dr. Georg Straller für das Lesen meiner Dissertation danken. Obwohl wir uns noch gar nicht so lange kennen, weiß ich deine Unterstützung, Expertise und Freundschaft wirklich sehr zu schätzen lieber Georg – du bist einfach der Beste.
Herzlicher Dank gebührt auch meiner liebgewonnen Freundin Julia Zahn, die mir durch gemeinsame Unternehmungen Kraft und Ausgleich für die Promotion gegeben hat.

Diese ganze Arbeit wäre allerdings nie möglich gewesen ohne die unermüdliche Unterstützung meiner lieben Eltern Willy und Waltraud. Danke, dass ihr immer für mich da seid.
Zuletzt danke ich meiner lieben Schwester Michaela. Liebe Michi, es lässt sich nicht in Worte fassen, wie sehr ich dir von ganzem Herzen danke. Du hast mir stets geholfen, mich ermutigt und aufgebaut und ich habe so viel von dir lernen können. Danke für ALLES!